HYDRAULIC EFFICIENCY OF GRATE AND CURB INLETS FOR URBAN STORM DRAINAGE

Prepared for

The Urban Drainage and Flood Control District

Prepared by

Brendan C. Comport
Christopher I. Thornton
Amanda L. Cox

December 2009

Colorado State University
Daryl B. Simons Building *at the*
Engineering Research Center
Fort Collins, CO 80523

Colorado State University

HYDRAULIC EFFICIENCY OF GRATE AND CURB INLETS FOR URBAN STORM DRAINAGE

Prepared for

The Urban Drainage and Flood Control District

.

Prepared by

Brendan C. Comport
Christopher I. Thornton
Amanda L. Cox

December 2009

Colorado State University
Daryl B. Simons Building *at the*
Engineering Research Center
Fort Collins, CO 80523

TABLE OF CONTENTS

LIST OF FIGURES

LIST OF TABLES

LIST OF SYMBOLS, UNITS OF MEASURE, AND ABBREVIATIONS

Symbols

a	gutter depression relative to the street cross slope (ft)
a	width of openings between bars
a	local inlet (and gutter) depression
a	coefficient of discharge
a,b,c,d,e,f	regression exponents
A	area (ft^2)
A	cross-sectional flow area (ft^2)
b	depth exponent
b	width of bars
D	hydraulic depth (ft)
depth	critical depth parameter
E	efficiency (inlet capture) (%)
E_o	ratio of flow in a depressed gutter section to total gutter flow
f	function relating dimensional analysis parameters q
F, Fr	Froude number
g	unspecified function different from f
g	acceleration due to gravity (ft/s^2)
G	function relating the dimensionless Pi parameters, related to the function f
h	flow depth (in the gutter) (ft)
h	depth for a rectangular cross section
H	head above the weir crest (ft)
H	total hydraulic head
L	length (of grate or inlet and curb opening) (ft)
L	curb opening length in the direction of flow (ft)
L_2	length of the downstream slope transition
L_e	effective length of grate (ft)
L_0	length required to trap the central portion of gutter flow
L_r	length, width, and depth scaling ratio
L_T	curb opening length required to capture 100% of gutter flow

m	number of dimensions required to specify the dimensions of all parameters
N	Pi parameter
N	coefficient of regression
n	Manning roughness coefficient (or parameter)
n-1	independent parameters
n_r	Manning roughness scaling ratio
n-m	independent dimensionless Pi parameters
Pr	level of confidence that a parameter estimate has not arisen by chance (called the significance level) evaluated by SAS
q	flow bypassing the inlet
q_1	dependent parameter
$q_2 \ldots q_n$	n-1 independent parameters
q_i	parameter
Q	discharge (cfs)
Q	volumetric flow rate or theoretical volumetric flow rate (cfs)
Q	gutter flow (cfs)
$Q_{captured}$	captured flow
Q_0	total flow
Q_r	discharge scaling ratio
Q_s	flow rate in the section above the depressed section (cfs)
Q_s	discharge in street section (cfs) (UDFCD, 2008)
Q_s	total gutter flow separated into side flow
Q_{Total}	total flow
Q_w	flow rate in the depressed section of the gutter (cfs)
Q_w	captured flow
Q_w	total gutter flow separated into frontal flow
Q_{wi}	frontal flow intercepted by the inlet (cfs)
R	hydraulic radius
R_f	ratio of frontal flow captured by the inlet to the total frontal flow
R_s	ratio of side flow captured to total side flow
R^2	coefficient of determination for regression analysis

S_c, *Sc, cross slope*	cross (or lateral) slope
S_e	equivalent street cross slope (ft/ft)
S_f	friction slope
S_L	longitudinal (street) slope (ft/ft)
S_o	bottom slope of the channel
S_w	gutter cross slope (ft/ft) (UDFCD, 2008)
S_x	street cross slope (ft/ft) (UDFCD, 2008)
S_x	side slope
t	dividing the standard error of the parameter estimate by the estimate itself in SAS
T	top width of gutter flow
T	top width for a general cross section
T	top width of flow (spread) (ft) (UDFCD, 2008)
T	top width of flow spread from the curb face (ft)
T_s	spread of flow in street (ft) (UDFCD, 2008)
T_w	top width parameter
V	velocity (of cross-sectional averaged flow, flow in the gutter, and approaching flow) (ft/s)
V	velocity of flow at the inlet (ft/s), determined from Q/A
$\overline{V}$	cross-sectional average flow velocity (ft/s)
V_o	splash-over velocity (ft/s)
V_0	velocity of approaching flow
V_r	velocity scaling ratio
velocity	flow velocity parameter
W	width (of the gutter, gutter section, and depressed gutter section) (ft)
W	width of gutter pan (ft) (UDFCD, 2008)
W_p	wetted perimeter
y	depth (of flow in the gutter and flow in the depressed gutter section) (ft)
y_0	depth of flow over the first opening
α,β,γ,η	constants (UDFCD, 2008)
θ	angle formed by the curb and gutter

Π	Pi parameter for dimensional analysis
Φ	unit conversion constant, equal to 1.49 for U. S. Customary and 1.00 for SI

Units of Measure

acre ft	acre foot
cfs	cubic feet per second
º	degree(s), as a measure of angular distance
ft	feet or foot
ft/ft	feet per foot
ft/s	feet per second
ft/s^2	feet per second squared
ft^2	square feet
GB	gigabyte(s)
hp	horse power
in.	inch(es)
%	percent
SI	International System of Units

Abbreviations

3d	type 2 debris
annubar	differential pressure meter
AT	additional test
BMP	Best Management Practice
CDOT	Colorado Department of Transportation
CSU	Colorado State University
DP	differential pressure
ERC	Engineering Research Center
FHWA	Federal Highway Administration
flat	type 1 debris
HEC 22	*Hydraulic Engineering Circular 22*

ID	identification
mag meter	electro-magnetic flow meter
No.	number
QC	quality control
®	registered
R5	5-ft Type R curb inlet
R9	9-ft Type R curb inlet
R12	12-ft Type R curb inlet
R15	15-ft Type R curb inlet
SAS	Statistical Analysis Software
SDHC	Secure Digital High Capacity
™	trademark
Type 13, Type 16	UDFCD grates tested at CSU
Type R	CDOT curb tested at CSU
UDFCD	Urban Drainage and Flood Control District
USB	Universal Serial Bus
USBR	U. S. Bureau of Reclamation
USDCM	*Urban Storm Drainage Criteria Manual*

1 INTRODUCTION

A research program was conducted at Colorado State University (CSU) to evaluate the hydraulic efficiency of three storm-drain inlets. Inlets tested in this study are currently used by the Urban Drainage and Flood Control District (UDFCD) of Denver, and consist of the Denver Type 13 and 16 grates, and the Colorado Department of Transportation (CDOT) Type R curb. These inlets have never been specifically studied or tested for development of hydraulic efficiency relationships. Current design practices are based upon a document produced by the Federal Highway Administration (FHWA, 2001) titled "*Hydraulic Engineering Circular 22*" (*HEC 22*). General inlet types are addressed in *HEC 22*, but no specific guidance is provided for these three inlets used by the UDFCD. The study presented in this report focused on collecting data on these inlets under physically-relevant design conditions, and developing improved design methods for determining inlet efficiency under varying road geometries. A 1/3 Froude-scale model of a two-lane road section was designed and built at the Engineering Research Center (ERC) of CSU. The model consisted of an adjustable slope road surface, gutter panels, and three interchangeable inlet types positioned in a testing flume. Details pertaining to model construction, testing procedure, resulting database, and data analysis are presented in this report.

1.1 Project Background

Storm-water runoff is typically conveyed through a network comprised of streets, gutters, inlets, storm sewer pipes, and treatment facilities. Streets of developed areas often serve as collectors for runoff, and convey water into gutters and eventually to storm sewer inlets. Storm-water management in the metropolitan Denver area falls under the jurisdiction of the UDFCD. Policies, design procedures, and Best Management Practices (BMPs) are provided in the "*Urban Storm Drainage Criteria Manual*" (*USDCM*; UDFCD, 2008). Design methods presented in the

USDCM for determining inlet efficiency provide the currently accepted methodology for design of storm-water collection systems throughout the region depicted in Figure 1-1. Guidance is provided in the *USDCM* for local jurisdictions, developers, contractors, and industrial and commercial operations in selecting, designing, maintaining, and carrying-out BMPs to effectively handle storm-water runoff (UDFCD, 2008). Other agencies participating in this study include the University of Colorado at Denver and the Colorado Department of Transportation.

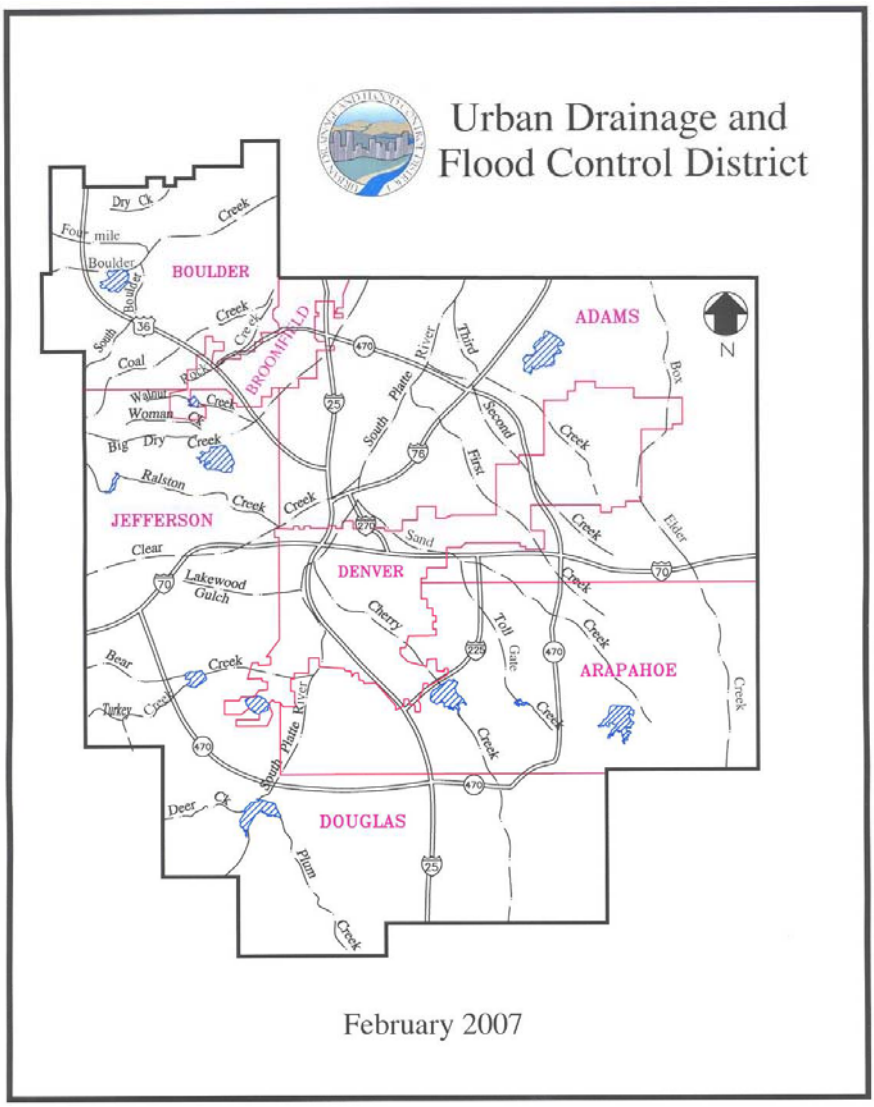

Figure 1-1: Map of the Urban Drainage and Flood Control District (UDFCD, 2008)

The need for this study arose from uncertainty in selecting appropriate design equations presented in the *USDCM* for the Type 13, 16, and R inlets. Local jurisdictions depicted in Figure

1-1 often require use of these three inlets. Methods presented in the *USDCM* for determining efficiency of grate and curb inlets were adopted from *HEC 22*, and do not include these three inlets. When the most similar inlets in the *USDCM* were selected for calculation purposes, uncertainties in sizing the inlets and in the level of flood protection afforded by them were realized. Uncertainty in design practice often leads to over-design and wasted expense. A need existed for greater accuracy in design for the three inlets tested in this study. Results of this research program will be used to supplement the *USDCM* design methodology.

Improving the accuracy of current design methods for the three inlets tested in this study requires addressing several deficiencies that exist in the procedures given in the *USDCM* (from *HEC 22*). Seven grate inlets are specified in *HEC 22* and some are similar to, but not exactly the same as, the Type 13 and 16 grates tested in this study. Subtle differences exist in the flow area and geometry of the grates. A second difference relates to the use of what is commonly referred to as a "combination inlet," a term used when a grate and a curb inlet are used together. Guidance provided in the *USDCM* is to ignore the curb inlet and determine efficiency based solely on the grate capacity. Some degree of conservatism is provided when determining efficiency in this manner, but performance of the combination inlet may be under-predicted when flow submerges the grate portion. A third difference relates to the curb inlet design used. The curb inlet specified in *HEC 22* is of a general type, with design parameters that do not fully describe the Type R curb inlet used by the UDFCD. Differences exist in the dimensions of the local inlet depression for the Type R curb inlet that are not considered in the *HEC 22* calculations. The Type R curb inlet depression is greater than what is described in *HEC 22* and capable of capturing some degree of additional flow. Lastly, typical design practices in the *USDCM* are based on the assumption of steady, uniform gutter flow. Hydraulics of street flow may or may not be uniform in any given situation, and the assumption of uniform flow may not be entirely valid. The relevance of uniform flow in analysis of the test data will be examined.

1.2 Research Objectives

A testing program was developed by the UDFCD to address known deficiencies in the *USDCM* design methods, and the primary purpose of this study was to collect data for further analysis by the UDFCD. After testing was completed, an analysis was performed to illustrate how current design methods given in the *USDCM* can be improved.

Objectives of this project were to:

- Construct a 1/3 scale model of a two-lane roadway with adjustable street slopes, gutter panels, and interchangeable inlet types.
- Collect data on total, captured, and bypassed flow for each inlet type, flow depth, and slope configuration.
- Determine efficiency for each test configuration as the ratio of captured flow to total input flow.
- Provide qualitative and quantitative interpretation of the performance of each configuration tested.
- Provide relevant analysis of the data to improve current design methods given in the *USDCM* for the inlets tested.

1.3 Report Organization

This report presents the project background and research objectives, literature review, description of the test facility and model fabrication, test data, analysis and results, and conclusions and recommendations. Included in each of the reports is a CD that contains the report Microsoft Word® (.doc) and Adobe® Acrobat® (.pdf) files, along with the Microsoft Excel® (.xls) analysis spreadsheet files. Also provided with this report is an Electronic Data Supplement (stored on a 16-GB SDHC™ card) that contains the CD contents and all test data and photographic documentation. Because only one SDHC™ card is provided and will not accompany each report, the reader is referred to the UDFCD for obtaining photographs and video documentation.

2 LITERATURE REVIEW

Urban storm drainage is an extensive topic that can range in scope from application of BMPs at a system level, to analysis of any given component in a large drainage network. Inlets tested in this study are used at the component level. The scope of this literature review is to provide background necessary for use of the collected test data in developing improved design methods. This chapter describes the model utilized to supply data for development of current UDFCD design methods for grate and curb inlets. Current design methods are explained and equations are presented from the *USDCM*. Two velocity-depth numerical relationships commonly known as Manning's equation and the Froude number are defined. The dimensional analysis method, which is commonly used for developing equations to predict observed test data, is explained.

2.1 Relevant Street Drainage Studies

HEC 22 was developed, in part, from a FHWA report titled "*Bicycle-safe Grate Inlets Study*." Ultimately, it was that FHWA study that provided data for development of the inlet equations provided in *HEC 22* and used in the *USDCM* for the Type 13 and 16 inlets. Volume 1 of the FHWA study titled "*Hydraulic and Safety Characteristics of Selected Grate Inlets on Continuous Grades*" (FHWA, 1977) describes the model built and the testing methods used. Table 2-1 provides a summary of physical characteristics of the FHWA model.

Table 2-1: Summary of FHWA model characteristics

Feature	FHWA
Scale (prototype : model)	1:1
Gutter section width (ft)	2
Street section width (ft)	6
Street section length (ft)	60
Approach section length (ft)	none
Curb height (ft)	none
Longitudinal slopes (%)	0.5 - 13
Cross slopes (%)	2 - 6.25
Maximum flow (cubic feet per second (cfs))	5.6
Manning's roughness	0.016 - 0.017
Surface material	3/4-in. PermaPly® (fiberglass)
Inflow control	vertical sluice gate
Inflow measurement	Orifice-Venturi meter
Outflow measurement	weir / J-hook gage
Flow type (uniform or non-uniform)	uniform
Inlet length (ft)	2 - 4
Gutter cross slope type	uniform
Maximum depth of flow (ft)	0.45

A total of eleven grate inlets were tested for structural integrity and bicycle-safety characteristics in the FHWA study. Of these, seven were tested hydraulically under the conditions given previously in Table 2-1. Efforts were made to separately measure frontal-captured flow and side-captured flow by blocking-off portions of the inlet opening. Grate efficiency was defined as the ratio of captured flow to total street flow. Flow into the model was from a large headbox reservoir. The vertical sluice gate was used to provide flow control from the headbox at the upstream end of the road section, and to ensure uniform flow conditions in the model. A total of 1,680 tests were carried out at the U. S. Bureau of Reclamation (USBR) Hydraulic Laboratory. Several of the qualitative findings are summarized here:

- Grates with wide longitudinal bar spacing were found to perform the best.
- For a given width of flow spread, grates were most efficient at flatter slopes.
- For a constant gutter flow and cross slope, grate efficiency increased as longitudinal slope was increased.
- Longer grates reached higher efficiencies at steeper slopes than shorter grates.
- Velocity is the factor that determined the most efficient longitudinal slope.
- At test conditions where splash carried completely across one or more of the grate designs, differences in efficiency were caused mostly by the grate type.

- All grates showed patterns of increasing efficiency with increased flow and longitudinal slope until the increased velocity caused splashing completely across the grate.

2.2 UDFCD Methods for Determining Inlet Efficiency

Calculations presented in this section are summarized from the *USDCM* for determination of the hydraulic efficiency of grate inlets, combination inlets, and curb inlets in the on-grade configuration. Presented in Figure 2-1 is an illustration of the grate, combination, and curb inlets. The on-grade configuration of inlet design is defined as a condition where a portion of the total flow on a road section is captured by the inlet, and the remainder bypasses the inlet and continues on to the next inlet. Several parameters related to the nature of street flow are determined from the street geometry in the on-grade configuration. For any of the inlet types shown in Figure 2-1, inlet efficiency can be determined using several calculations based on the inlet type and flow conditions in the street.

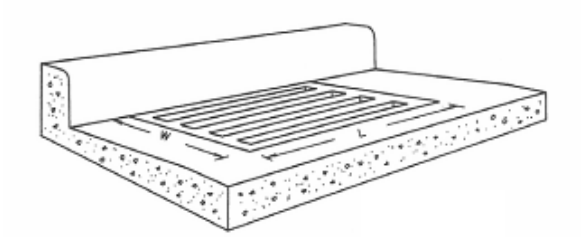

(a) grate inlet

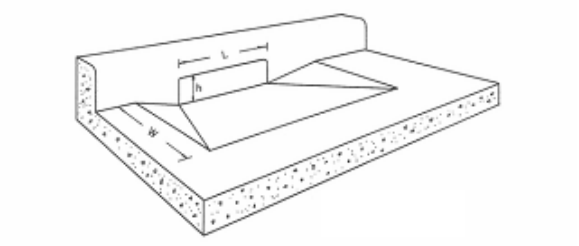

(b) curb opening inlet

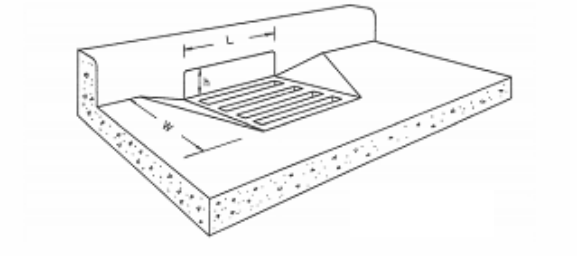

(c) combination inlet

Figure 2-1: Inlet types (UDFCD, 2008)

2.2.1 On-grade Conditions

On-grade configurations typically result in less than 100% capture of street flow at any given inlet location. In design practice, inlets are grouped and spaced to maintain an acceptable flow depth in the gutter and spread of water on the street (UDFCD, 2008). Efficiency of any single inlet group is defined as the ratio of captured flow to total flow. A composite gutter cross slopes is defined as a configuration where the gutter cross slope differs from the street cross slope, and is shown in Figure 2-2 with applicable dimensions given in Table 2-2. Calculations summarized in this section are specific to gutters with composite cross slopes used in the on-grade configuration.

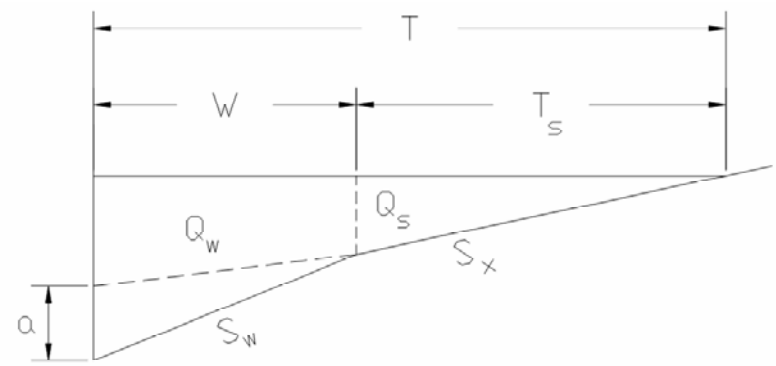

Figure 2-2: Typical gutter section with composite cross slope (UDFCD, 2008)

Table 2-2: Composite gutter dimensions (modified from UDFCD (2008))

Variable	Description
a	gutter depression (ft)
Q_s	discharge in street section (cfs)
Q_w	discharge in depressed section of gutter (cfs)
S_w	gutter cross slope (ft/ft)
S_x	street cross slope (ft/ft)
T	top width of flow (spread) (ft)
T_s	spread of flow in street (ft)
W	width of gutter pan (ft)

Total flow is divided into flow in the depressed section of the gutter (Q_w) and flow on the street section (Q_s), and is defined by Equation 2-1. Frontal flow is the portion of the flow that approaches directly in line with the width of the grate, and side flow occurs outside of the grate width:

$$Q = Q_w + Q_s \qquad \textbf{Equation 2-1}$$

where:

Q = volumetric flow rate (cfs);
Q_w = flow rate in the depressed section of the gutter (cfs); and
Q_s = flow rate in the section above the depressed section (cfs).

Theoretical total flow rate in a composite gutter section can be computed using Equation 2-2:

$$Q = \frac{Q_s}{1 - E_o} \qquad \textbf{Equation 2-2}$$

where:

Q = theoretical volumetric flow rate (cfs);
Q_s = flow rate in the section above the depressed section (cfs); and
E_o = ratio of flow in the depressed section of the gutter to the total gutter flow (and is defined below).

The ratio of flow in the depressed section of the gutter to the total gutter flow (E_o) can be found from Equation 2-3:

$$E_o = \frac{1}{1 + \dfrac{S_w / S_x}{\left[1 + \dfrac{S_w / S_x}{(T/W) - 1}\right]^{8/3} - 1}} \qquad \textbf{Equation 2-3}$$

where:

S_w = gutter cross slope (ft/ft) (and is defined below);
S_x = street cross slope (ft/ft);
W = width of the gutter section (ft); and
T = total width of flow (ft).

Gutter cross slope is defined from Equation 2-4:

$$S_w = S_x + \frac{a}{W} \qquad \textbf{Equation 2-4}$$

where:

S_w = gutter cross slope (ft/ft);
S_x = street cross slope (ft/ft);
a = gutter depression relative to the street cross slope (ft); and
W = width of the gutter (ft).

Equation 2-5 and Equation 2-6 can be derived from the gutter geometry presented previously in Figure 2-2:

$$y = a + TS_x \qquad \textbf{Equation 2-5}$$

and

$$A = \frac{1}{2} S_x T^2 + \frac{1}{2} aW \qquad \textbf{Equation 2-6}$$

where:

A = cross-sectional flow area (ft^2);
T = total width of flow (ft);
S_x = street cross slope (ft/ft);
W = width of the gutter (ft);
a = gutter depression relative to the street cross slope (ft); and
y = depth of flow in the depressed gutter section (ft).

From Equation 2-1 through 2-6, gutter flow, street flow, and the depth and spread of flow on the street can be determined. With these quantities known, inlet efficiency can be determined for grate and curb inlets as described in the following sections.

2.2.2 Grate Inlets

Grate inlet efficiency is governed by the grate length and width, and is reduced when width of flow is greater than the grate width, or the flow has sufficient velocity to splash over the inlet. Table 2-3 describes the grates given in the *USDCM* and corresponding schematics are provided in Appendix A. Determination of grate inlet efficiency as presented in the *USDCM* requires that total gutter flow be separated into frontal flow (Q_w) and side flow (Q_s), which were defined previously. Side flow can be found from Equation 2-2 and from Equation 2-1 the frontal flow can be determined.

Table 2-3: Grate nomenclature and descriptions

Inlet Name	Description
Bar P-1-7/8	parallel bar grate with bar spacing 1-7/8 in. on center
Bar P-1-7/8-4	parallel bar grate with bar spacing 1-7/8 in. on center and 3/8-in. diameter lateral rods spaced at 4 in. on center
Bar P-1-1/8	parallel bar grate with 1-1/8 in. on center bar spacing
Vane Grate	curved vane grate with 3-1/4 in. longitudinal bar and 4-1/4 in. transverse bar spacing
45° Bar	45°-tilt bar grate with 3-1/4 in. longitudinal bar and 4-in. transverse bar spacing on center
30° Bar	30°-tilt bar grate with 3-1/4 in. longitudinal bar and 4-in. transverse bar spacing on center
Reticuline	"honeycomb" pattern of lateral bars and longitudinal bearing bars

The ratio of frontal flow captured by the inlet to the total frontal flow (R_f) can be expressed by Equation 2-7:

$$R_f = Q_{wi} / Q_w = 1.0 - 0.09(V - V_o) \qquad \textbf{Equation 2-7}$$

where:

R_f = ratio of frontal flow captured to total frontal flow;
Q_w = flow rate in the depressed section of the gutter (cfs);
Q_{wi} = frontal flow intercepted by the inlet (cfs);
V = velocity of flow at the inlet (ft/s) determined from Q/A; and
V_o = splash-over velocity (ft/s).

The relationship given in Equation 2-7 is only valid for splash-over velocity (V_o) less than cross-sectional averaged velocity (V), otherwise $R_f = 1$ and all frontal flow is captured by the grate. Splash-over velocity is defined as the minimum velocity causing some frontal flow to escape capture by the grate, and may be defined by Equation 2-8:

$$V_o = \alpha + \beta L_e - \gamma L_e^2 + \eta L_e^3 \qquad \textbf{Equation 2-8}$$

where:

V_o = splash-over velocity (ft/s);
L_e = effective length of grate (ft); and
α,β,γ,η = constants from Table 2-4.

Constants in Equation 2-8 are associated with specific grates listed in Table 2-4.

Table 2-4: Splash-over velocity constants for inlet grates (UDFCD, 2008)

Type of Grate	α	β	γ	η
Bar P-1-7/8	2.22	4.03	0.65	0.06
Bar P-1-1/8	1.76	3.12	0.45	0.03
Vane Grate	0.30	4.85	1.31	0.15
45º Bar	0.99	2.64	0.36	0.03
Bar P-1-7/8-4	0.74	2.44	0.27	0.02
30º Bar	0.51	2.34	0.20	0.01
Reticuline	0.28	2.28	0.18	0.01

The ratio of side flow captured to total side flow approaching the grate can be determined using Equation 2-9:

$$R_s = \frac{1}{1 + \frac{0.15V^{1.8}}{S_x L^{2.3}}}$$ **Equation 2-9**

where:

R_s = ratio of side flow captured to total side flow;
S_x = side slope;
L = length of grate (ft); and
V = velocity of flow in the gutter (ft/s).

Capture efficiency of a grate inlet may be determined using Equation 2-10, which uses the parameters determined previously:

$$E = R_f\left(\frac{Q_w}{Q}\right) + R_s\left(\frac{Q_s}{Q}\right)$$ **Equation 2-10**

where:

E = grate inlet efficiency;
R_s = ratio of side flow captured to total side flow;
R_f = ratio of frontal flow captured to total frontal flow;
Q = volumetric flow rate (cfs);
Q_w = flow rate in the depressed section of the gutter (cfs); and
Q_s = flow rate in the section above the depressed section (cfs).

Efficiency for combination inlets is typically determined by only considering the grate when the curb opening and grate are of equal length (UDFCD, 2008), and Equation 2-10 is used.

2.2.3 Curb Opening Inlets

Curb opening inlets can be located in either depressed or not depressed gutters. Depressed gutters are defined as a configuration in which the invert of the curb inlet is lower than the bottom of the gutter flow line. Various curb inlet types used by the UDFCD are shown in Figure 2-3. Type R curb inlets are used alone; the curb inlet used with the combination inlet typically has a grate component (UDFCD, 2008). Calculations presented in this section apply to the Type R curb inlet only, because the grate portion of a combination inlet typically diverts flow away from the curb inlet.

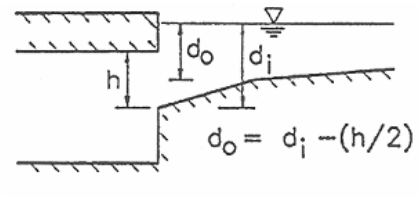

(a) horizontal throat

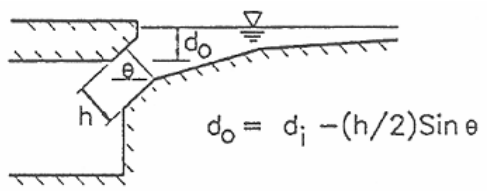

(b) inclined throat

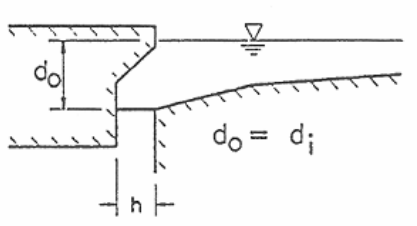

(c) vertical throat

Figure 2-3: Curb inlet openings types (UDFCD, 2008)

Efficiency (E) of curb inlets is primarily a function of the curb opening length. Equation 2-11 is used for determining the efficiency of the Type R curb inlets:

$$E = 1 - \left[1 - \left(L/L_T\right)\right]^{1.8} \qquad \textbf{Equation 2-11}$$

where:

L = curb opening length in the direction of flow (ft); and
L_T = curb opening length required to capture 100% of gutter flow.

Equation 2-11 is valid for a curb opening length (L) less than the length required for 100% flow capture (L_T), otherwise the efficiency (E) is equal to one. The parameter L_T is a

function of street characteristics and the storm-water discharge in the street. For an inlet located in a gutter that is not depressed relative to the street slope, Equation 2-12 applies:

$$L_T = 0.6Q^{0.42}S_L^{0.3}\left(\frac{1}{nS_x}\right)^{0.6} \qquad \textbf{Equation 2-12}$$

where:

Q = gutter flow (cfs);
S_L = longitudinal street slope (ft/ft);
S_x = street cross slope (ft/ft); and
n = Manning's roughness coefficient.

For an inlet that is depressed relative to the street slope, Equation 2-13 applies:

$$L_T = 0.6Q^{0.42}S_L^{0.3}\left(\frac{1}{nS_e}\right)^{0.6} \qquad \textbf{Equation 2-13}$$

where:

L_T = curb opening length required to capture 100% of gutter flow;
Q = gutter flow (cfs);
S_L = longitudinal street slope (ft/ft);
S_e = equivalent street cross slope (ft/ft); and
n = Manning's roughness coefficient.

The equivalent street cross slope (S_e) required for Equation 2-13 is determined from Equation 2-14:

$$S_e = S_x + \frac{a}{W}E_o \qquad \textbf{Equation 2-14}$$

where:

S_x = street cross slope (ft/ft);
a = gutter depression (ft);
W = depressed gutter section width (ft), illustrated in Figure 2-2; and
E_o can be found using Equation 2-3.

Once the parameter L_T has been determined, efficiency of the curb inlet may be calculated using Equation 2-11.

2.3 Manning's Equation

Uniform flow is a state of open-channel flow that occurs when accelerating and decelerating forces acting on the flow are equal (Chaudhry, 2008). In this state, the channel itself exerts hydraulic control over the flow. Often, uniform flow occurs in long and straight prismatic channels that do not vary in bottom slope or cross-sectional character with distance. Flow depth corresponding to uniform flow is called normal depth. The numerical relationship of Manning's equation commonly used to describe uniform flow is provided as Equation 2-15. Known channel geometry, flow depth, roughness, and bottom slope can be used in Manning's equation to solve for flow velocity. Alternatively, surface roughness can be solved for. The friction slope (S_f) term in Manning's equation represents the rate of energy dissipation caused by frictional forces acting along the channel perimeter. When a state of uniform flow exists, the friction slope is equal to the bottom slope of the channel (S_o). Manning's equation is then simplified by assuming that S_f is equal to S_o. Conversely, Manning's equation can provide an explicit solution for the friction slope when uniform flow does not exist:

$$V = \frac{\Phi}{n} R^{2/3} S_f^{1/2} \qquad \textbf{Equation 2-15}$$

where:

V = cross-sectional averaged flow velocity (ft/s);
Φ = unit conversion constant, equal to 1.49 for U. S. Customary and 1.00 for SI;
R = hydraulic radius (ft), which is a function on depth;
S_f = friction slope; and
n = Manning's roughness coefficient.

2.4 Froude Number

In open-channel flow, where gravity is the driving force, the Froude number represents the ratio of inertial to gravity forces (Chaudhry, 2008). Stated another way, it is the ratio of bulk flow velocity to elementary gravity wave celerity. The Froude number (Fr) is defined as Equation 2-16:

$$Fr = \frac{\overline{V}}{\sqrt{gD}} \qquad \textbf{Equation 2-16}$$

where:

$\overline{V}$ = cross-sectional average flow velocity (ft/s);
g = acceleration due to gravity (ft/s^2); and
D = hydraulic depth (ft), equal to area (A) divided by top width (T) for a general cross section or depth (h) for a rectangular cross section.

The celerity of an elementary gravity wave is defined as the velocity with which the wave travels relative to the bulk flow velocity (Chaudhry, 2008). When the Froude number is greater than one, for flow velocity greater than wave celerity, a disturbance in the flow can only propagate in the direction of flow. This type of flow is commonly classified as supercritical. When the Froude number is less than one, for flow velocity less than wave celerity, a disturbance in the flow can propagate either upstream of downstream. This type of flow is commonly classified as subcritical.

2.5 Dimensional Analysis

Development of equations by the process of dimensional analysis requires identifying and utilizing parameters that are significant in describing the process or phenomena in question. A survey of parameter groups identified as significant in determining inlet efficiency is presented in this section. Many phenomena in fluid mechanics depend, in a complex way, on geometric and flow parameters (Fox, 2006). For open-channel street flow, such parameters are associated with the geometry of the street and gutter sections, and the flow velocity. Through the process of dimensional analysis, significant parameters are combined to produce dimensionless quantities that are descriptive of the phenomena in question. One approach to developing equations is to collect experimental data on these dimensionless quantities and fit a mathematical model to them.

The Buckingham Pi theorem is a method for determining dimensionless groups that consist of parameters identified as significant. The theorem is a statement of the relation between a function expressed in terms of dimensional parameters and a related function expressed in terms of non-dimensional parameters (Fox, 2006). Given a physical problem in which the dependent parameter is a function of n-1 independent parameters, the relationship among the variables can be expressed in functional form as Equation 2-17:

$$q_1 = f(q_2, q_3, ..., q_n) \quad \text{or} \quad g(q_1, q_2, ..., q_n) = 0 \qquad \textbf{Equation 2-17}$$

where:

q_1 = dependent parameter;
$q_2 \ldots q_n$ = n-1 independent parameters;
f = function relating dimensional analysis parameters q; and
g = unspecified function different from f.

The Buckingham Pi theorem states that, given a relation among n parameters in the form of Equation 2-17, the n parameters may be grouped into n-m independent dimensionless ratios also called Pi (Π) groups (Fox, 2006). In functional form this is expressed as Equation 2-18:

$$\Pi_1 = G_1(\Pi_2, \Pi_3, ..., \Pi_{n-m}) \text{ or } G(\Pi_1, \Pi_2, ..., \Pi_{n-m}) = 0 \qquad \textbf{Equation 2-18}$$

where:

Π = Pi parameter; and
G = function relating the dimensionless Pi parameters, related to the function f.

The number m is often, but not always, equal to the number of dimensions required to specify the dimensions of all the parameters (q_i) of the problem or phenomena in question. The n-m dimensionless Pi parameters obtained from this procedure are independent of one another. The Buckingham Pi theorem does not predict the functional form of G, which must be determined experimentally.

2.6 Significant Parameter Groups for Calculating Inlet Efficiency

A review of available literature has shown that the complex nature of street inlet flow has precluded the development of purely theoretical equations. Often the approach of developing empirical equations has been used. Physical variables related to gutter flow and inlet characteristics are typically identified and combined into meaningful parameter groups using dimensional analysis. Tests are performed on parameter groups to quantify their relevance. Although the method of dimensional analysis is universally applicable to development of parameter groups, there are many forms that these dimensionless groups may take depending upon what parameters are used. Two of the larger studies conducted on the topic of inlet efficiency were the FHWA study on bicycle-safe grate inlets described previously (FHWA, 1977) and a study completed at The Johns Hopkins University (Li, 1956). Equations developed from the FHWA study were incorporated into *HEC 22* and were presented previously. The Johns Hopkins University study took a slightly different approach of regression analysis. For an

un-depressed grate inlet with longitudinal bars, the following parameter groups in Equation 2-19 were identified:

$$\frac{L_0}{V_0}\sqrt{\frac{g}{y_0}} = f\left(\frac{V_0}{\sqrt{gy_0}}, \frac{a}{b}, \frac{y_0}{a}\right) \qquad \textbf{Equation 2-19}$$

where:

L_0 = length required to trap the central portion of gutter flow;
V_0 = velocity of approaching flow;
y_0 = depth of flow over the first opening;
g = unspecified function different from f;
a = width of openings between bars; and
b = width of bars.

For a depressed curb inlet, the following parameter groups in Equation 2-20 were identified:

$$\frac{Q}{Ly\sqrt{gy}} = f\left(\frac{V^2}{gy}, \frac{L}{a}, \theta, \frac{L_2}{a}, \frac{q}{Q_0}\right) \qquad \textbf{Equation 2-20}$$

where:

Q = captured flow;
Q_0 = total flow;
θ = angle formed by the curb and gutter;
L = length of the curb opening;
L_2 = length of the downstream slope transition;
V = velocity of approaching flow;
y = depth of flow in the gutter;
g = acceleration due to gravity;
a = local inlet depression; and
q = flow bypassing the inlet.

For both of these inlets, the Froude number appears as a parameter group, as do several length and flow ratios.

In a study performed at the Istanbul Technical University (Uyumaz, 2002), several parameter groups were identified in Equation 2-21 for a depressed curb opening inlet in a gutter with uniform cross section (for a uniform gutter cross section, the gutter slope is equal to the street cross slope):

$$Q_w = f\left(\frac{L}{FT}, \frac{L}{h}, \frac{Q_w}{Q}\right) \qquad \textbf{Equation 2-21}$$

where:

Q = total flow;
Q_w = captured flow;
L = inlet length;
F = Froude number;
T = top width of gutter flow; and
h = depth of flow in the gutter.

For this inlet, the Froude number appears in the first parameter group, and ratios of lengths and flows are used. The flow ratio used is typically called the inlet efficiency or capture efficiency.

2.7 Summary

Currently-accepted design procedures, which represent the state-of-the-art for inlet design from the UDFCD, were explained for each inlet used in this study. *USDCM* methods (which originated in *HEC 22*) are based upon theoretical parameters which must be determined from empirical relationships. The FHWA model, which provided data for development of *HEC 22* methods, was described. In addition, Manning's equation and the Froude number were each defined as unique velocity-depth relationships. The process of dimensional analysis was explained as a commonly-used method for developing significant parameter groups that can be used in equation development. A survey of parameter groups identified as significant in determining inlet efficiency was conducted. Empirical equations have been used for determining the capacity of curb and grate inlets for composite gutter sections (in which the gutter cross slope does not equal the street cross slope). Most of the available research has been on gutters with uniform cross slopes. For gutters of uniform cross slope, Manning's equation for a triangular cross section is frequently used for determining flow. Relationships exist for determining either curb or grate inlet capacity. Few relationships exist for combination inlets; they are typically treated as only a grate inlet. This is due to the observation that, when the grate is not depressed below the gutter flow line, little or no gain in performance results from the grate. A need exists for design equations, based on physically relevant and easy to determine parameters, which address use of combination inlets with the grate depressed below the gutter flow line.

3 HYDRAULIC MODELING

Testing was performed on three different types of curb and grate inlet from January 2006 through November 2008. Emphasis was placed on collection of curb depth and flow data to facilitate completion of research objectives. Two basic street drainage conditions were tested in this study for a total of 318 tests. First was a sump condition, in which all of the street flow was captured by the inlets. Second was an on-grade condition, in which only a portion of the total street flow was captured and the rest of the flow bypassed the inlets. All three inlets (Type 13, Type 16, and Type R) were tested in the sump and on-grade conditions at three depths. With development of the model and testing program for this study, there was an opportunity to improve upon the FHWA model. This chapter provides details of the testing facility, conditions tested, model construction, and testing methods used in obtaining data.

3.1 Testing Facility Description and Model Scaling

Model construction and testing was performed at the ERC of Colorado State University. A photograph of the flume, pipe network, and drainage facilities is presented in Figure 3-1. The model consisted of a headbox to supply water, a flume section containing the street and inlets, supporting pumps, piping, several flow-measurement devices, a tailbox to capture returning flow, and the supporting superstructure.

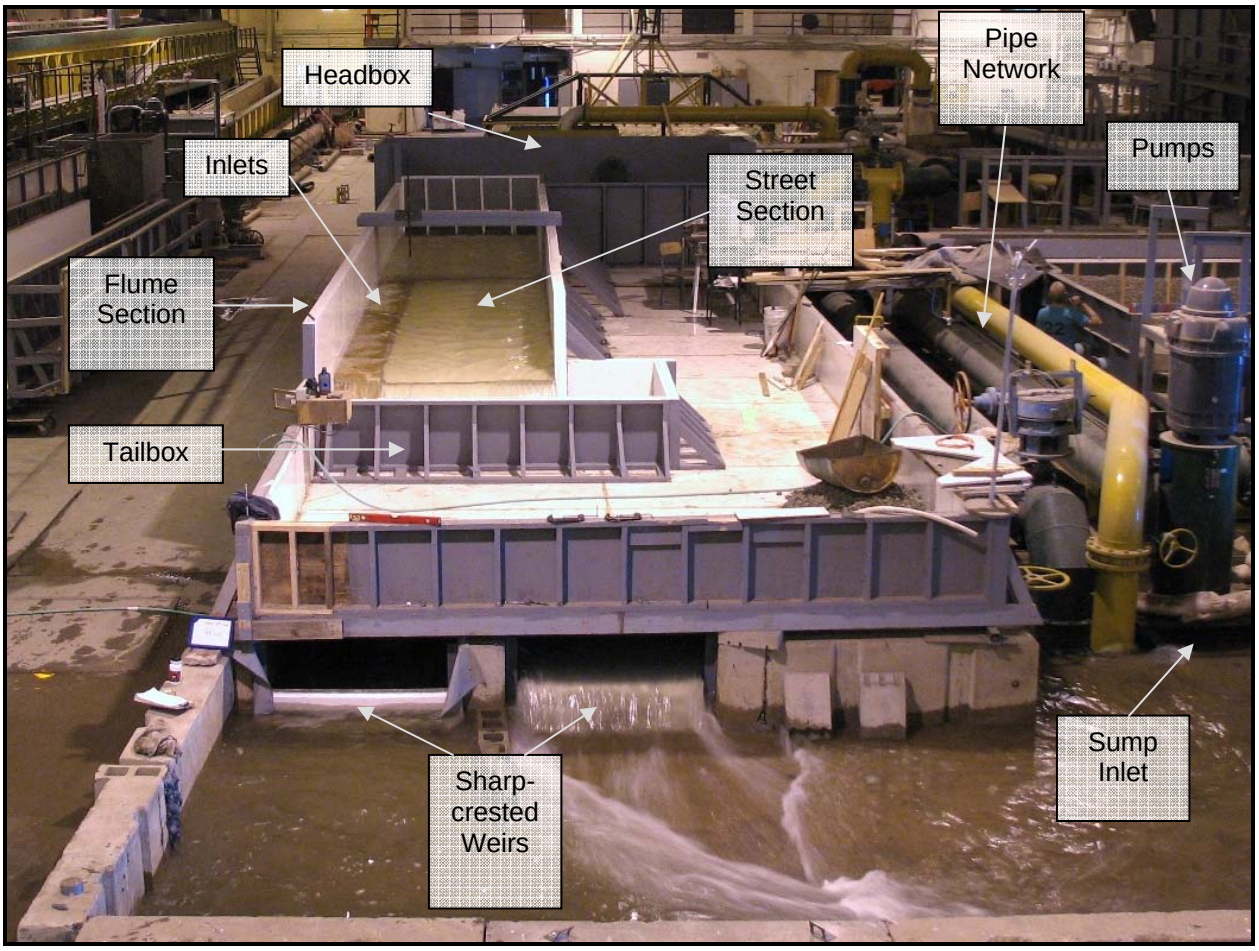

Figure 3-1: Photograph of model layout

Contained within the flume section were the model's road surface and all curb and inlet components. Sufficient laboratory space allowed for construction of a two-lane street surface. A cross section of the flume including the street section, gutter panel, and sidewalk is presented in Figure 3-2. The street section was constructed as a 2-by-4 in. tubular steel framework and decked with 1/8-in. thick sheet steel. Slope adjustment was achieved by the use of eight scissor jacks placed under the street section, and adjustment ranged from 0.5% to 4% longitudinally and from 1% to 2% laterally. Upstream of the street section, an approach section was constructed to allow flow to stabilize after exiting the headbox. A diffuser screen was installed at the junction between the headbox and the approach section to minimize turbulence and to distribute flow evenly across the width of the model. The long horizontal approach section provided stabilized flow. Prototype dimensions and characteristics are presented in Table 3-1, which can be directly compared to Table 2-1 for the FHWA model. The physical model used provided a broader range

of test conditions likely to be encountered in the field. Primary advantages include the two-lane road section, higher flow capacity afforded by a scaled model, a composite gutter cross slope, greater inlet length, greater depth of flow, and the curb component. A composite gutter cross slope is one in which the street cross slope does not equal the gutter cross slope, and provides higher gutter flows (UDFCD, 2008).

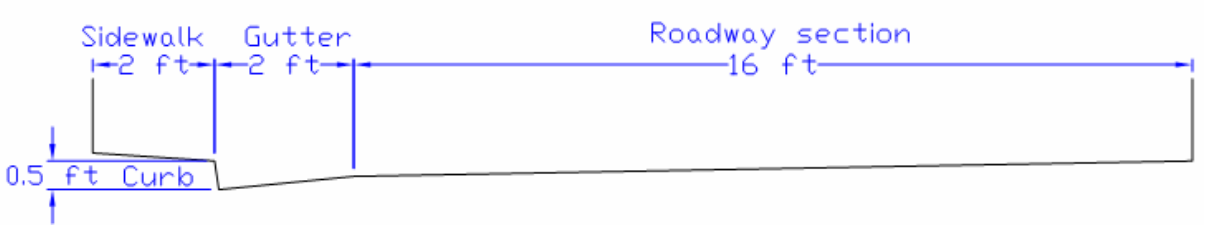

Figure 3-2: Flume cross-section sketch (prototype scale)

Table 3-1: Prototype dimensions

Feature	Prototype design
Scale (prototype : model)	3:1
Gutter section width (ft)	2
Street section width (ft)	16
Street section length (ft)	63
Approach section length (ft)	42
Curb height (ft)	0.5
Longitudinal slopes (%)	0.5 - 4
Cross slopes (%)	1 - 2
Maximum flow (cfs)	Over 100
Manning's roughness	0.015
Surface material	1/80-in. steel plate
Inflow control	butterfly valve / diffuser screen
Inflow measurement	electro-magnetic flow meter or differential pressure meter
Outflow measurement	weir / point gage
Flow type (uniform or non-uniform)	varies
Inlet length (ft)	3.3 - 9.9
Gutter cross slope type	composite
Maximum depth of flow (ft)	1

Use of an exact Froude-scale model was chosen for this study. Table 3-2 provides scaling ratios used in the model. An exact scale model is well suited for modeling flow near hydraulic structures, and the x-y-z length-scale ratios are all equal (Julien, 2002). The length scaling ratio was determined to be 3 to 1 (prototype : model) based on available laboratory space and pump

capacity. A similar study performed at The Johns Hopkins University identified the minimum reliable scale to be 3 to 1 based on correlation of laboratory and field test data (Li, 1956).

Table 3-2: Scaling ratios for geometry, kinematics, and dynamics

Geometry	Scale Ratios
Length, width, and depth (L_r)	3.00
All slopes	1.00
Kinematics	**Scale Ratios**
Velocity (V_r)	1.73
Discharge (Q_r)	15.62
Dynamics	**Scale Ratios**
Fluid density	1.00
Manning's roughness (n_r)	1.20

An analysis of Manning's roughness coefficient was conducted for the model street section to create a surface with the scaled roughness of asphalt. An average friction slope over the range of expected flows was used with Manning's equation to calculate the roughness value. Figure 3-3 presents the results of testing the painted street surface. Roughness was established by adding coarse sand to industrial enamel paint (at about 15% by weight), and painting the street section. Subsequent tests showed that, for anticipated flows, the roughness was within the acceptable range for asphalt. An average value of 0.013 was determined for the model, which corresponds to a prototype value of 0.015 (the mean value for asphalt).

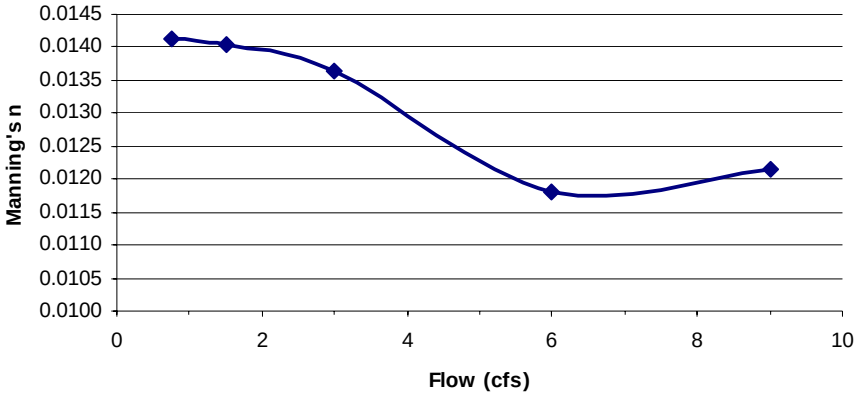

Figure 3-3: Manning's roughness for the model-scale street section at expected flows

3.2 Conditions Tested

A test matrix was developed to organize the variation of parameters through three inlet types, two lateral slopes, four longitudinal slopes, three flow depths, and several inlet lengths. Type 13 and 16 combination inlets were configured to 3.3-, 6.6-, and 9.9-ft prototype lengths. Type R curb inlets were configured to 5-, 9-, 12-, and 15-ft prototype lengths. Required flow depths were provided by the UDFCD and consisted of 0.33-, 0.5-, and 1-ft depths at the prototype scale. Rationale for selection of these depths was based on curb height. A depth of 0.33 ft is below a standard 0.5-ft curb, a depth of 0.5 ft is at the curb height, and a depth of 1 ft is above the standard 0.5-ft curb. A total of 318 independent tests resulted from variation of these parameters, and each test matrix is presented in Table 3-3 through Table 3-6 by depth of flow. At the request of the UDFCD, twelve additional sump tests and twenty additional debris tests were performed beyond the original 286 tests. Additional debris tests were performed at 4% longitudinal and 1% cross slope to provide data for combination inlets of varying lengths. They were performed for type 1 (flat – 50% coverage) and type 2 (3d – 25% coverage) debris. Additional sump condition tests were performed to provide two additional depths for the Type 13 and 16 combination inlets. Table 3-6 provides a list of these additional sump tests. Tabular versions of each test matrix were developed with test identification (ID) numbers for organizing the results and are presented in Appendices B and C. In the tabular version, each unique slope and inlet configuration was given an ID number (1 through 286), with additional sump tests AT1 through AT12 and additional debris tests AT287 through AT305. Each inlet was tested under two basic conditions. First was the sump condition, where the inlet was placed such that all the flow was captured and none of the flow was bypassed. Roadway cross slope was a constant 1% with no longitudinal slope. Second was an on-grade condition, where some of the flow was captured by the inlets and the remainder was bypassed off the road section. Both the longitudinal and cross slope were varied for the on-grade condition, for a total of six slope configurations ranging from 0.5% to 4% longitudinal and 1% to 2% lateral.

Table 3-3: Test matrix for 0.33-ft prototype flow depth

	Flow Depth = 0.33 ft							
	SUMP TEST	ON-GRADE TEST						
Longitudinal Slope	**0.00%**	**0.50%**	**0.50%**	**2.00%**	**2.00%**	**4.00%**	**4.00%**	
Cross Slope	**1.00%**	**1.00%**	**2.00%**	**1.00%**	**2.00%**	**1.00%**	**2.00%**	**TOTAL:**
Single No. 13	1	1	1	1	1	1	1	7
Single No. 13 - Debris Test One			1		1		1	3
Single No. 13 - Debris Test Two			1		1	1	1	4
Double No. 13 - Debris Test One						1		1
Double No. 13 - Debris Test Two						1		1
Triple No. 13 - Debris Test One						1		1
Triple No. 13 - Debris Test Two						1		1
Double No. 13	1	1	1	1	1	1	1	7
Triple No. 13	1	1	1	1	1	1	1	7
Single No. 16	1	1	1	1	1	1	1	7
Single No. 16 - Debris Test One			1		1	1	1	4
Single No. 16 - Debris Test Two			1		1		1	3
Double No. 16 - Debris Test One						1		1
Double No. 16 - Debris Test Two						1		1
Triple No. 16 - Debris Test One						1		1
Triple No. 16 - Debris Test Two						1		1
Double No. 16	1	1	1	1	1	1	1	7
Triple No. 16	1	1	1	1	1	1	1	7
5-ft Type R (R5)	1	1	1	1	1	1	1	7
9-ft Type R (R9)	1	1	1	1	1	1	1	7
12-ft Type R (R12)	1	1	1	1	1	1	1	7
15-ft Type R (R15)	1	1	1	1	1	1	1	7
TOTAL:	10	10	14	10	14	20	14	92

No. 13 – Type 13; No. 16 – Type 16

Table 3-4: Test matrix for 0.5-ft prototype flow depth

	Flow Depth = 0.5 ft							
	SUMP TEST	ON-GRADE TEST						
Longitudinal Slope	**0.00%**	**0.50%**	**0.50%**	**2.00%**	**2.00%**	**4.00%**	**4.00%**	
Cross Slope	**1.00%**	**1.00%**	**2.00%**	**1.00%**	**2.00%**	**1.00%**	**2.00%**	**TOTAL:**
Single No. 13	1	1	1	1	1	1	1	7
Single No. 13 - Debris Test One			1		1		1	3
Single No. 13 - Debris Test Two			1		1	1	1	4
Double No. 13 - Debris Test One						1		1
Double No. 13 - Debris Test Two						1		1
Triple No. 13 - Debris Test One						1		1
Triple No. 13 - Debris Test Two						1		1
Single No. 13 - Curb Opening Only	1		1		1		1	4
Single No. 13 - Grate Only	1		1		1		1	4
Single No. 13 - Grate & 4-in. Curb Opening	1		1		1		1	4
Double No. 13	1	1	1	1	1	1	1	7
Triple No. 13	1	1	1	1	1	1	1	7
Single No. 16	1	1	1	1	1	1	1	7
Single No. 16 - Debris Test One			1		1	1	1	4
Single No. 16 - Debris Test Two			1		1		1	3
Double No. 16 - Debris Test One						1		1
Double No. 16 - Debris Test Two						1		1
Triple No. 16 - Debris Test One						1		1
Triple No. 16 - Debris Test Two						1		1
Single No. 16 - Grate Only	1		1		1		1	4
Single No. 16 - Grate & 4-in. Curb Opening	1		1		1		1	4
Double No. 16	1	1	1	1	1	1	1	7
Triple No. 16	1	1	1	1	1	1	1	7
5-ft Type R (R5)	1	1	1	1	1	1	1	7
5-ft Type R (R5) - Horizontal Safety Bar	1		1		1		1	4
5-ft Type R (R5) - 4-in. Curb Opening	1		1		1		1	4
9-ft Type R (R9)	1	1	1	1	1	1	1	7
12-ft Type R (R12)	1	1	1	1	1	1	1	7
15-ft Type R (R15)	1	1	1	1	1	1	1	7
TOTAL:	17	10	21	10	21	20	21	120

No. 13 – Type 13; No. 16 – Type 16

Table 3-5: Test matrix for 1-ft prototype flow depth

	Flow Depth = 1 ft							
	SUMP TEST	ON GRADE TEST						
Longitudinal Slope	**0.00%**	**0.50%**	**0.50%**	**2.00%**	**2.00%**	**4.00%**	**4.00%**	
Cross Slope	**1.00%**	**1.00%**	**2.00%**	**1.00%**	**2.00%**	**1.00%**	**2.00%**	**TOTAL:**
Single No. 13	1	1	1	1	1	1	1	7
Single No. 13 - Curb Opening Only	1		1		1		1	4
Single No. 13 - Grate Only	1		1		1		1	4
Single No. 13 - Grate & 4-in. Curb Opening	1		1		1		1	4
Double No. 13	1	1	1	1	1	1	1	7
Triple No. 13	1	1	1	1	1	1	1	7
Single No. 16	1	1	1	1	1	1	1	7
Single No. 16 - Grate Only	1		1		1		1	4
Single No. 16 - Grate & 4-in. Curb Opening	1		1		1		1	4
Double No. 16	1	1	1	1	1	1	1	7
Triple No. 16	1	1	1	1	1	1	1	7
5-ft Type R	1	1	1	1	1	1	1	7
5-ft Type R - 4-in. Curb Opening	1		1		1		1	4
9-ft Type R	1	1	1	1	1	1	1	7
12-ft Type R	1	1	1	1	1	1	1	7
15-ft Type R	1	1	1	1	1	1	1	7
TOTAL:	16	10	16	10	16	10	16	94

No. 13 – Type 13; No. 16 – Type 16

Table 3-6: Additional sump tests (prototype scale)

	Flow Depth = 0.75 ft	Flow Depth = 1.5 ft	
Longitudinal Slope	**0.00%**	**0.00%**	
Cross Slope	**1.00%**	**1.00%**	**TOTAL:**
Single No. 13	1	1	2
Double No. 13	1	1	2
Triple No. 13	1	1	2
Single No. 16	1	1	2
Double No. 16	1	1	2
Triple No. 16	1	1	2
TOTAL:	6	6	12

No. 13 – Type 13; No. 16 – Type 16

3.3 Inlet Construction

Curb and gutter sections were fabricated from 1/8-in. thick sheet metal, and construction is shown in Figure 3-4 and Figure 3-5. Removable gutter sections for both the Type R curb inlet and the Type 13 and 16 combination inlets allowed the inlet length to be adjusted. Modular

construction methods were utilized to facilitate exchanging curb inlets with combination inlets, which simplified reconfiguration of the model. Construction drawings of each inlet type are presented in Appendix D.

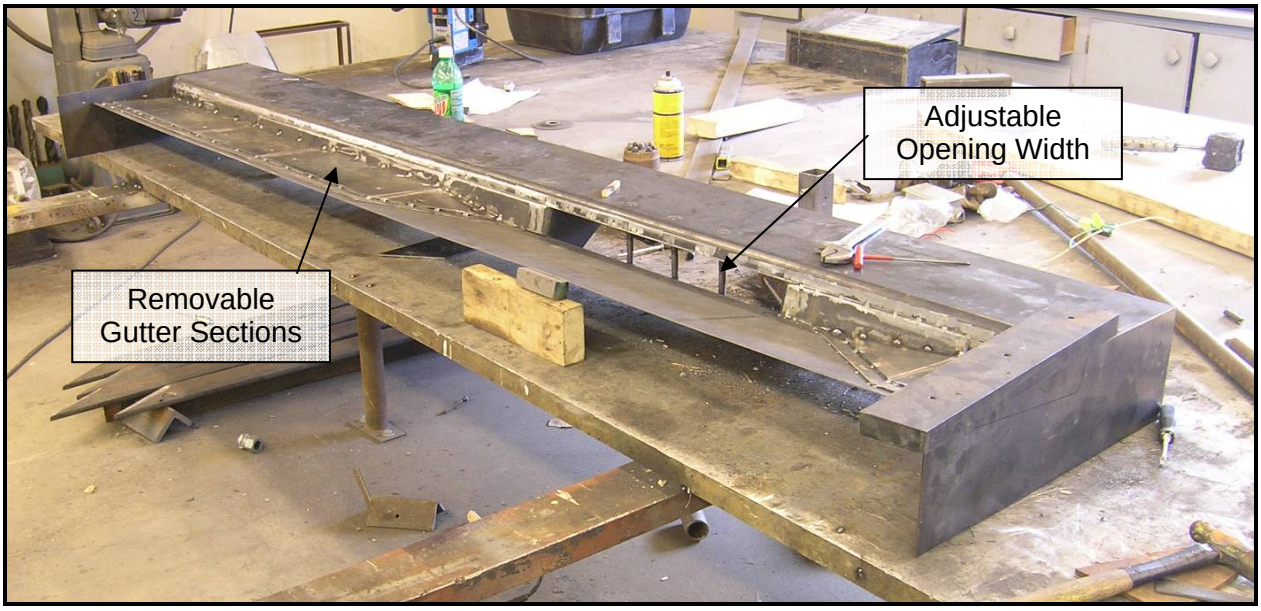

Figure 3-4: Curb inlet gutter panel during fabrication (Type R)

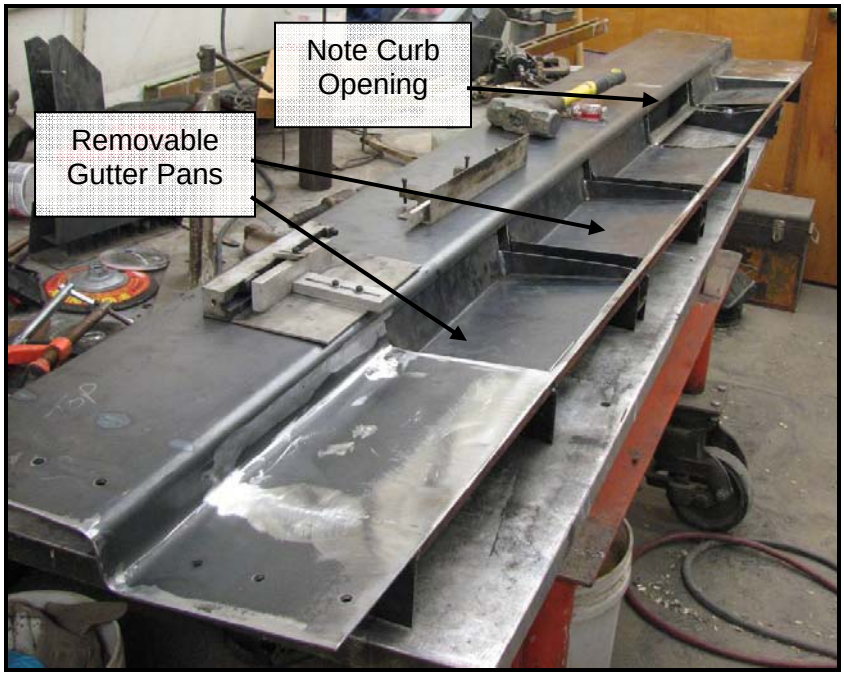

Figure 3-5: Combination-inlet gutter panel during fabrication (Type 13 and 16 grates)

Solid Plexiglas® was milled to produce the Type 13 grate shown in Figure 3-6. Copper pipe and brass bar stock were used to fabricate the Type 16 grate shown in Figure 3-7. Curved vanes on the Type 16 grate were constructed of copper pipe. Transitions from the gutter cross slope to the inlet cross slope were built into the gutter panels. As a result of the need for variable opening lengths in each inlet type, the gutter panels were built as modular elements which could be removed and relocated within the gutter panel framework. Modeling clay was used to smooth-out any irregularities in the curb, gutter, and inlet surfaces.

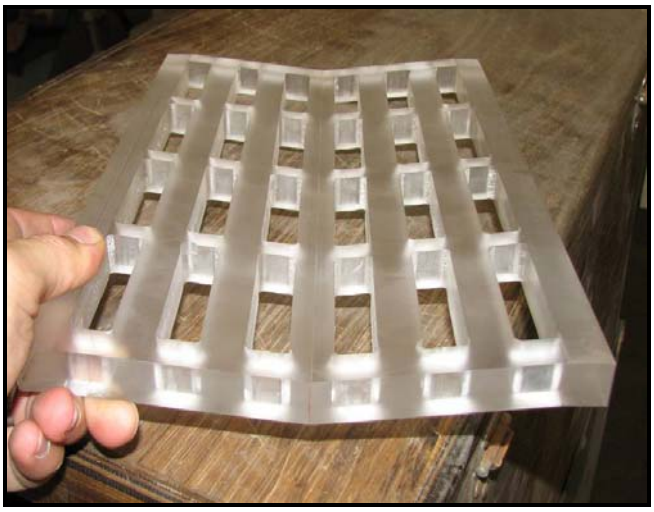

Figure 3-6: Type 13 grate photograph

Figure 3-7: Type 16 grate during fabrication

Type 13 and 16 inlets were used in a combination-inlet configuration, in which there was a curb opening in addition to the grate. The Type R inlet is only a curb opening, which differed from the curb opening used in the combination-inlet configuration. The model incorporated depressed gutters in which the invert of the curb inlet was lower than the bottom of the gutter flow line. With reference to Figure 2-3 presented previously, the curb inlet portion of the combination inlet is most similar to the vertical throat type, whereas the Type R curb inlet is most similar to the inclined throat type. There were several other configurations in which the flow area of the inlet was reduced in some way: the curb portion of a combination inlet was reduced to a "4-in." height, the curb portion of a combination inlet was blocked-off completely,

the grate portion of a combination inlet was obstructed with debris, the grate portion of a combination inlet was blocked-off completely, or a horizontal safety bar was used across the Type R curb inlet. The photographs provided in Figure 3-8 through Figure 3-28 illustrate the inlet types and configurations.

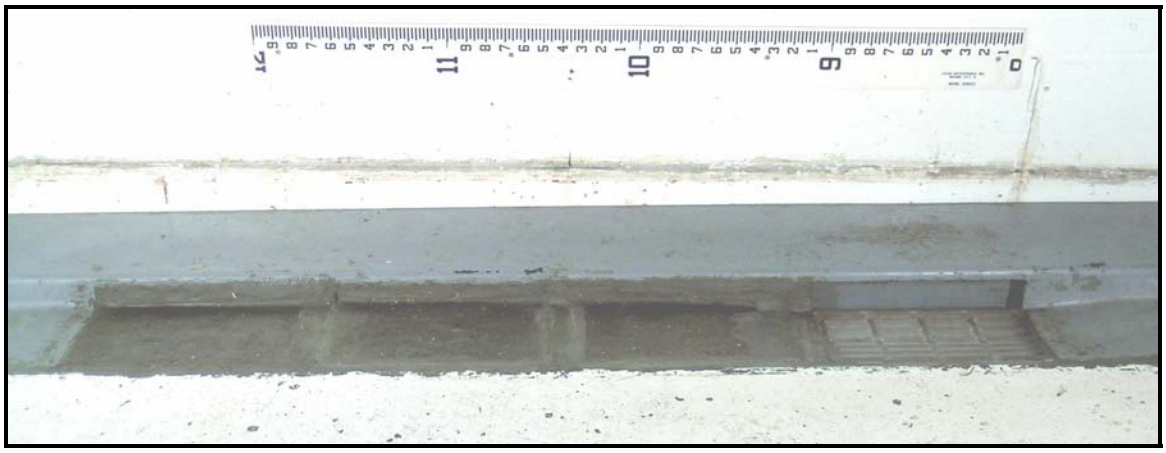

Figure 3-8: Single No. 13 combination photograph

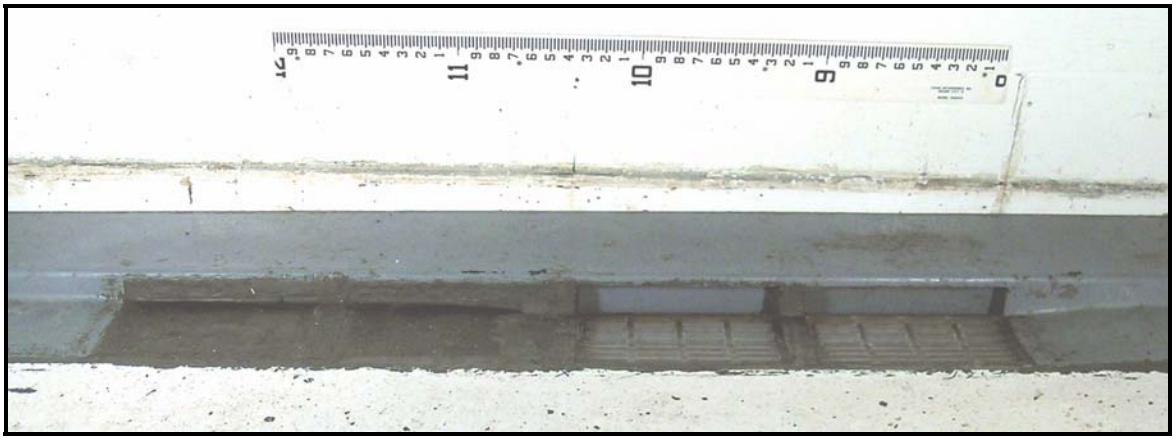

Figure 3-9: Double No. 13 combination photograph

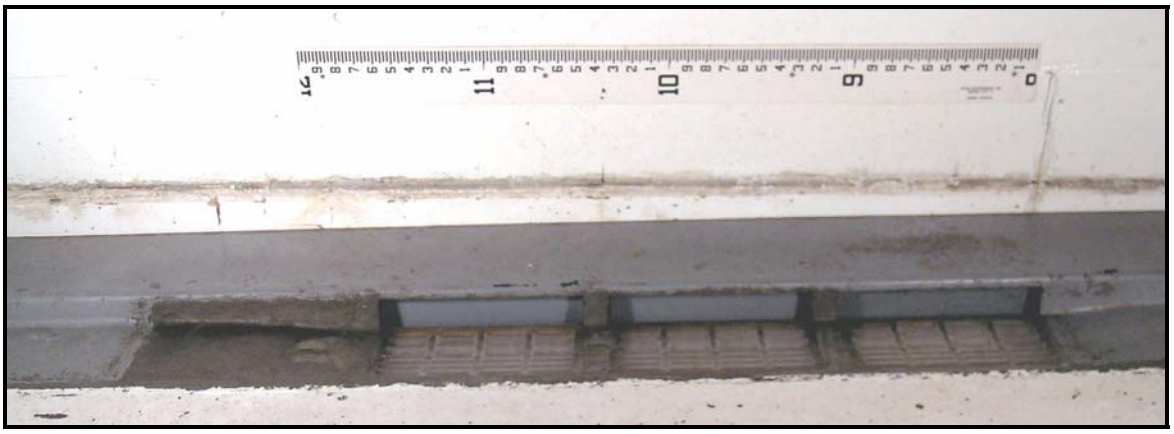

Figure 3-10: Triple No. 13 combination photograph

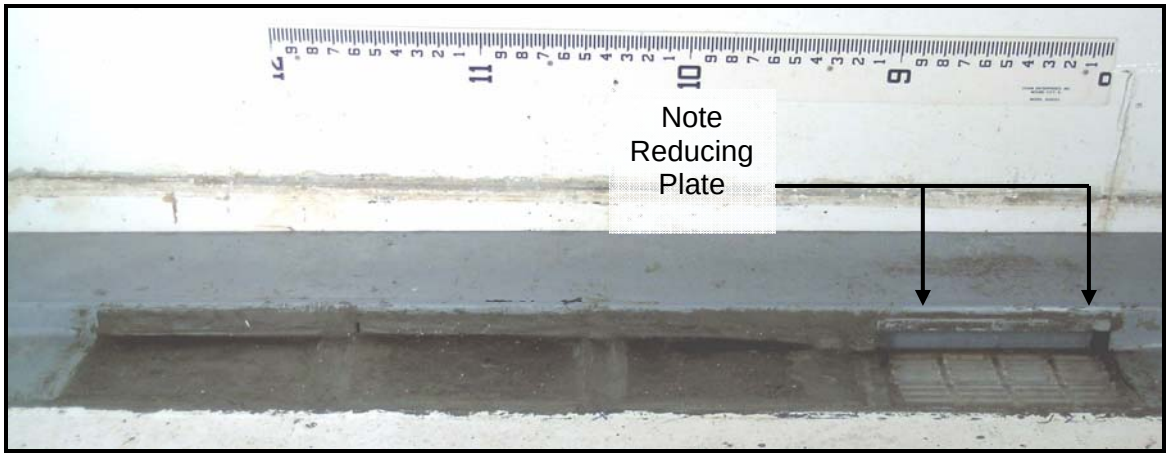

Figure 3-11: Single No. 13 combination with 4-in. curb opening photograph

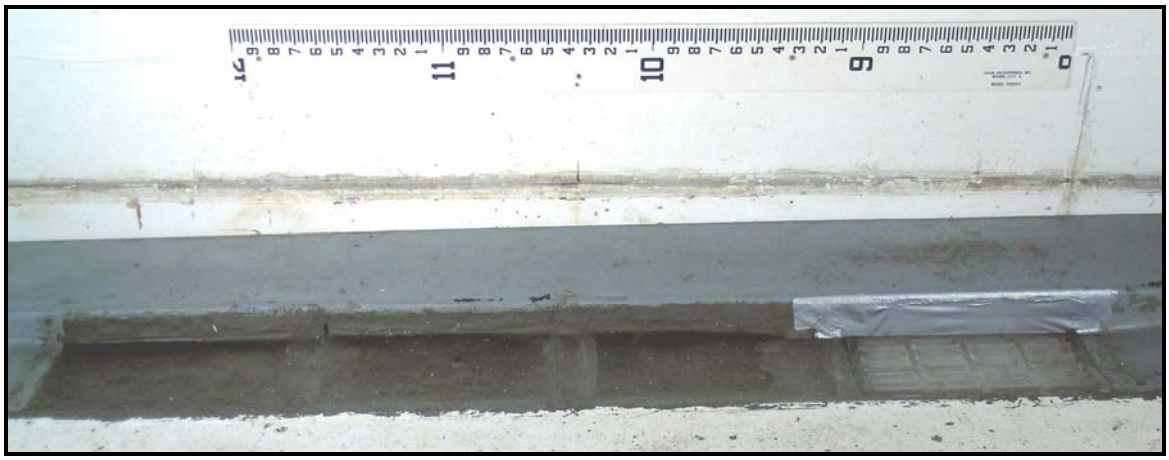

Figure 3-12: Single No. 13 combination with grate only photograph

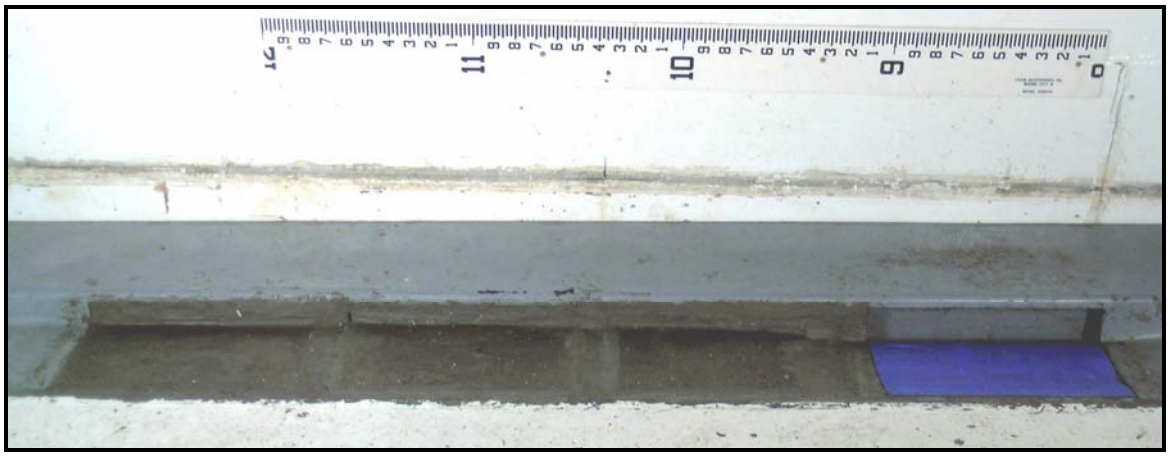

Figure 3-13: Single No. 13 curb opening only photograph

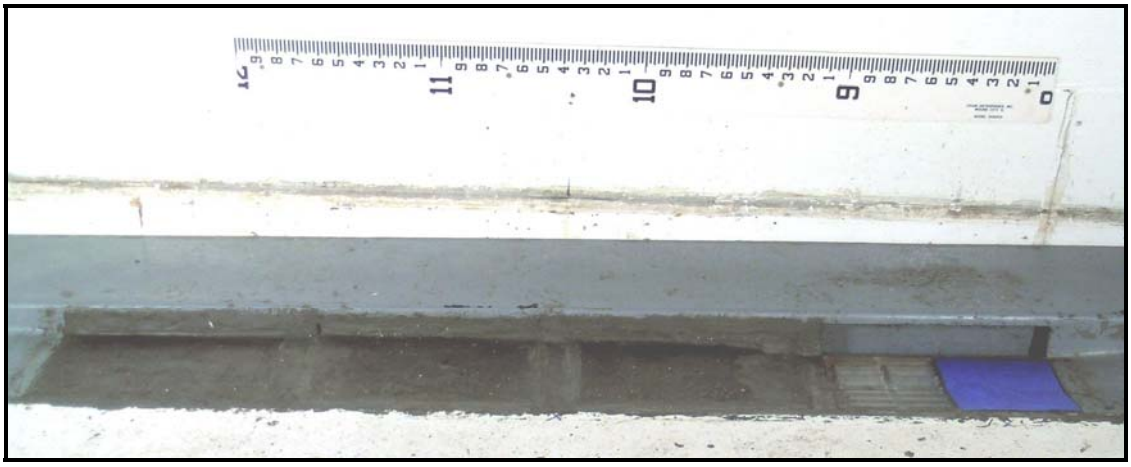

Figure 3-14: Single No. 13 combination debris test one photograph

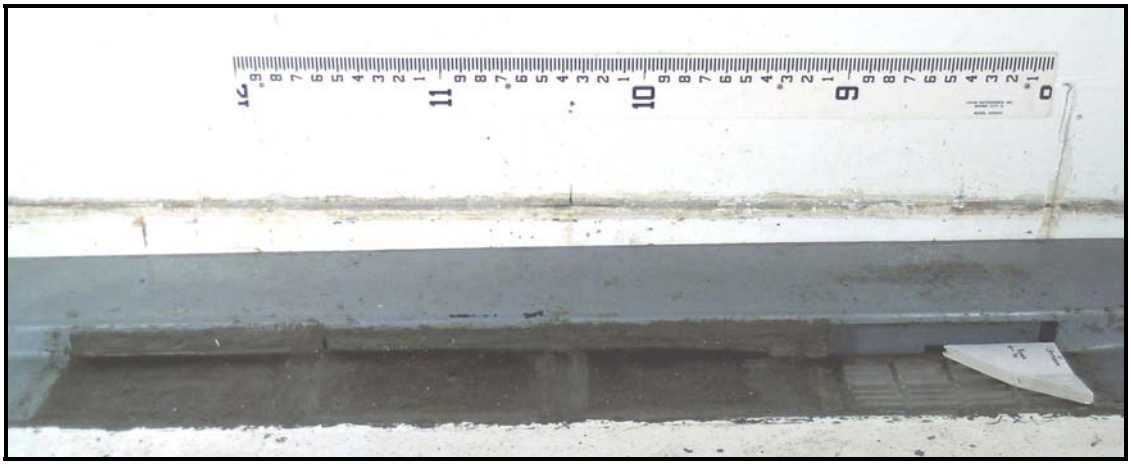

Figure 3-15: Single No. 13 combination debris test two photograph

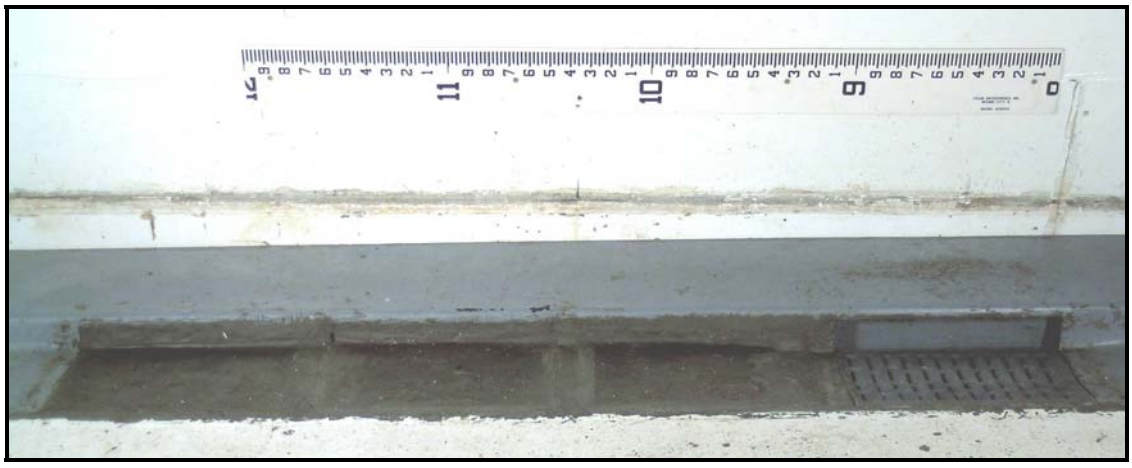

Figure 3-16: Single No. 16 combination photograph

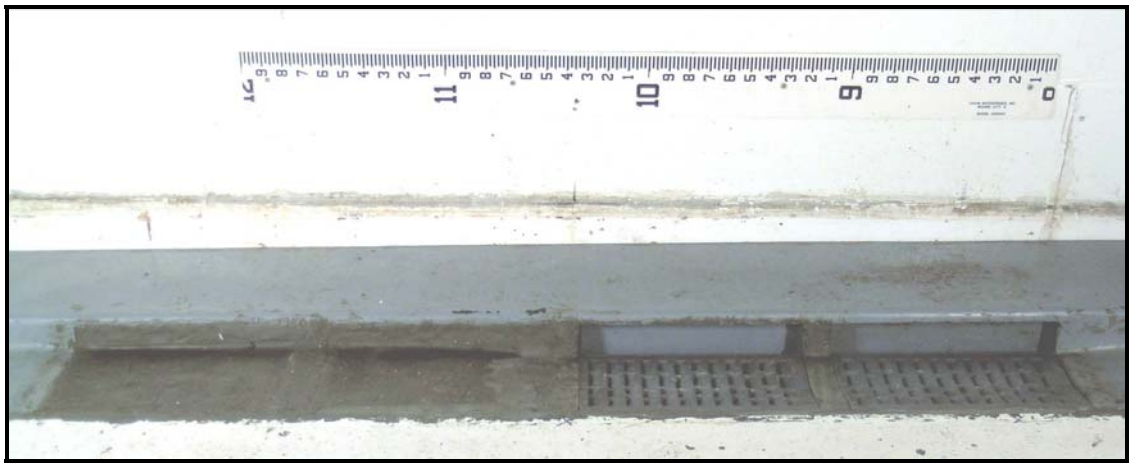

Figure 3-17: Double No. 16 combination photograph

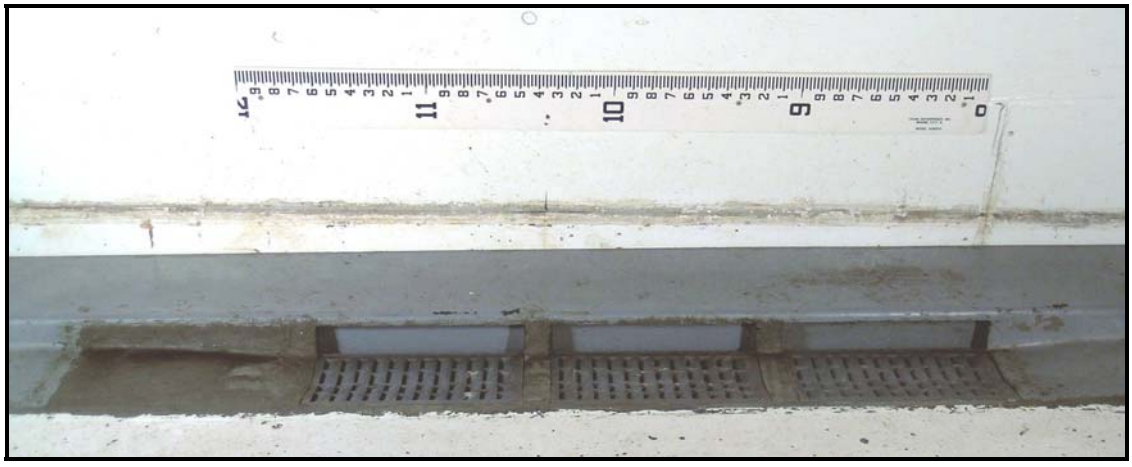

Figure 3-18: Triple No. 16 combination photograph

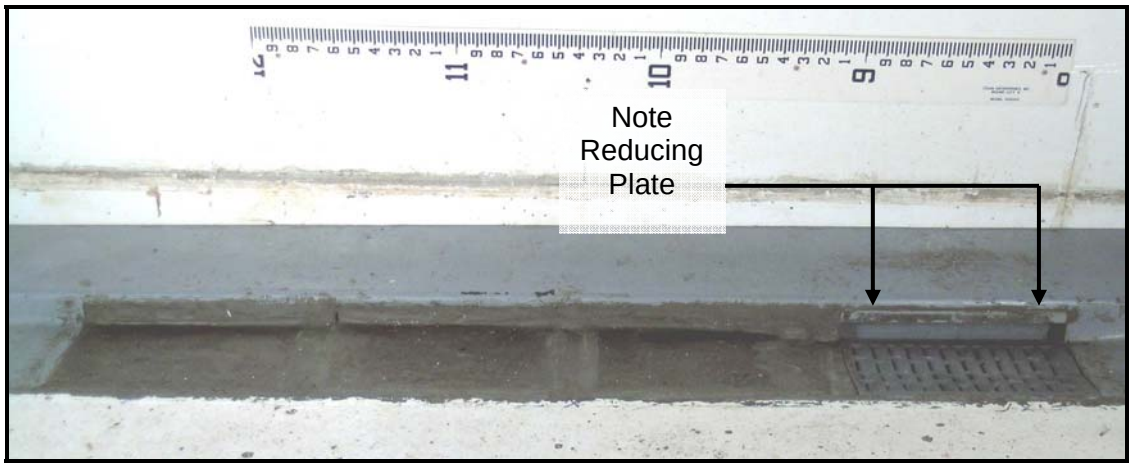

Figure 3-19: Single No. 16 with 4-in. curb opening photograph

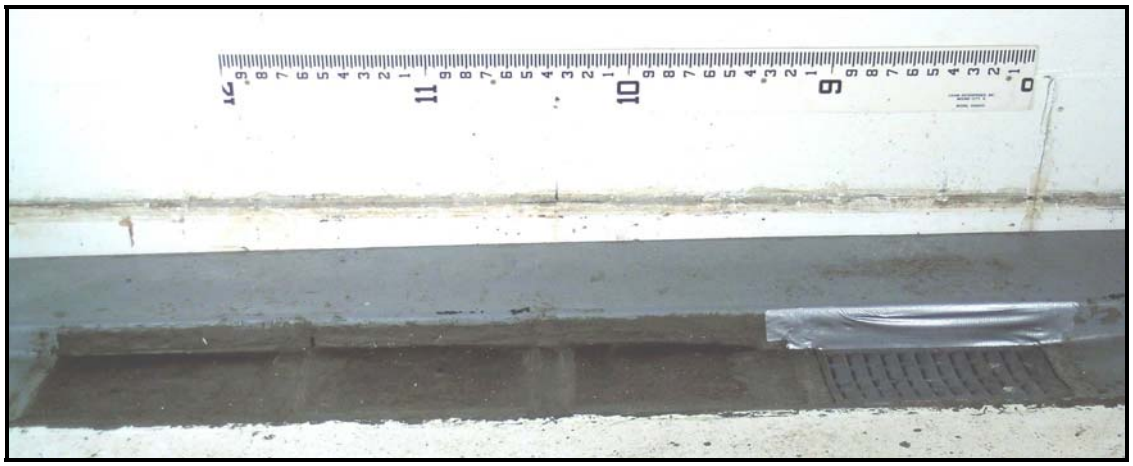

Figure 3-20: Single No. 16 grate only photograph

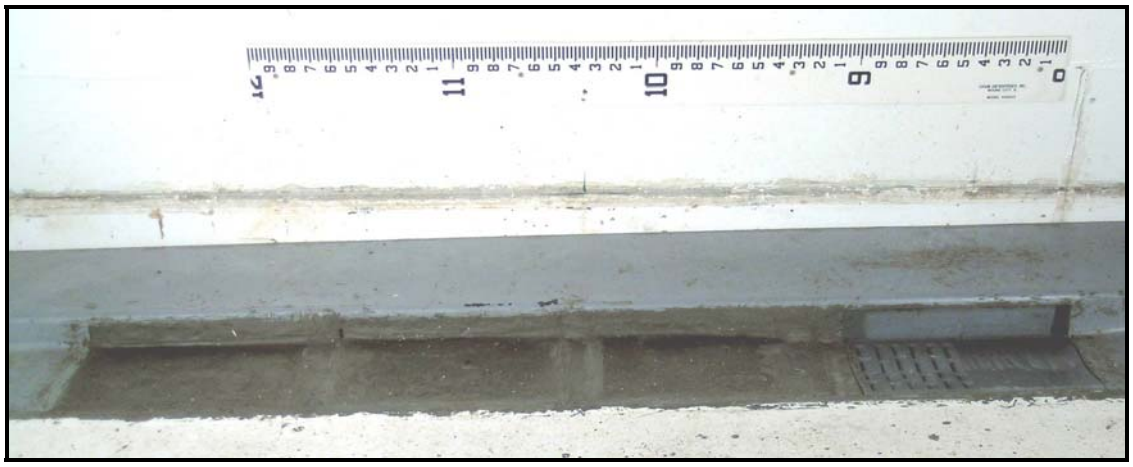

Figure 3-21: Single No. 16 combination debris test one photograph

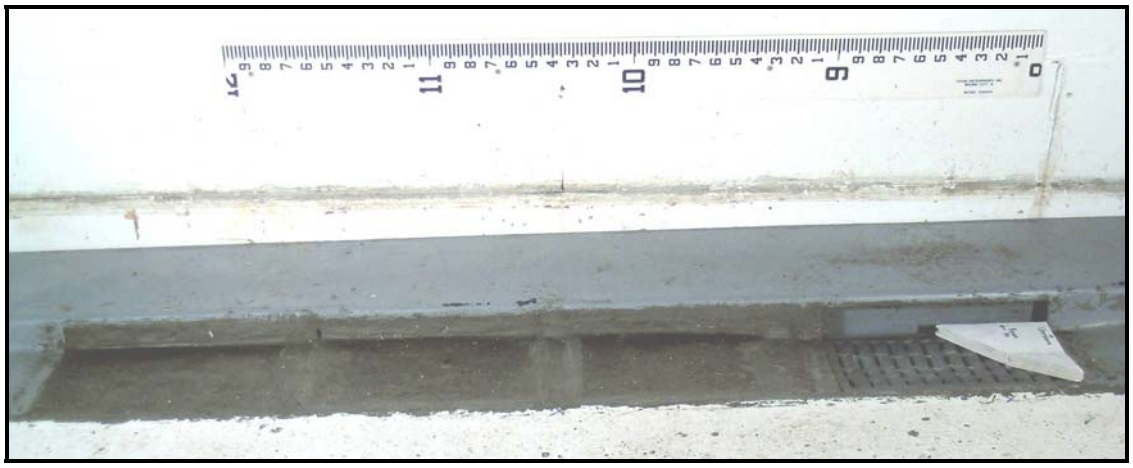

Figure 3-22: Single No. 16 combination debris test two photograph

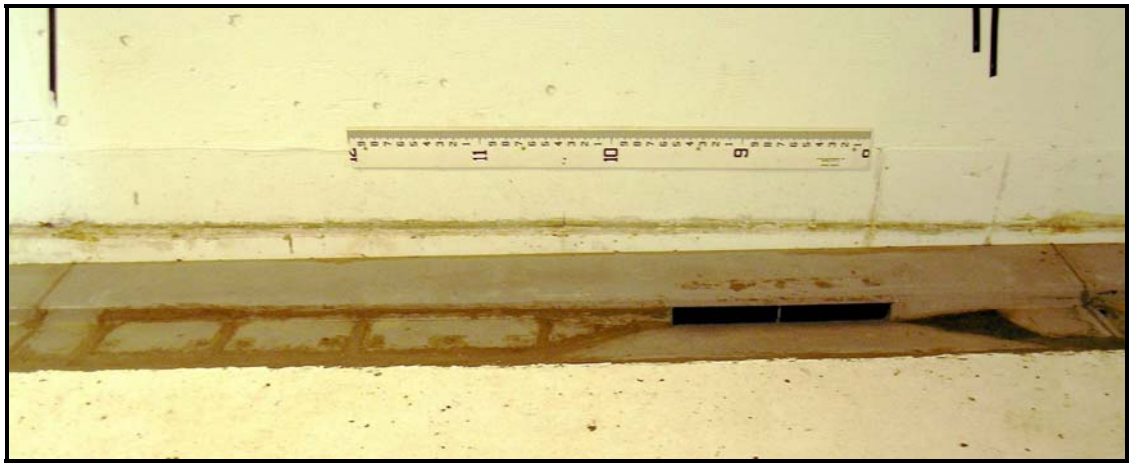

Figure 3-23: R5 curb inlet photograph

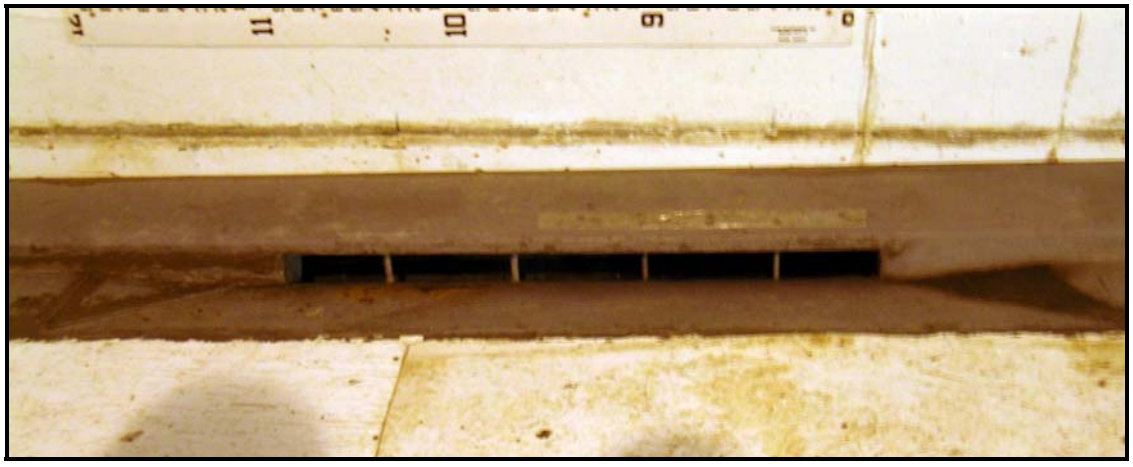

Figure 3-24: R9 curb inlet photograph

Figure 3-25: R12 curb inlet photograph

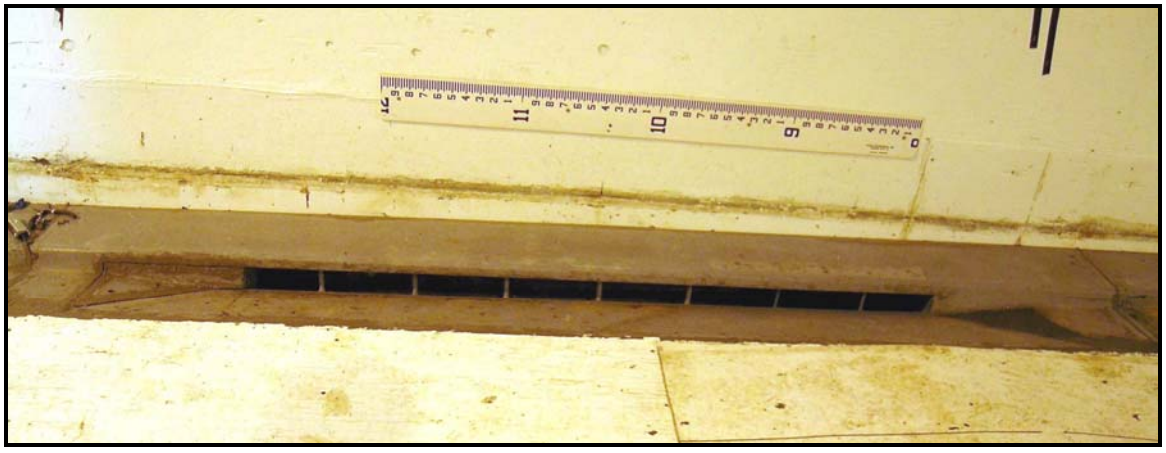

Figure 3-26: R15 curb inlet photograph

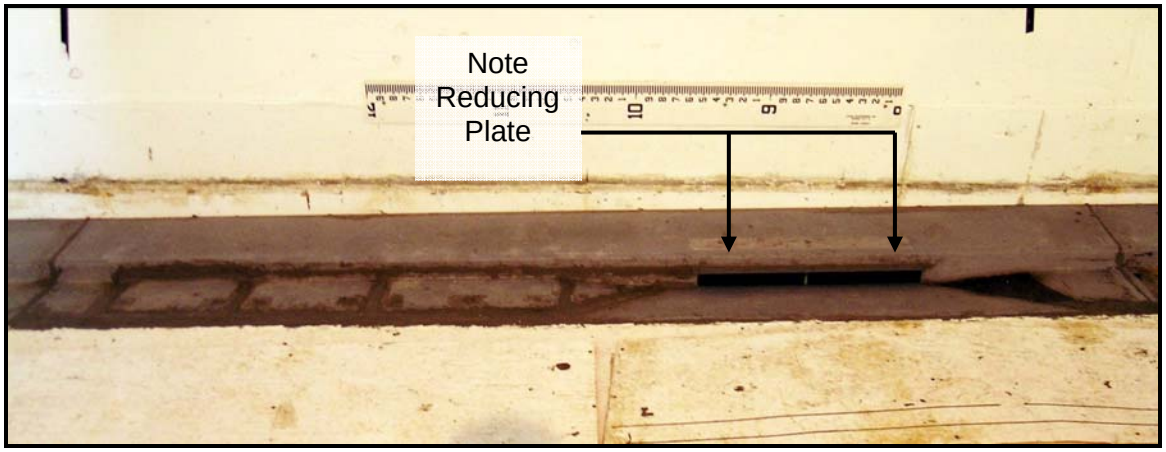

Figure 3-27: R5 with 4-in. curb opening photograph

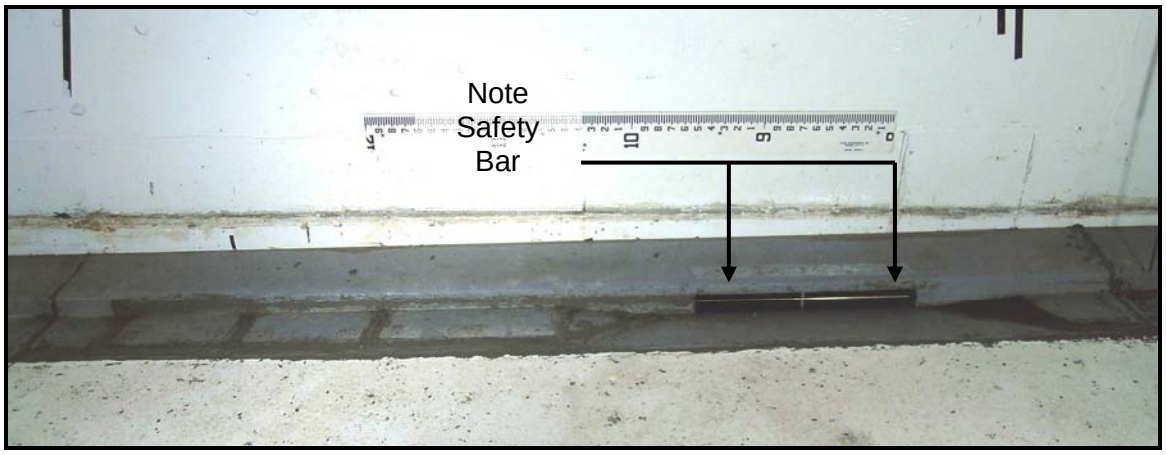

Figure 3-28: R5 with safety bar photograph

3.4 Model Operation and Testing Procedures

A headbox was used to supply water to the model, a flume section contained the street and inlet components, and a tailbox was used to catch flow that bypassed the inlets. Figure 3-29 provides a sketch of the entire model. Water flowed from the inlet valve to the headbox, through the flume section, then exits into the tailbox. Two pumps fed water to the headbox through a network of large pipes and valves. A 40-horsepower (hp) pump was used for the 0.33-ft and 0.50-ft prototype-scale depths, and a 75-hp pump was used for the 1-ft prototype-scale flow depth. Both pumps drew water from a sump located beneath the laboratory floor, which was approximately 1 acre ft in volume. Lined channels below the flume conveyed flow away from the tailbox and back into the sump.

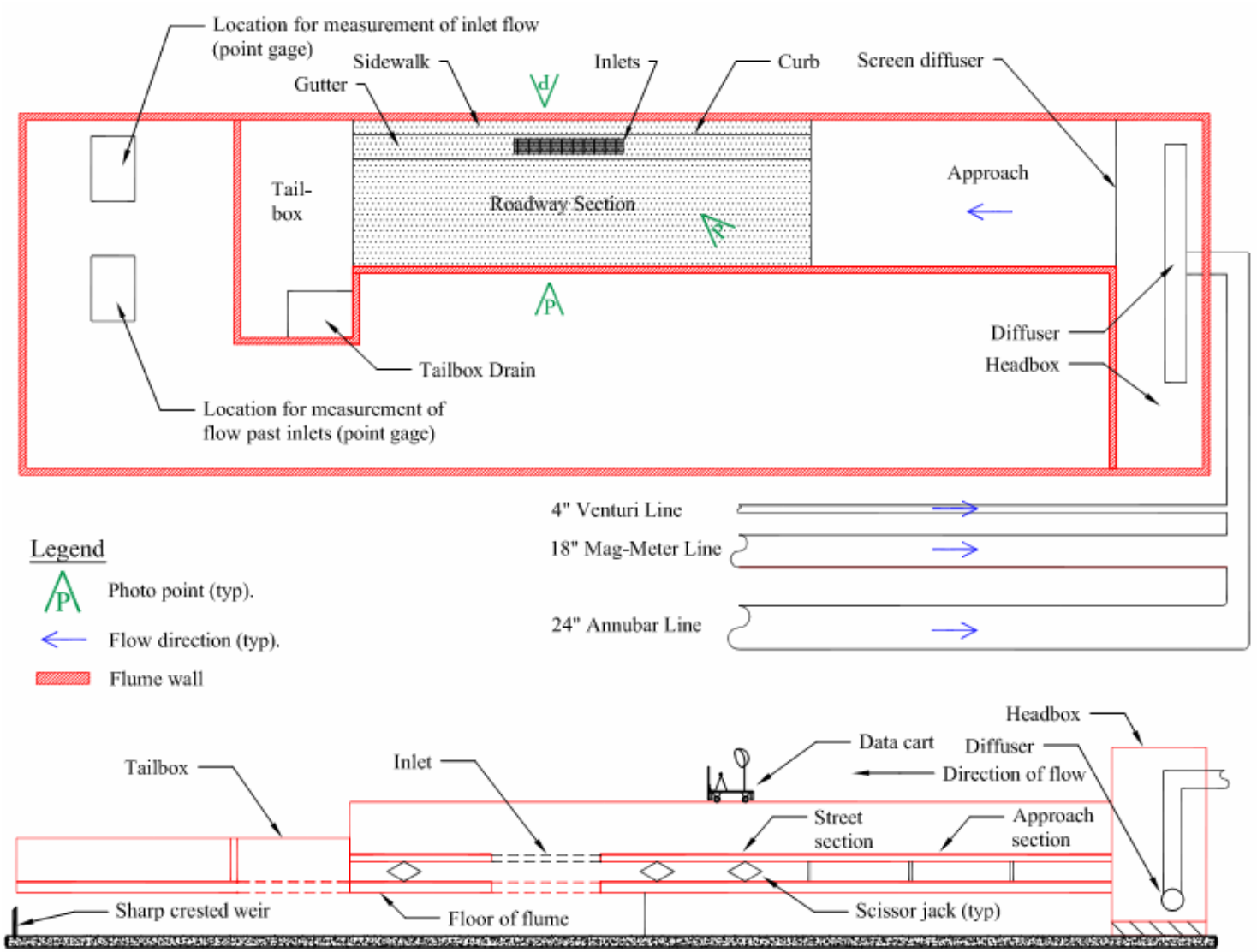

Figure 3-29: Model schematic

Flow entering and exiting the model was measured as part of the data-collection process. Flow entered the model headbox through pipes as pressurized flow. Measurement-instrument selection for inflow was based on the anticipated flow required for each test, and the associated pump and pipelines used. Two instruments were used: 1) a differential pressure meter (annubar) manufactured by the Rosemount division of the Emerson Process Management Company, and 2) an electro-magnetic flow meter (mag meter) manufactured by the Endress and Hauser Company. Table 3-7 summarizes flow-measurement characteristics of each instrument.

Table 3-7: Discharge measurement-instrument ranges

Instrument Type	Flow Range (cfs)	Pipeline (in.)	Pump (hp)	Accuracy (%)
mag meter	0.13 - 10	18	40	0.5
annubar	6.5 - 15	24	75	2.5

Outflow from the model flume section was either conveyed through the inlets or bypassed off the road section. In either case, the flow passed through an opening in the tailbox of the flume and into channels below. Flow exiting the channels was measured by either a rectangular weir for bypassed flow or V-notch sharp-crested weir for inlet captured flow. Both weirs were constructed in accordance with published specifications (Bos, 1989; USBR, 2001). Calibration was performed for each weir prior to testing of the model. Rating equations in the form of Equation 3-1 were developed by regression analysis of depth-flow data over the expected operating range of each weir. Coefficients and exponents used in these equations are given in Table 3-8. For slope configurations greater than 0.5% longitudinal, the tailwater depth was noted to rise significantly in the tailbox of the model. When this occurred, the weirs were raised and recalibrated:

$$Q = aH^{b} \qquad \textbf{Equation 3-1}$$

where:

Q = discharge (cfs);
a = coefficient of discharge;
H = head above the weir crest (ft); and
b = depth exponent.

Table 3-8: Empirically-derived weir parameters

Slopes	V-notch Weir	Rectangular Sharp-crested Weir
4% and 2%; 4% and 1%; 2% and 2%; 2% and 1%	a = 2.64 b = 2.50 R^2 = 0.999	a = 15.78 b = 1.58 R^2 = 0.999
0.5% and 1%; 0.5% and 2%	a = 2.52 b = 2.45 R^2 = 0.999	a = 13.50 b = 1.35 R^2 = 0.999

Flow depth required for each test was measured at the same location roughly 5 prototype feet upstream of the first inlet. This location was chosen to be free of surface curvature from flow being drawn into the inlets, free of ripples generated from the upstream approach transition, and served as a control section to establish the depth and adjust the flow into the model for each test. Depth of flow was measured using a point gage with ±0.001 ft accuracy, which was mounted on a data-collection cart designed to slide along the model and perform other water-surface measurements as well. Figure 3-30 provides a photograph of the data-collection cart. A camera tripod was mounted on the data-collection cart providing one of the three photograph points: 1) an elevated oblique view from the data-collection cart, 2) a view laterally opposite from the inlets, and 3) a plan view from directly above the inlets.

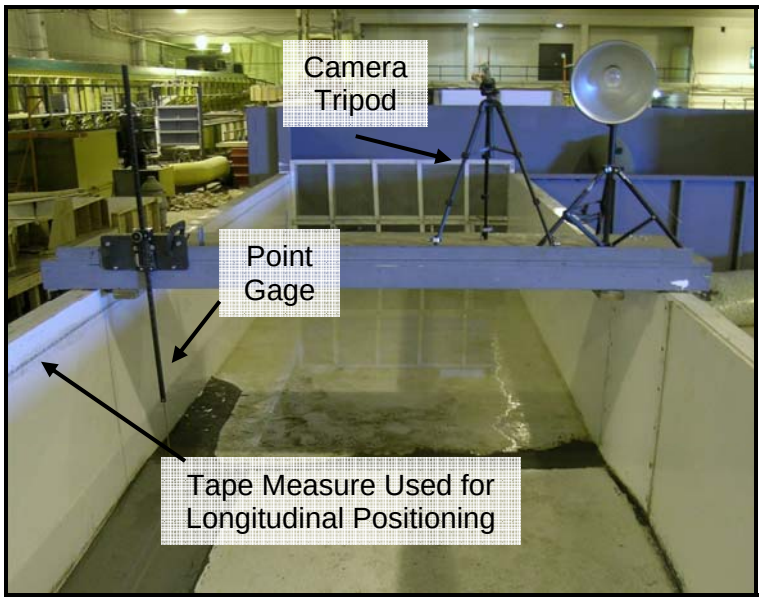

Figure 3-30: Data-collection cart photograph (looking upstream)

Following a standardized testing procedure assured consistency and facilitated data collection by multiple technicians. Prior to testing, the street slope and inlet type were configured. The flow depth was then set on the point gage and the flow into the model was adjusted to contact the point gage. Technicians waited approximately 10 minutes once the target depth was achieved for flow conditions to stabilize. Outflow measurement point gages were checked periodically during this time until the readings stabilized. Test conditions were then checked and recorded on the data sheet. If the slope and inlet configurations did not change for a subsequent test, a new depth was set on the point gage and the flow adjusted accordingly. If a new slope or inlet configuration was required, the pumps were shut off and the model was reconfigured. If the spread of water did not cover the street section for any given test, the extent of flow was recorded to provide a top width at every longitudinal station. A fixed measuring tape was used to determine longitudinal stations along the flume. Lateral positions across the flume were determined with a measuring tape affixed to the data-collection cart. Both tapes were graduated in tenths of a foot and had ±0.01 ft accuracy.

Data collection was documented by completing a data sheet for each test, taking still photographs, and shooting short videos. The data-collection sheet used for all testing is presented in Appendix E. Data collection was comprised of the following information: date, operator name, water temperature, test ID number, start and end times, slope configuration, inlet configuration, discharge and measurement devices used, depth of flow, extent of flow, and flow characteristics. Flow characteristics consisted of any general observations that the operator recorded for a particular test. Typical observations included the condition of flow around the inlets (if waves emanated or splashing occurred), and if possible an approximation of flow percentage passing through each inlet was made.

Several measures were taken to maintain data quality. After the testing procedures described above were followed, data were entered into the database by the operator, and then checked by another person for accuracy with the original data sheets. A survey of the model was performed every time the model inlet type was changed. This confirmed that the model was not shifting or settling, and that the slope was accurate to within allowable limits of 0.05% for longitudinal and cross slopes.

3.5 Summary

A testing program designed for evaluating the performance of Type 13, 16, and R inlets, comprised of 318 tests, was conducted at Colorado State University. A 1/3-scale model of a two-lane street section was constructed. Variations in street longitudinal slope, cross slope, inlet length, and flow depth were accomplished to provide data on captured inlet flow and bypassed street flow. In addition, the spread of flow was measured along the street section. Surface roughness of the prototype was designed to be 0.015, which is the mean value for asphalt. Inflow to the model was measured using either a magnetic flow meter or a differential pressure meter. Outflow from the model was measured using sharp-crested weirs for captured inlet flow and bypassed street flow. Photographs were taken and video recordings were made to facilitate later inspection of flow conditions in the model. From the collected test data, qualitative and quantitative observations will be made for determination of efficiency for each inlet.

4 DATA AND OBSERVATIONS

Testing results presented in this report have been collected using the previously described test procedures and quality control (QC) measures, and are presented at the prototype scale. The large quantity of data is presented in this section in graphical form, organized by inlet type, and qualitative observations are made concerning the performance of the Type 13, 16, and R inlets. Sample tables of on-grade and sump test data are also presented. The entire collected test data set is presented in tabular form in Appendices B and C, where it is organized by: test ID number, inlet configuration, slopes, flow depth, total flow, efficiency, top width of flow at the upstream control section, and top width of flow downstream of the inlets.

4.1 On-grade Tests

A tabular sample of the on-grade test data is presented as Table 4-1. The entire on-grade data set in included as Appendix B. Inlet efficiency was determined as the ratio of captured flow to total street flow for each test as shown in Equation 4-1:

$$E = \frac{captured\ inlet\ \ flow}{total\ street\ \ flow} \times 100 \qquad \textbf{Equation 4-1}$$

where:

E = inlet efficiency (%).

Table 4-1: Sample on-grade test data

Test ID Number	Configuration	Longitudinal Slope (%)	Cross Slope (%)	Flow Depth (ft)	Prototype Total Flow (cfs)	Efficiency (%)	Top Width at Control (ft)	Top Width Downstream of Inlets (ft)
56	Triple No. 13	0.5	1	0.333	4.4	82.1	15.8	9.0
57	Triple No. 13	0.5	1	0.501	20.6	43.2	18.2	18.2
58	Triple No. 13	0.5	1	0.999	126.6	22.7	18.2	18.2
59	Double No. 13	0.5	1	0.333	4.7	73.3	16.0	10.7
60	Double No. 13	0.5	1	0.501	22.6	35.9	18.2	18.2
61	Double No. 13	0.5	1	0.999	127.8	16.2	18.2	18.2
62	Single No. 13	0.5	1	0.333	4.8	61.3	16.0	15.8
63	Single No. 13	0.5	1	0.501	26.2	23.8	18.2	18.2
64	Single No. 13	0.5	1	0.999	126.4	9.9	18.2	18.2

For illustration purposes, trend lines are fitted to the on-grade test data (as second-order polynomials) in Figure 4-1 through Figure 4-3. Each trend line illustrates how efficiency increases with increasing inlet length. Velocity was chosen as the independent variable in these figures because of its significant effect on inlet efficiency.

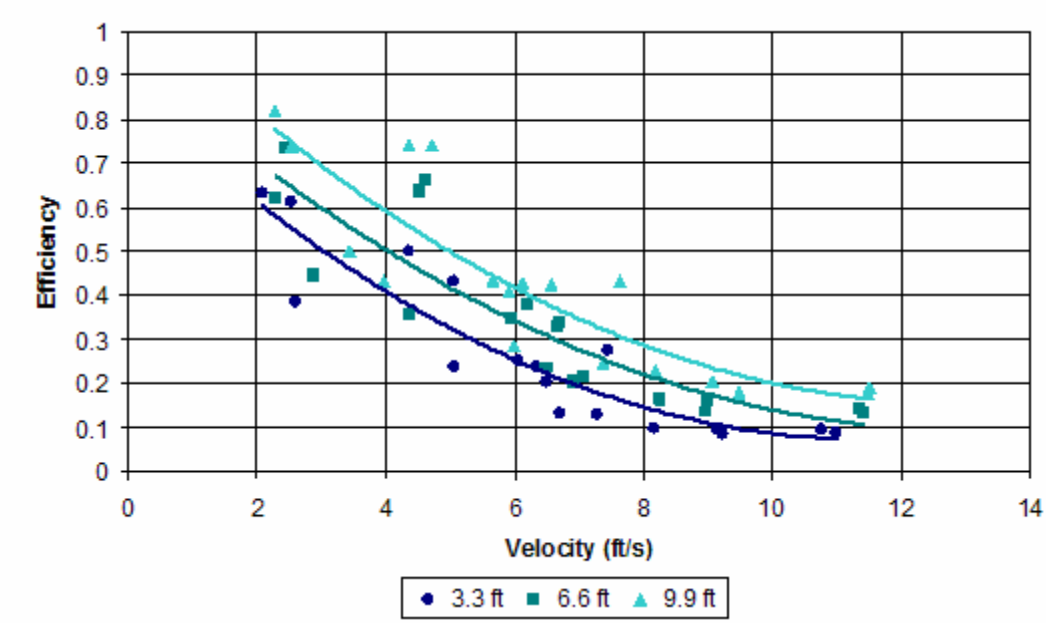

Figure 4-1: Type 13 combination-inlet on-grade test data

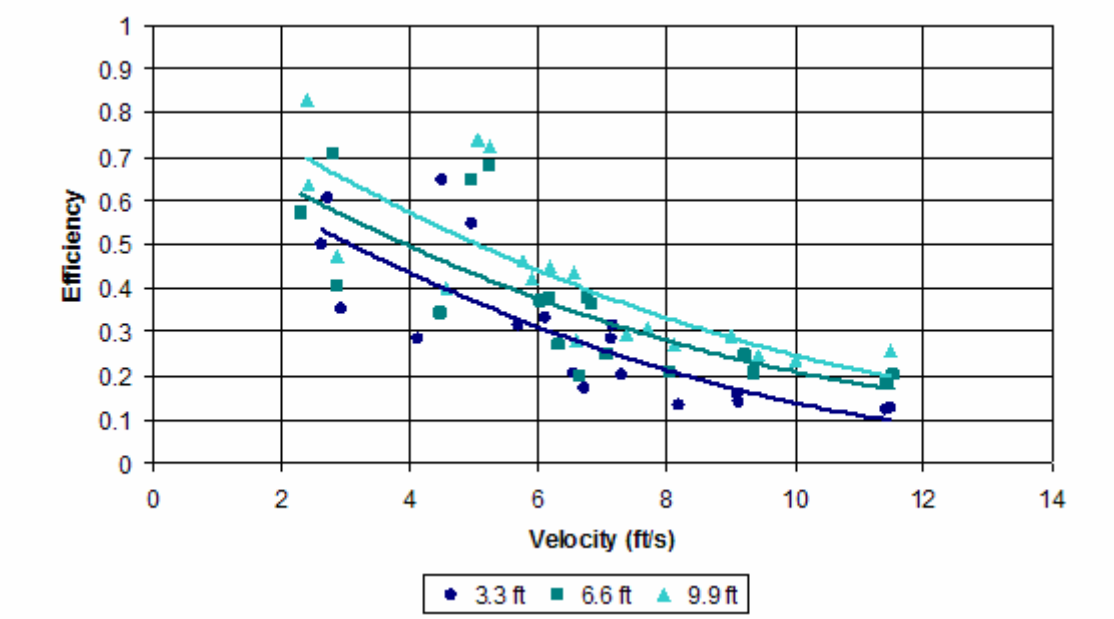

Figure 4-2: Type 16 combination-inlet on-grade test data

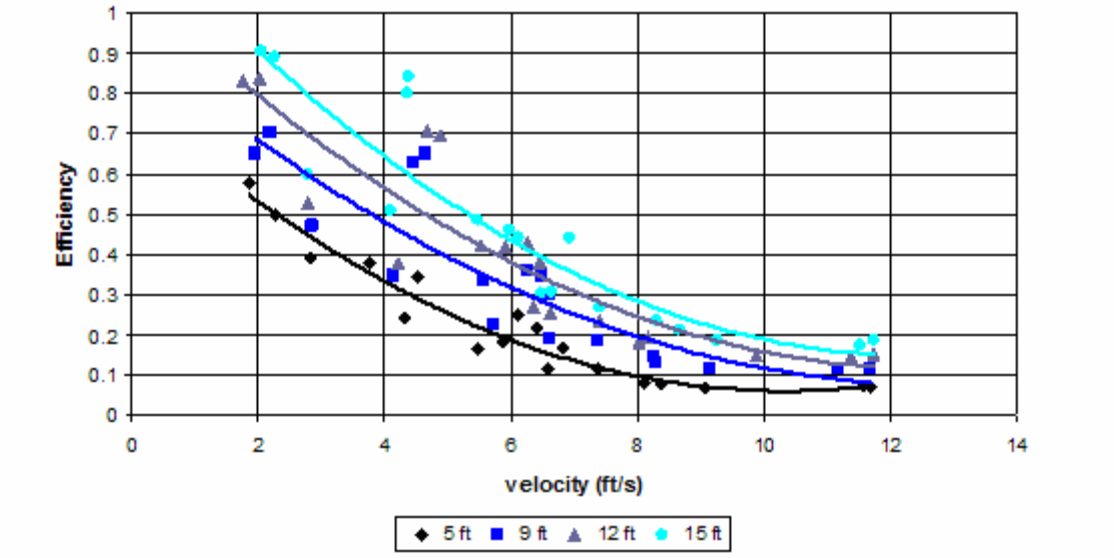

Figure 4-3: Type R curb inlet on-grade test data

Several general trends can be found in the on-grade test data:

- The highest inlet efficiency occurs at the lowest flow velocity.
- The velocity of flow is influenced by the longitudinal and cross slopes, and lower slopes produce lower velocity.
- Flow on the model street section was almost always supercritical

- The inlet efficiency appears to asymptotically approach a minimum value as the velocity increases.
- As the inlet length increases for a given flow velocity, the efficiency increases.
- The spread of water across the street section for a given flow decreases as either of the slopes increase.
- For a given longitudinal slope, a lower cross slope shows a slightly faster rate of decrease in efficiency as the velocity increases.
- For a given cross slope, a lower longitudinal slope shows a slightly faster rate of decrease in efficiency as the velocity increases.
- For a given inlet length, the Type 16 inlet is generally the most efficient, followed by the Type 13 and Type R.

4.2 Sump Tests

A tabular sample of the sump test data is presented as Table 4-2. All of the flow into the model was captured by the inlets in the sump test condition. The entire sump test data set is included as Appendix C.

Table 4-2: Sample sump test data

Test ID Number	Configuration	Longitudinal Slope (%)	Cross Slope (%)	Flow Depth (ft)	Prototype Flow (cfs)
1	Triple No. 13	0	1	0.333	2.5
2	Triple No. 13	0	1	0.501	8.6
3	Triple No. 13	0	1	0.999	42.2
4	Double No. 13	0	1	0.333	2.3
5	Double No. 13	0	1	0.501	7.8
6	Double No. 13	0	1	0.999	27.1
7	Single No. 13	0	1	0.333	2.0
8	Single No. 13	0	1	0.501	5.9
9	Single No. 13	0	1	0.999	15.3

The sump test data are plotted in Figure 4-4 through Figure 4-6 for increasing flow depth for the three inlets tested.

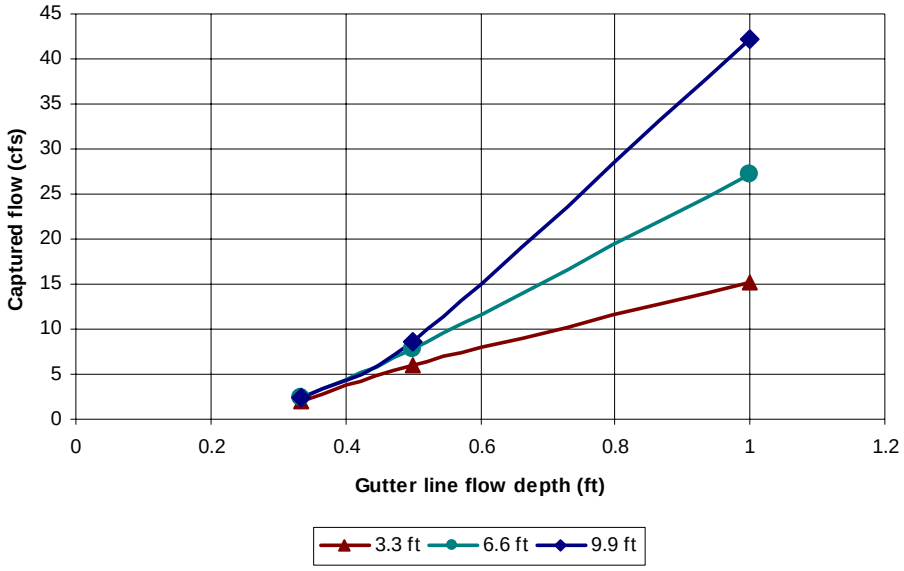

Figure 4-4: Type 13 combination-inlet sump test data

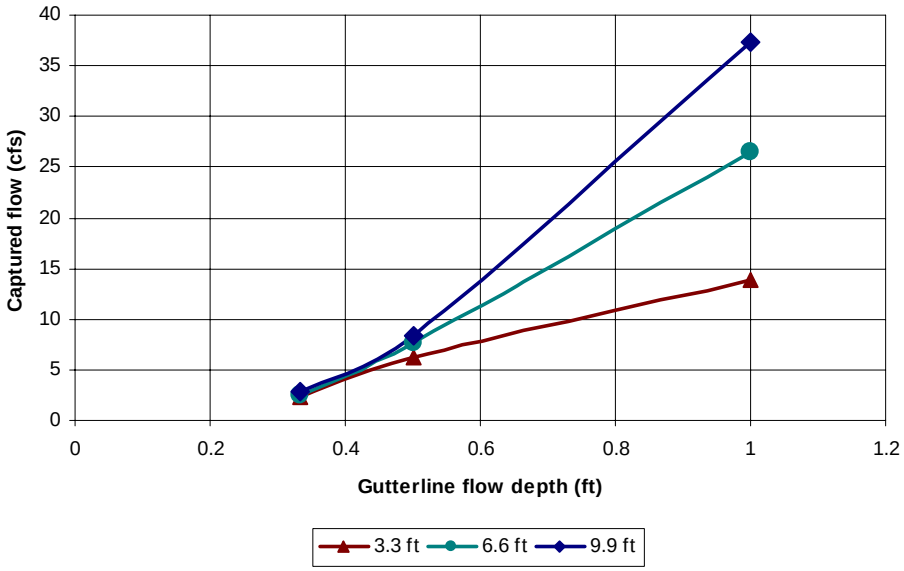

Figure 4-5: Type 16 combination-inlet sump test data

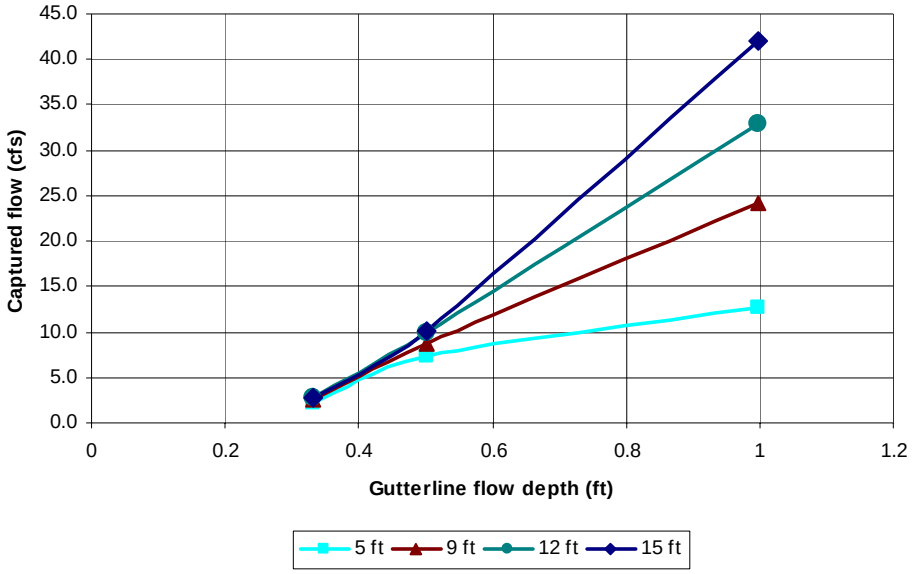

Figure 4-6: Type R curb inlet sump test data

Several general trends can be found in the sump test data:

- For a given flow depth, a longer inlet results in higher captured flow.
- As the flow depth increases, the corresponding captured flow increases.
- For a given inlet length, the Type 13 inlet is generally the most efficient, followed by the Type 16 and Type R.

4.3 Summary

A sample of the collected data set was presented in tabular form and all of the data presented in graphical form. The entire data set in presented in Appendices B and C. Qualitative observations were made regarding the nature of flow in the model and performance of the inlets tested. For the on-grade tests, flow velocity and depth were found to be the primary influencing parameters on efficiency. Street longitudinal slope primarily affected flow velocity, and cross slope primarily affected the spread of flow across the model street section. A detailed regression analysis of the on-grade test data, development of design equations, and qualitative observations are presented in the analysis chapter of this report.

5 ANALYSIS AND RESULTS

Data selected for analysis consisted of the unobstructed, on-grade configuration tests for Type 13 and 16 combination inlets and the Type R curb inlet. Analysis presented in this chapter is intended to provide improved methods for determining the efficiency of Type 13, 16, and R inlets in the on-grade configuration. Included in the unobstructed, on-grade, test category is 180 out of 318 tests. Remaining test data including sump tests and debris tests will be analyzed by other participating agencies. Presented in this chapter is a comparison between the observed inlet efficiency from testing, inlet efficiency determined from current and improved UDFCD calculation methods, and inlet efficiency determined from independent empirical equations developed using the process of dimensional analysis. Presented in Figure 5-1 is a flow chart illustrating the analysis. Empirical equations developed are intended to provide an independent alternative to the UDFCD methods for determining inlet efficiency. Also examined in this analysis is the relevance of achieving uniform flow in the model and a comparison is made between combination and grate inlet performance for the Type 13 and 16 inlets.

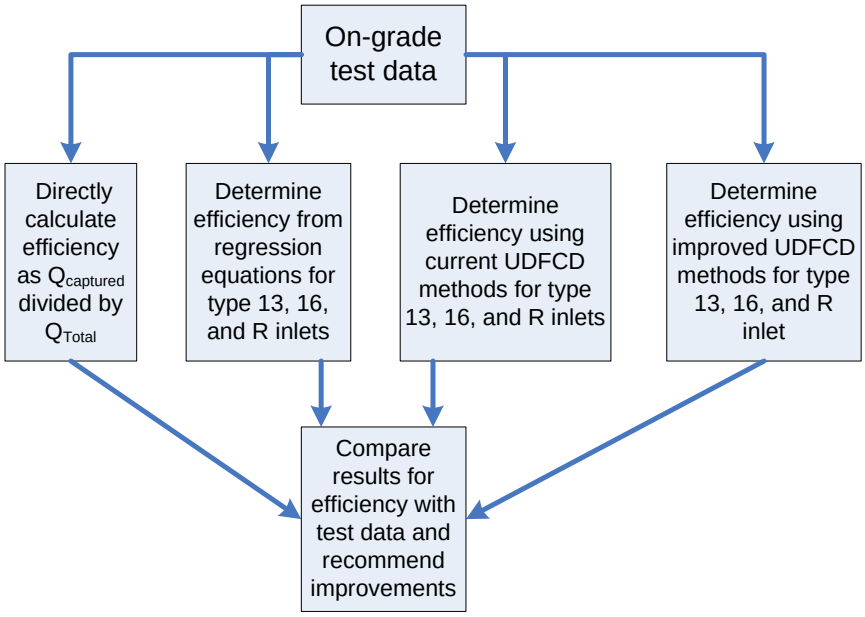

Figure 5-1: Analysis flow chart

5.1 Efficiency from UDFCD Methods

In this section, efficiency is determined for the Type 13, 16, and R inlets using the currently-accepted calculation methods presented previously in Section 2.2. For the Type 13 and 16 combination inlets, efficiency was determined using Equation 2-1 through Equation 2-4, and Equation 2-7 through Equation 2-10 as a direct calculation. Guidance in the *USDCM* to ignore the curb component of these combination inlets was followed by applying those equations. It was necessary to match the Type 13 and 16 inlets to comparable inlets from the UDFCD methods given in Section 2.2. From Table 2-4, the Type 13 inlet grate was found to be most similar to the Bar P-1-7/8-4 (also known as a P50x100 in *HEC 22*) by visual inspection, and the Type 16 grate was most similar to the vane grate. Applicable coefficients from Table 2-4 were used in Equation 2-8 for calculation of splash-over velocity. The local gutter depression (a), shown in Figure 2-2, was determined as a function of cross slope and gutter width. For a cross slope of 1% the value of "a" was 0.13 ft, and for a cross slope of 2% the value of "a" was 0.11 ft. Additional parameters were determined directly from the collected test data. Efficiency was then calculated from Equation 2-10, and compared to the observed efficiency in Figure 5-2 and Figure 5-3. Deviation of UDFCD methods from the observed test data becomes greater with increasing flow depth and increasing inlet length for Type 13 and 16 inlets. Differences in efficiency are

likely due to the nature of the original FHWA test data used to develop Equation 2-4 through Equation 2-10 for grate inlets. The FHWA study, summarized in Section 2.1, only tested to a maximum flow depth of 0.45 ft and a maximum inlet length of 4 ft. Therefore, the data would have had to be extrapolated to greater depths and inlet lengths. Analysis of the observed test data presented here does not extrapolate beyond the actual conditions tested.

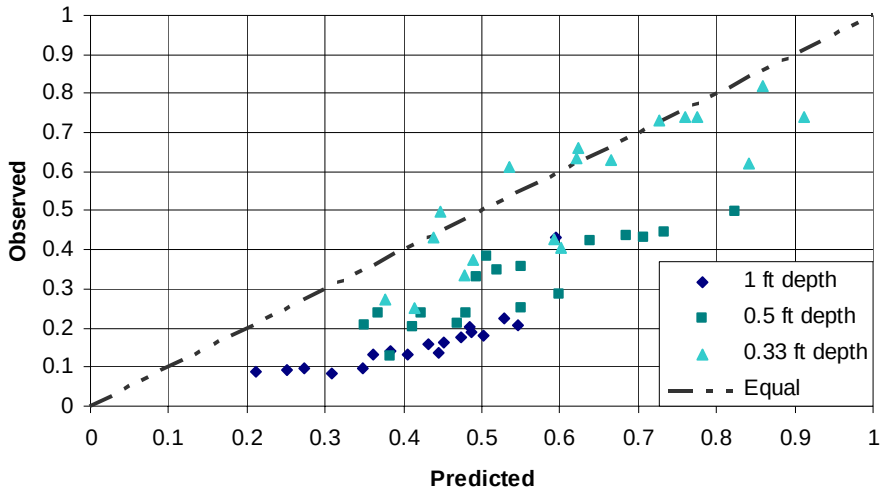

R^2	Average efficiency error (%)	Maximum efficiency error (%)
0.719	18.8	34.0

Figure 5-2: Predicted vs. observed efficiency for Type 13 combination inlet from UDFCD methods

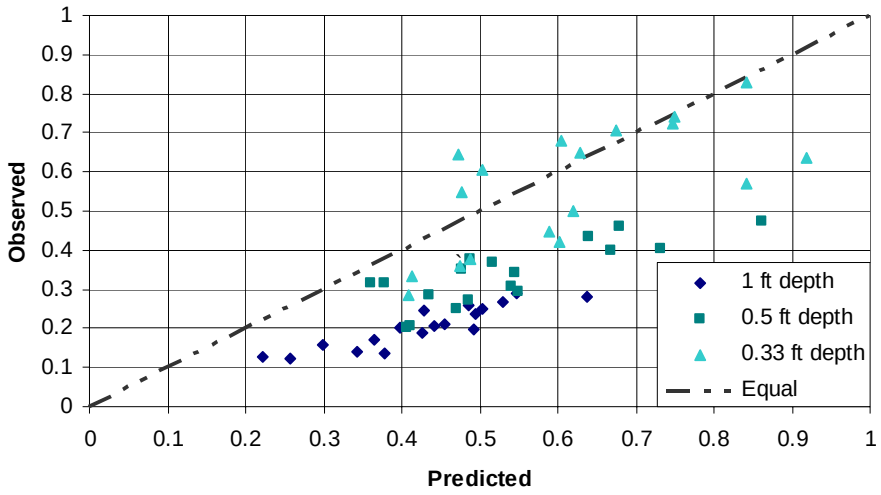

R^2	Average efficiency error (%)	Maximum efficiency error (%)
0.574	17.7	39.0

Figure 5-3: Predicted vs. observed efficiency for Type 16 combination inlet from UDFCD methods

For the Type R curb inlet, efficiency was determined using Equation 2-11, Equation 2-13, and Equation 2-14 as a direct calculation. Efficiency comparison with the observed test data is presented in Figure 5-4, where agreement is best for high flow depths. Measured top width, velocity, and cross-sectional flow area for each inlet test were used in the calculations and are provided in Appendix F. Accuracy of these methods for the Type 13, 16, and R inlets will be improved in Section 5.2 when the UDFCD methods are extended to include them directly.

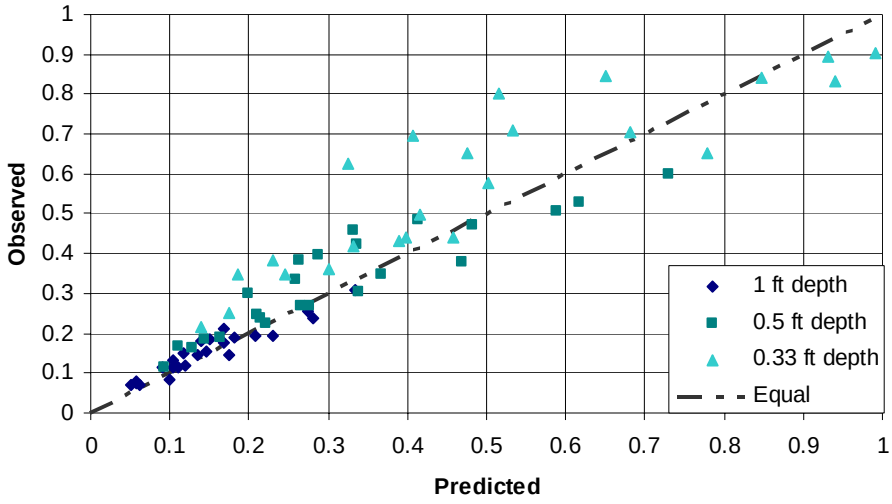

R^2	Average efficiency error (%)	Maximum efficiency error (%)
0.861	6.5	30.2

Figure 5-4: Predicted vs. observed efficiency for Type R curb inlet from UDFCD methods

For the most similar inlets to the Type 13 and 16 combination inlets currently available in the *USDCM*, the UDFCD methods over-predict efficiency by an average of about 20%. For the most similar inlet to the Type R curb inlet currently available in the *USDCM*, the UDFCD methods generally under-predict efficiency by an average of 7%. These predictions can be improved by slight modification of the currently-accepted design methods.

5.2 Improvements to UDFCD Efficiency Calculation Methods

One of the research objectives of this study was to extend the UDFCD methods for determining inlet efficiency to include the Type 13 and 16 inlets, and to improve methods for the Type R curb inlet. From the plots presented in Section 5.1, it can be seen that efficiency was generally over-predicted for the combination inlets and under-predicted for the curb inlet. For grate-type inlets, the only equation given in the *USDCM* that is grate-specific was presented previously as Equation 2-8 for calculating splash-over velocity (V_o). Coefficients used in the third-order polynomial of Equation 2-8 to calculate V_o are what need to be developed for the Type 13 and 16 inlets. Splash-over velocity is a unique value for a given grate type and length. By inspection of testing photographs and recorded videos, it was concluded that flow velocity in

the model was often either lower or higher than the exact point of splash-over velocity for a given grate length. No efforts were made to directly measure splash-over velocity in this study. It was possible, however, to determine a theoretical splash-over velocity from the efficiency, velocity, and flow characteristics of each applicable test. The approach presented here is to back-calculate V_o from the equations given previously in Sections 2.2.1 and 2.2.2. A unique value for V_o can then be determined for a given inlet length from a regression of the results. When Equation 2-7 is solved for V_o, the following form presented as Equation 5-1 results:

$$V_o = V - \left[\frac{\left(1 - R_f\right)}{0.09} \right] \qquad \textbf{Equation 5-1}$$

where:

V = velocity of flow at the inlet (ft/s) determined from Q/A;
V_o = splash-over velocity (ft/s); and
R_f = ratio of frontal flow captured by the inlet to the total frontal flow.

In Equation 5-1, the parameter R_f must be less than or equal to one to determine a physically-meaningful splash-over velocity. When R_f is greater than or equal to one, flow velocity is less than or equal to splash-over velocity and all frontal flow is captured by a grate. When R_f is less than one, flow velocity is greater than splash-over velocity and splashing of some frontal flow over a grate occurs. As grate length increases, flow velocity must increase for water to splash completely over a grate. When Equation 2-10 is solved for R_f, the following form presented as Equation 5-2 results:

$$R_f = \left[E - R_s \left(\frac{Q_s}{Q} \right) \right] \frac{Q}{Q_w} \qquad \textbf{Equation 5-2}$$

where:

E = inlet capture efficiency;
R_s = ratio of side flow captured to total side flow;
R_f = ratio of frontal flow captured by the inlet to the total frontal flow;
Q = volumetric flow rate (cfs);
Q_w = flow rate in the depressed section of the gutter (cfs); and
Q_s = flow rate in the section above the depressed section (cfs).

Parameters Q_w, Q_s, and R_s were calculated directly from the geometry of the street and gutter sections using the applicable equations presented previously in Sections 2.2.1 and 2.2.2.

Total flow (Q) is known from the observed test data, and efficiency can be calculated as the ratio of captured inlet flow to total street flow for each test. Data were collected for combination inlets of varying length, but no data were collected for grate inlets of varying length. Therefore, the only approach possible for determining splash-over velocity was to use the combination-inlet data. Equation 5-2 and Equation 5-1, when used together, give a calculated value for splash-over velocity. Use of these two equations for each grate type gave a range of values for V_o. Many of these values were negative, which implies that conditions for these tests exceeded the limitations of Equation 2-10. Remaining positive values for V_o were plotted against inlet length. A third-order polynomial regression in the form of Equation 2-8 was fit to the V_o data and the coefficients are provided in Table 5-1 for the Type 13 and 16 combination inlets. Also shown in this table is a comparison between the splash-over velocity regressions developed for the Type 13 and 16 combination inlets and those for the most similar inlets from the *USDCM*. Use of equations developed from regression procedures allowed splash-over velocity to be accounted for when it occurred at a velocity other than what was directly observed in the test data. It should be restated here that these results for V_o are applicable to combination inlets only, which is not consistent with development of the other coefficients in Table 2-4, which are for the grates only. Given the tests performed in this study, developing a V_o trend for grate-only inlets was not possible. By updating the splash-over velocity coefficients, a more accurate determination of combination-inlet efficiency by the UDFCD methods given in Sections 2.2.1 and 2.2.2 was possible. Efficiency predicted by these methods is compared to observed efficiency in Figure 5-5 and Figure 5-6. A tabular, test-by-test, comparison of efficiency data is presented in Appendix H for the Type 13 and 16 combination inlets.

Table 5-1: Updated splash-over velocity coefficients and plots

Grate	α	β	γ	η	R^2
Type 13	0	0.583	0.030	0.0001	0.43
Type 16	0	0.815	0.074	0.0024	0.24

where: $V_o = \alpha + \beta L_e - \gamma L_e^2 + \eta L_e^3$

Type 13 grate inlet

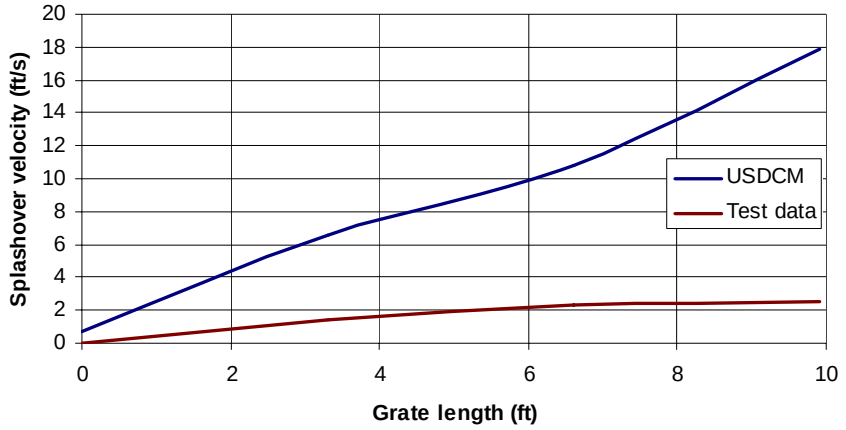

Type 16 grate inlet

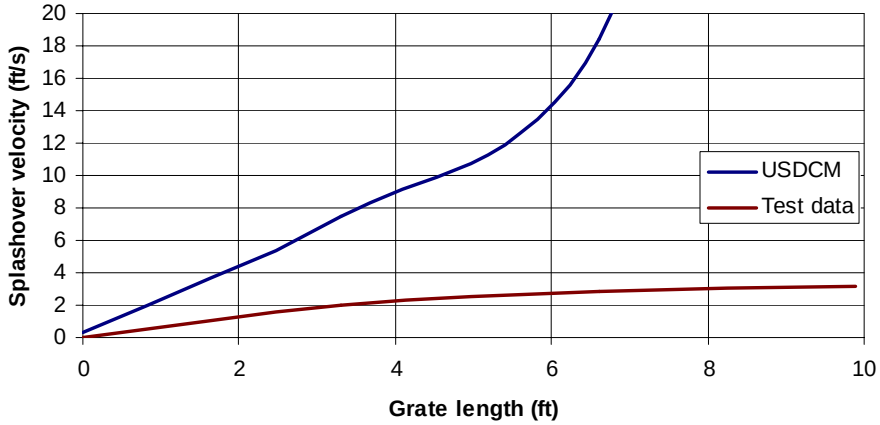

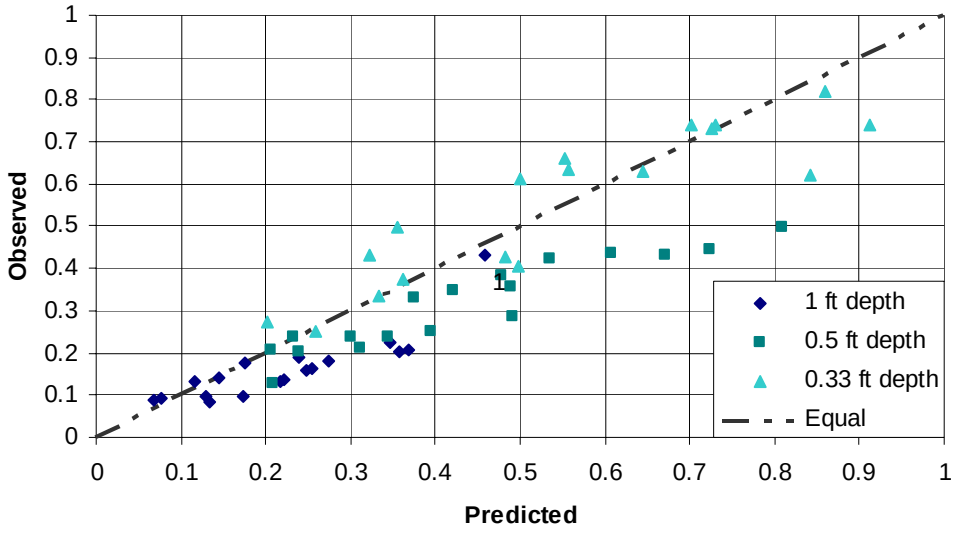

R^2	Average efficiency error (%)	Maximum efficiency error (%)
0.804	8.6	31.0

Figure 5-5: Predicted vs. observed efficiency for Type 13 combination inlet from improved UDFCD methods

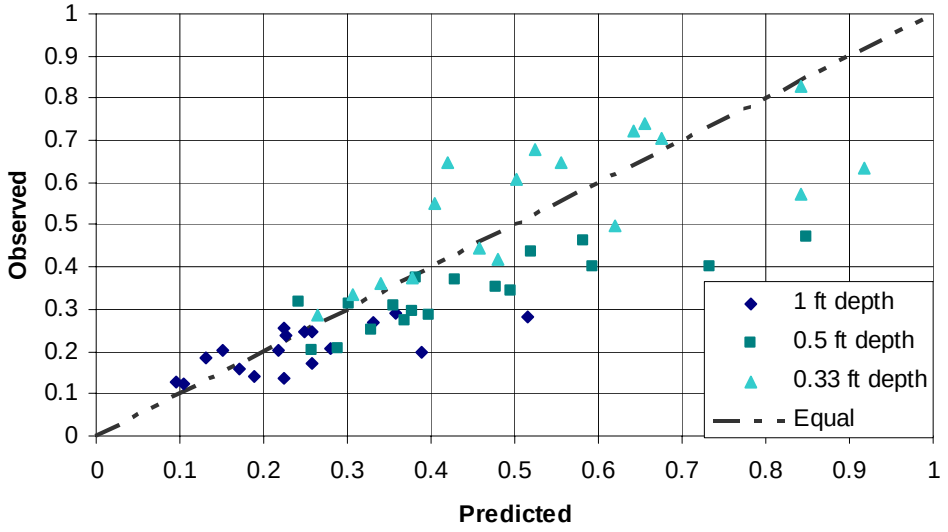

R^2	Average efficiency error (%)	Maximum efficiency error (%)
0.644	13.6	39.0

Figure 5-6: Predicted vs. observed efficiency for Type 16 combination inlet from improved UDFCD methods

Efficiency for the Type R curb inlet presented in Section 5.1 was calculated from Equation 2-11 and Equation 2-13. Calculated efficiency from these two equations can be improved by updating the coefficient and exponents of Equation 2-13. By doing this, the original form of the equation is preserved. Equation 5-3 illustrates the general form of this equation, where the coefficient *N* and the exponents *a*, *b*, and *c* will be determined by regression of the test data:

$$L_T = NQ^a S_L^b \left(\frac{1}{nS_e} \right)^c \qquad \textbf{Equation 5-3}$$

where:

L_T	=	curb opening length required to capture 100% of gutter flow;
Q	=	gutter flow (cfs);
S_L	=	longitudinal street slope (ft/ft);
S_e	=	equivalent street cross slope (ft/ft);
n	=	Manning's roughness coefficient;
N	=	regression coefficient; and
a,b,c	=	regression exponents.

The improved results of using Equation 5-3 to determine efficiency are presented in Figure 5-7. A tabular test-by-test comparison is presented in Appendix B for the Type R curb inlet. The final form of this equation is presented as Equation 5-4:

$$L_T = 0.38 Q^{0.51} S_L^{0.058} \left(\frac{1}{nS_e} \right)^{0.46} \qquad \textbf{Equation 5-4}$$

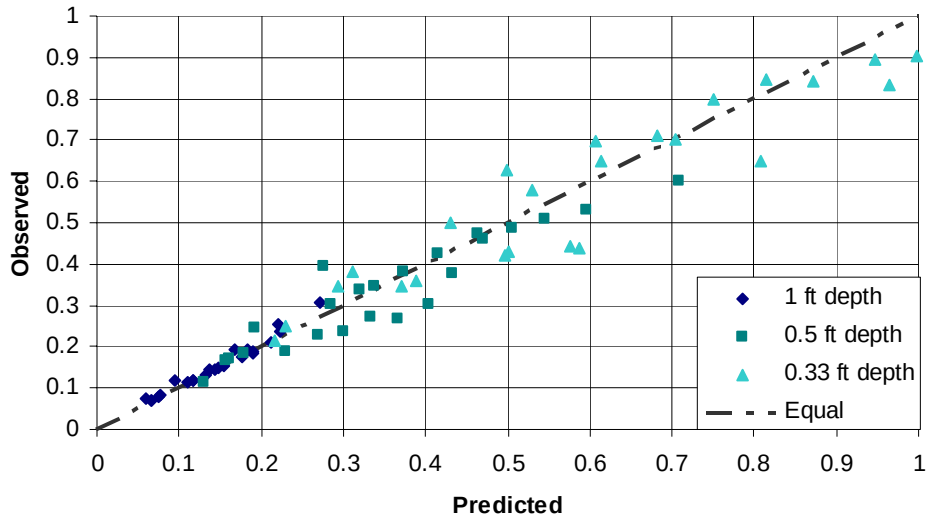

R^2	Average efficiency error (%)	Maximum efficiency error (%)
0.948	3.8	15.7

Figure 5-7: Predicted vs. observed efficiency for Type R curb inlet from improved UDFCD methods

Efficiency predictions by the UDFCD methods were improved slightly for each of the inlets tested. The methods were extended to include the Type 13 and 16 combination inlets, with efficiency over-predicted by an average of 10%. For these inlets, agreement with observed test data is still best at low flow depth. For the Type R curb inlet, UDFCD methods were modified slightly, and efficiency error spread evenly at 3.8%. Agreement is still best at higher flow depths, and has been improved for the lowest depth. Efficiency predictions can be further improved by developing new empirical relationships for each inlet.

5.3 Efficiency from Dimensional Analysis and Empirical Equations

In this section empirical equations are presented, as an alternative to the use of the UDFCD methods, for determination of inlet efficiency for the Type 13 combination, Type 16 combination, and Type R curb inlets. Equations presented will provide a simpler and more accurate method, than that presented in the *USDCM*, for determining efficiency in the on-grade condition. Methods presented in the *USDCM* suffer from, in part, use of theoretical parameters that can not be physically determined by a user (such as splash-over velocity, R_f, R_s, Q_w, and Q_s).

From a design perspective, a user approaching an inlet design situation will know several parameters: street flow (and velocity from continuity), design flow depth (and area), allowable spread of flow, street longitudinal slope, and street cross slope. Given values for those parameters, a suitable inlet length is typically sought that provides an acceptable degree of flow capture efficiency for a particular street location. A desirable equation will utilize physically-known parameters in a form that is easily applied to determine efficiency.

It was possible to develop one equation for each inlet type to predict the basic on-grade test data. Power regression equations were used because of their easy integration with dimensional analysis, which was described as the process of selecting parameter groups for use in equation development. Application of dimensional analysis began with simply identifying the parameters of interest. Parameters typically known or desired by a designer are re-stated in functional form as:

$$E = f(S_c, S_L, V, L, h, A, T) \qquad \textbf{Equation 5-5}$$

where:

E = inlet capture efficiency;
S_c = cross slope;
S_L = longitudinal slope;
V = velocity (ft/s);
L = grate or inlet length (ft);
h = depth of flow in the gutter (ft);
A = flow area (ft^2); and
T = top width of flow spread from the curb face (ft).

Calculation of values for parameters in Equation 5-5 was necessary for each test, and they are given in Appendix F by test number. Parameters in Equation 5-5 were arranged into dimensionless groups (called Pi groups) using the Buckingham Pi theorem described previously in Section 2.5. Units were made consistent in several dimensionless groups by use of the gravitational constant (g). Applying the Buckingham Pi theorem, with repeating variables of V and h or V and L, resulted in the following dimensionless parameter groups:

$$\Pi_1 = \frac{h}{L}, \Pi_2 = \frac{V^2 T}{gA}, \Pi_3 = \frac{V^2}{gh}, \Pi_4 = \frac{V^2}{gL}, \Pi_5 = S_c, \Pi_6 = S_l, \Pi_7 = E$$

The second Pi group is the square of the Froude number for a general channel cross section, and the third Pi group is the Froude number for a rectangular channel. Both forms of the Froude number were tested for statistical significance, and either form was used in the final equations. Compiling the Pi groups into power-equation form resulted in Equation 5-6:

$$E = N\left(\frac{h}{L}\right)^{a}\left(\frac{V^2T}{gA}\right)^{b}\left(\frac{V^2}{gh}\right)^{c}\left(\frac{V^2}{gL}\right)^{d}(S_c)^{e}(S_l)^{f} \qquad \textbf{Equation 5-6}$$

where:

N	=	coefficient of regression;
a,b,c,d,e,f	=	regression exponents to be determined by statistical analysis of the test data; and

remaining parameters were defined previously.

The computer application Statistical Analysis Software (SAS) was used to efficiently analyze the large amount of test data. Analysis was carried-out using the logarithms of each Pi group so a multi-variable linear regression model could be fit to the data. Coefficients given by a linear model for each independent variable are the exponents (*a*, *b*, *c*, *d*, *e*, and *f*) and the y-intercept given is the logarithm of the coefficient *N* for the equivalent power-equation form, as shown in Equation 5.7:

$$\Pi_6 = N\,\Pi_1^{a}\,\Pi_2^{b}\,\Pi_3^{c}\,\Pi_4^{d}\,\Pi_5^{e}\,\Pi_7^{f}\text{, or}$$

$$\log\Pi_6 = \log N + a\log\Pi_1 + b\log\Pi_2 + c\log\Pi_3 + d\log\Pi_4 + e\log\Pi_5 + f\log\Pi_7 \qquad \textbf{Equation 5-7}$$

The Statistics Department at CSU was consulted to assist in examination of the regression statistics from SAS. When a regression is performed using SAS, the significance of each parameter is examined and the effect of each possible parameter combination on the regression fit is tested. Significance of each parameter is evaluated by dividing the standard error of the parameter estimate by the estimate itself. The result is called the "*t*" value and a significant parameter has an absolute *t* value greater than 2 (i.e., the estimate itself is at least two times larger than its error, and the 95% confidence interval for the estimate is two times the standard error). The level of confidence that a parameter estimate has not arisen by chance (called the significance level) is also evaluated by SAS and reported as the *Pr* value. A *Pr* value

less than 0.0001 (the minimum level reported by SAS) means that there is less than a one in ten thousand chance that the parameter estimate could have arisen by chance. Parameter groups that did not give a *t* value >2 and a *Pr* value <0.0001 were eliminated from the model for each inlet type. The effect of each parameter group on the overall regression fit was examined by checking the R^2 value as different combinations of groups were used. By doing this, statistically-significant parameter groups were combined in the best possible way to achieve the highest R^2 value. Finally, the range of predicted values for the dependent variable was checked for outliers by application of the Studentized residual test by SAS. A Studentized residual greater than three is an indicator that a predicted value has exceeded three standard deviations from the mean predicted value. No outliers were noted in the analysis.

Equations developed are presented in their parameter group form and a simplified form determined by combining like terms. Final empirical equations and statistical summaries are presented in Table 5-2. A detailed statistical analysis from SAS for each equation in linear form is provided in Appendix G. Results from applying the empirical equations are plotted against the observed test data for efficiency in Figure 5-8 through Figure 5-10. The long slope parameter was not found to be statistically significant for any of the inlets. For the Type 13 and 16 inlets, the general form of the Froude number was preferred over the rectangular form, and use of the cross slope parameter was not necessary. For the Type R curb inlet, use of the first Pi group was not necessary and no statistical advantage was achieved by use of the general form of the Froude number, so the simplified form for a rectangular cross section was used. Tabular values of efficiency determined from these equations for each test are provided in Appendix H.

Table 5-2: Empirical equations for grate and curb inlets

Inlet	Predictive Equation	Simplified Form	
Type 13 Combination	$E = 0.063\left(\frac{h}{L}\right)^{0.665}\left(\frac{V^2T}{gA}\right)^{0.835}\left(\frac{V^2}{gL}\right)^{-1.138}$	$E = \frac{h^{0.665}T^{0.835}V^{-0.606}}{L^{-0.473}A^{0.835}g^{-0.303}}$	Equation 5-8

R^2	Average efficiency error (%)	Maximum efficiency error (%)
0.895	4.7	22.6

Type 16 Combination	$E = 0.095\left(\frac{h}{L}\right)^{0.573}\left(\frac{V^2T}{gA}\right)^{0.756}\left(\frac{V^2}{gL}\right)^{-0.920}$	$E = \frac{h^{0.573}T^{0.756}V^{-0.328}}{L^{-0.347}A^{0.756}g^{-0.164}}$	Equation 5-9

R^2	Average efficiency error (%)	Maximum efficiency error (%)
0.844	5.1	21.9

Type R Curb	$E = 0.076\left(\frac{V^2}{gh}\right)^{0.545}\left(\frac{V^2}{gL}\right)^{-0.879}(Sc)^{0.231}$	$E = \frac{V^{-0.328}S_c^{0.231}}{L^{-0.879}h^{0.545}g^{-0.334}}$	Equation 5-10

R^2	Average efficiency error (%)	Maximum efficiency error (%)
0.890	5.1	29.1

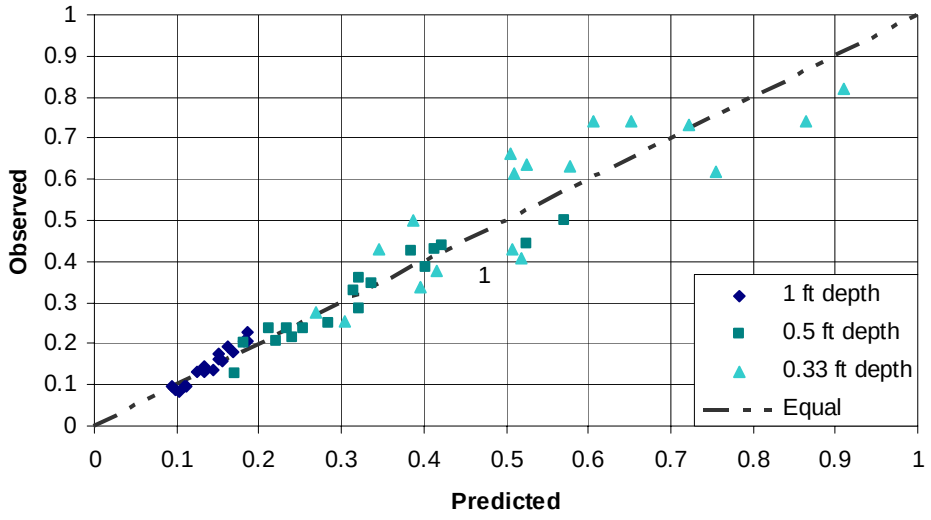

Figure 5-8: Predicted vs. observed efficiency for Type 13 combination-inlet from empirical equation

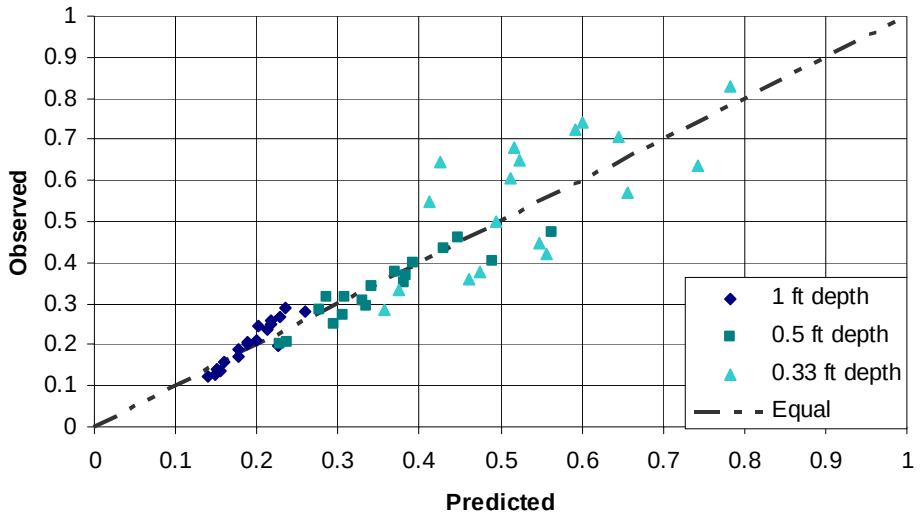

Figure 5-9: Predicted vs. observed efficiency for Type 16 combination-inlet from empirical equation

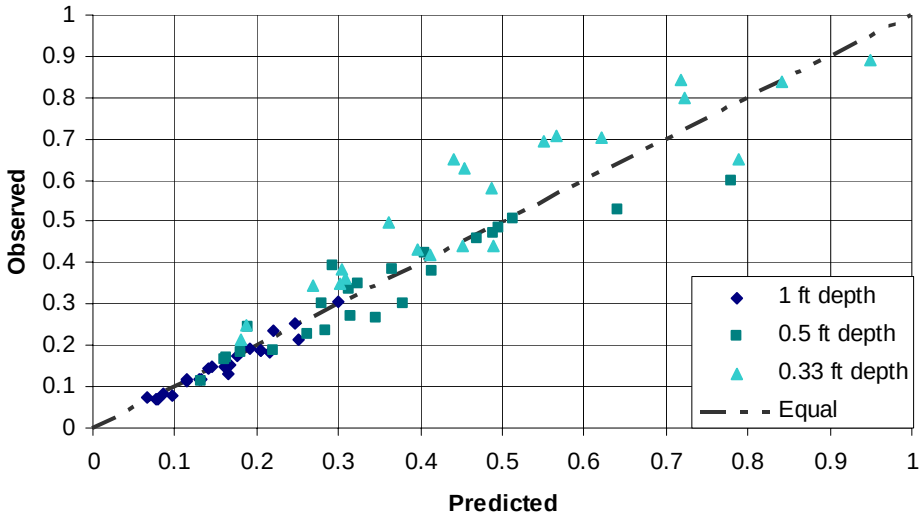

Figure 5-10: Predicted vs. observed efficiency for Type R curb inlet from empirical equation

By developing new equations to predict efficiency, it was possible to further improve predictions for inlet efficiency over previous sections. With new equations presented here, the average error in predicted efficiency was reduced to about 5% for all inlets with R^2 values between 0.84 and 0.90. Overall agreement between observed and predicted efficiency is improved over previous methods for all test depths. A comparison is shown in Figure 5-11 through Figure 5-13 between the empirical equations and the improved UDFCD methods.

Agreement is best at the smallest flow depth for the Type 13 and 16 inlets. This is due to the test conditions of the original FHWA model described previously which only tested to a maximum depth of 0.45 ft. For the Type R curb inlet, agreement is best at a high-flow depth.

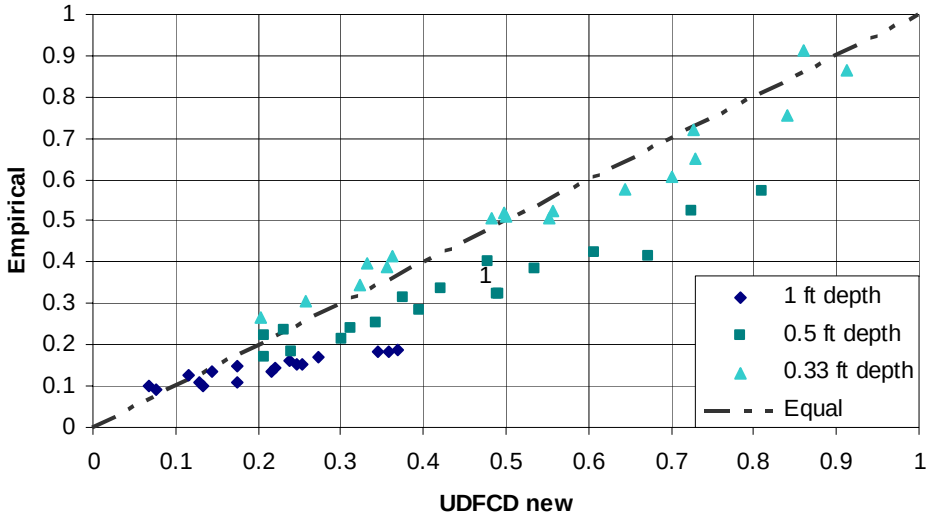

Figure 5-11: Type 13 combination-inlet efficiency comparison

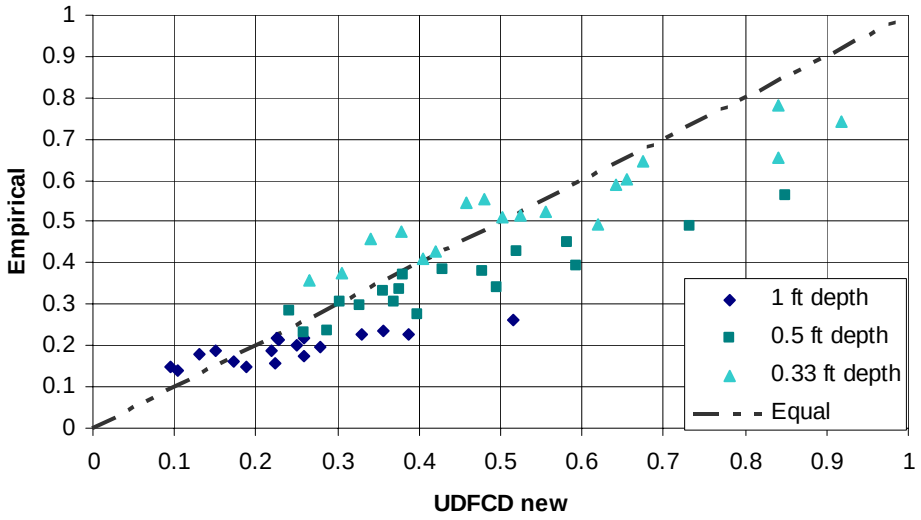

Figure 5-12: Type 16 combination-inlet efficiency comparison

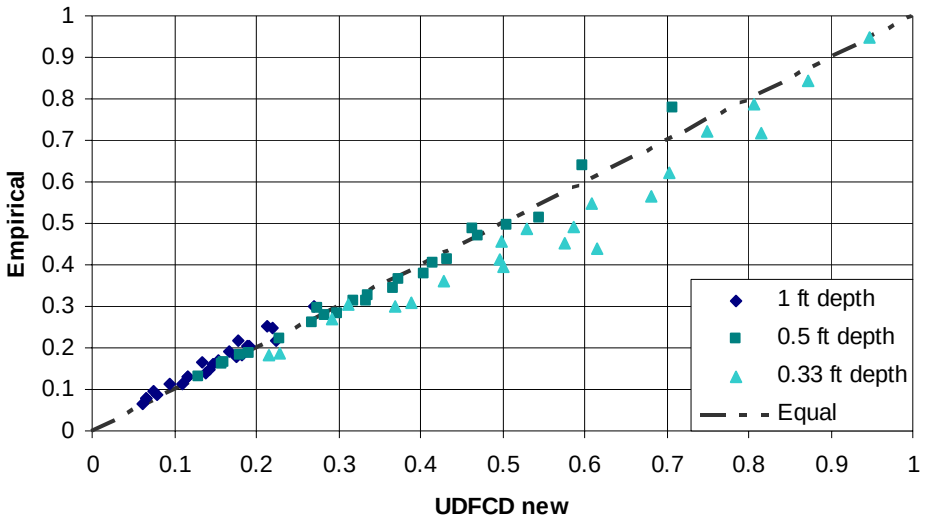

Figure 5-13: Type R curb inlet efficiency comparison

A sensitivity analysis was performed on each of the variables in Equation 5-8 through Equation 5-10 to quantify the magnitude of change in efficiency from a change in any of the independent variables, results are presented in Figure 5-14 through Figure 5-16, respectively. Base values for each parameter were chosen as the median values observed in testing. Each parameter was varied throughout the range of test conditions while other parameters were held at their base values, which produced a range of values for efficiency. Normalizing each parameter value and corresponding efficiency by their base values then produced a curve centered about one. Use of these figures allows for quantification of the effects from varying each parameter on inlet efficiency. For example, when the Type 13 and 16 combination inlets are increased in length by 50% the efficiency increases by approximately 20%. For the Type R curb inlet a 50 % increase in length results in an efficiency increase of about 40%. A similar comparison could be made for flow velocity, depth, or top width of flow. As expected, the equations are most sensitive to changes in velocity and flow area (or depth in the case of the Type R curb inlet). The Type 16 is less sensitive to changes in velocity than the Type 13 due to the directional vanes on the grate. Type 16 and 13 equations are least sensitive to changes in inlet length due to most flow entering the first grate for those inlets, whereas the Type R equation is least sensitive to changes in street cross slope due to the deep local inlet depression.

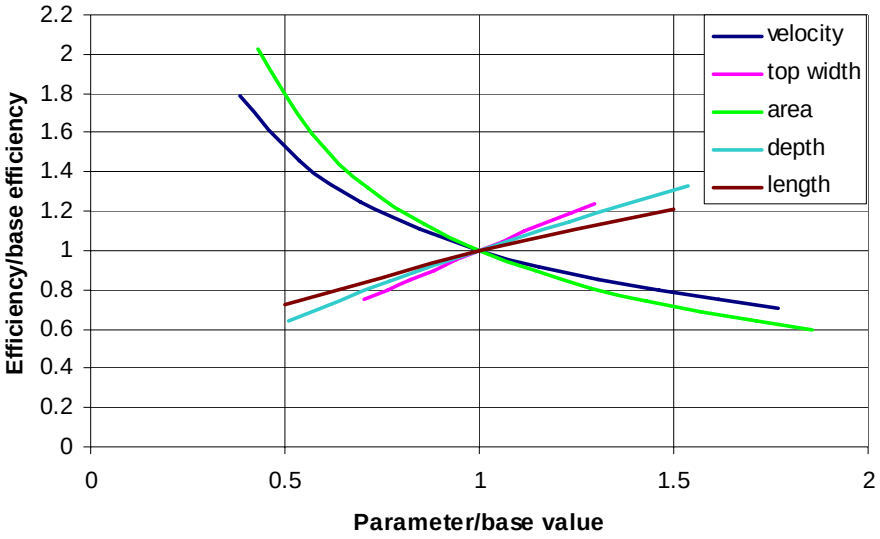

Figure 5-14: Type 13 combination-inlet regression parameter sensitivity

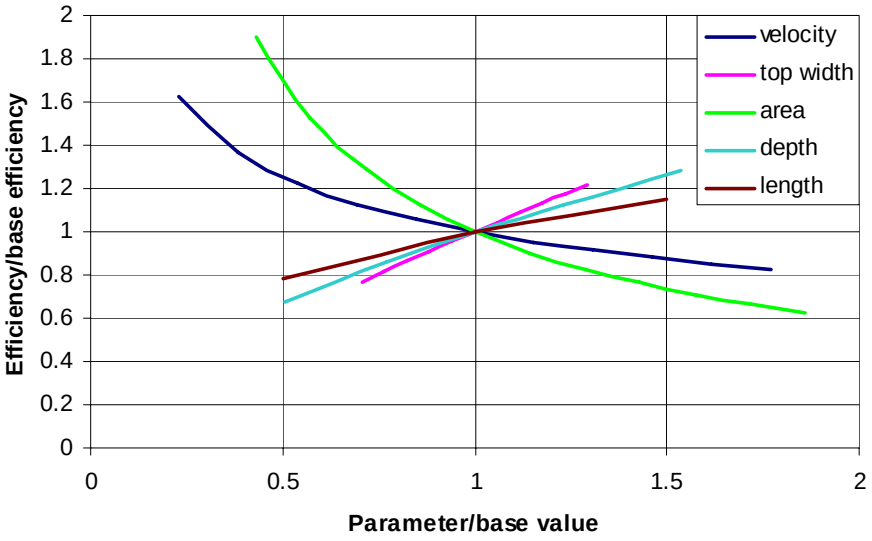

Figure 5-15: Type 16 combination-inlet regression parameter sensitivity

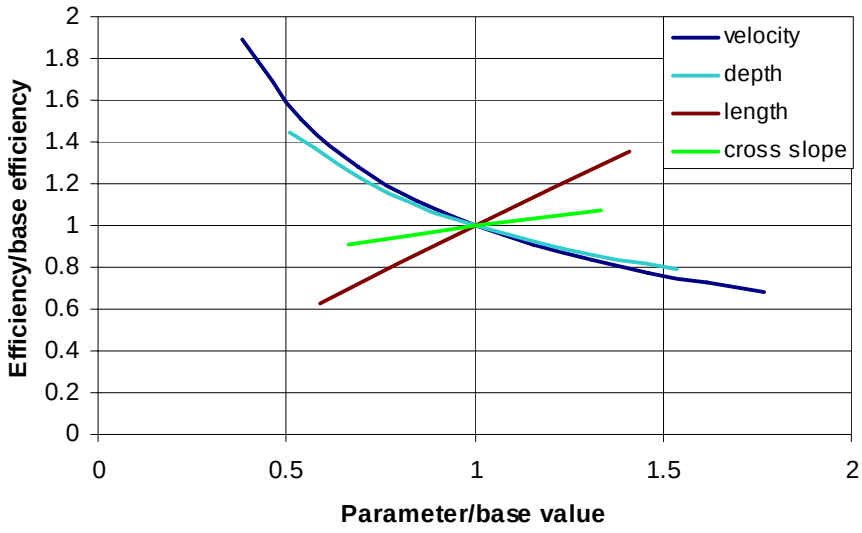

Figure 5-16: Type R curb inlet regression parameter sensitivity

5.4 Combination-inlet Efficiency Compared to Grate and Curb Inlet Efficiency

The difference in efficiency between a combination inlet, a grate-only inlet utilizing the same grate as the combination inlet, and a curb-only inlet utilizing the same curb opening as the combination inlet is illustrated in this section. Of the 318 tests performed, twelve test configurations were performed with the combination inlet and then repeated with the grate only and the curb opening only. These tests were performed with single Type 13 and 16 grates. Graphical comparisons were developed in which the efficiency for each configuration (grate only, curb only, and their sum) was plotted against the combination-inlet efficiency, and are presented in Figure 5-17 and Figure 5-18. An efficiency difference is read in these figures from the combination-inlet line to the desired inlet configuration line. Differences in efficiency can be determined from these figures when, for instance, the combination-inlet efficiency is known but the grate-only efficiency is desired. Similar comparisons can be made between the combination-inlet efficiency and the sum of the grate-only and curb-only efficiencies. An average difference of 3% efficiency was observed when the combination and the grate-only inlets were compared, and an average difference of 12% efficiency was observed when the combination and curb-only inlets were compared. When the curb-only and grate-only efficiencies are summed, they over-predict combination-inlet efficiency by an average of 7%. The largest differences in efficiency

were typically seen at higher flow depths when the inlets became submerged. Performing similar comparisons for two and three grates would be useful, but no data were collected for configurations consisting of more than one grate or curb inlet. At lower flow depths (where flow is entirely below the curb) for multiple curb openings, little difference would likely be seen due to the observation that, at lower depths, almost no flow enters through the second and third curb openings in the combination-inlet configuration. At higher flows (where the flow is at or above the curb) all curb openings are expected to contribute significantly due to submergence, and the difference in efficiency could be greater.

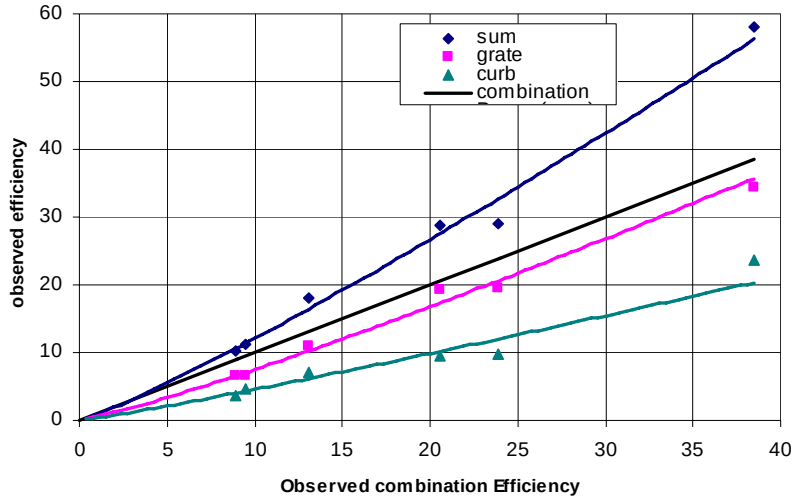

Figure 5-17: Type 13 inlet configurations and efficiency

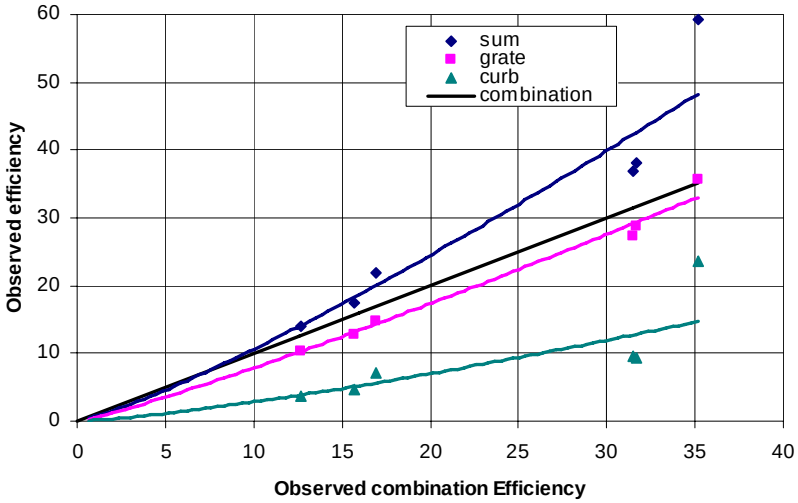

Figure 5-18: Type 16 inlet configurations and efficiency

5.5 Relevance of Uniform Flow in Data Analysis

Gutter flow is by nature unsteady and non-uniform during storm events, but is often assumed steady and uniform for design purposes (UDFCD, 2008). In the original FHWA study (FHWA, 1977) used to develop current methods given in the *USDCM* for the Type 13 and 16 inlets, it was stated that uniform flow conditions were created in the model. In contrast, uniform flow was not specifically sought in the model used in this study. A physically-relevant model was developed to reproduce actual field conditions in which the existence of uniform flow is uncertain. The horizontal approach section and diffuser screen used in the UDFCD model were intended to provide for energy dissipation and to allow flow conditions to stabilize. In this section, the relevance of achieving uniform flow in the model for data analysis purposes is explored.

A comparison was made between the observed test data and the test data adjusted to conditions of uniform flow. Test data were adjusted to conditions of uniform flow by using the observed roughness, depth, flow area, hydraulic radius, and bottom slope in Manning's equation to calculate velocity. Efficiency was assumed not to change between conditions of uniform flow or otherwise. Analysis presented in Sections 5.2 and 5.3 were repeated with the adjusted velocity. In Figure 5-19, the results of repeating the analysis of Section 5.3 are presented. Empirical equations were re-developed from the corrected data set, and efficiency is compared to that calculated from the original empirical equations.

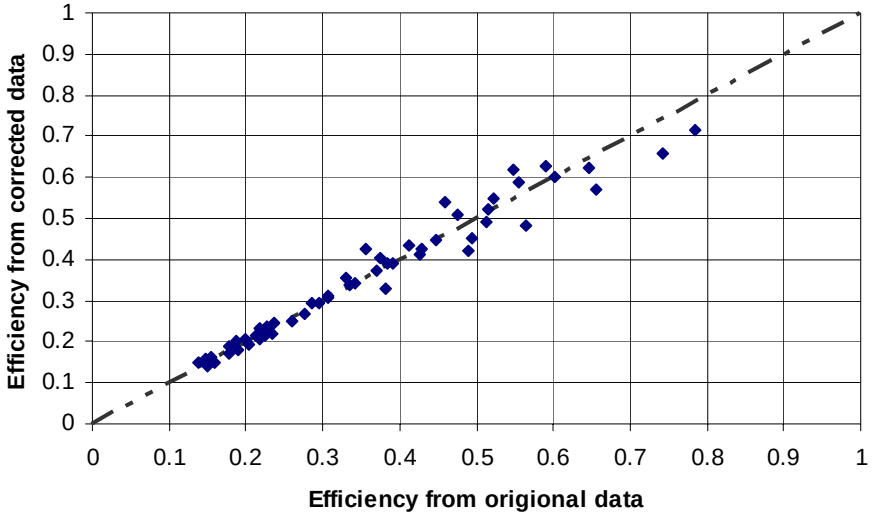

Figure 5-19: Efficiency comparison from empirical equations (Type 16 inlet)

Average difference in calculated efficiency between the corrected and uncorrected data sets was 2.3% and the R^2 value was 0.97, with the greatest differences occurring at lower velocities. Based on that small difference, the empirical equations are not sensitive to uniform-flow conditions. In Figure 5-20, the results of repeating the analysis of Section 5.2 are presented. The splash-over velocity coefficients were redeveloped for the corrected data set, the calculations presented in Section 2.2 for grate inlets were repeated, and the efficiencies are plotted against each other.

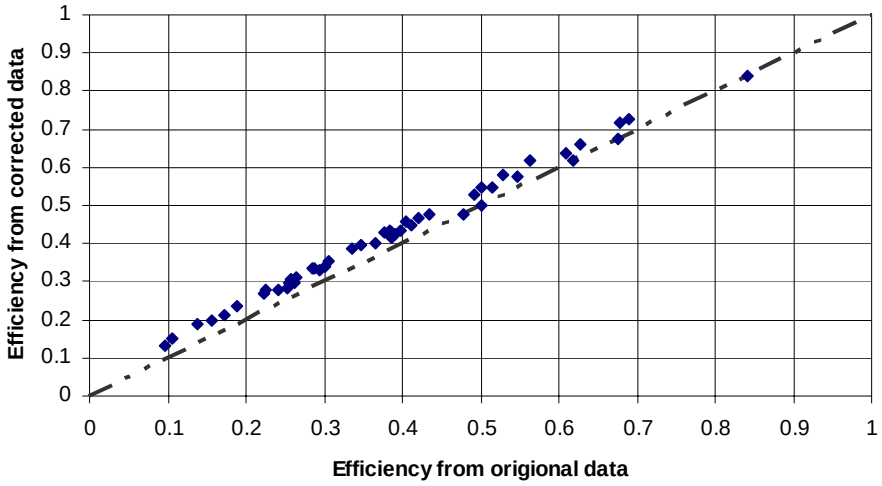

Figure 5-20: Efficiency comparison from UDFCD methods (Type 16 inlet)

Average difference in calculated efficiency between the corrected and uncorrected data sets was 4% and the R^2 value was 0.99, with the greatest differences occurring at lower velocities. This is due to the UDFCD methods being least accurate at low velocity. The existence of uniform flow is more significant for the UDFCD methods than for the empirical equations, and could be significant when the inlet efficiency is low (such as less than 10%). But typical inlet designs are made to be highly efficient (greater than 50%). Based upon the small differences in efficiency seen, the existence or non-existence of uniform flow in the model was found to not significantly affect the results of predicting efficiency by the methods used in this analysis.

5.6 Summary

The current state-of-the-art in determining inlet efficiency was illustrated in this chapter by application of methods provided in the *USDCM* to the Type 13, 16, and R inlets. Agreement with observed test data was generally very poor with efficiency over-predicted by an average of 20% for the Type 13 and 16 inlets and under-predicted by an average of 7% for the Type R curb inlet. Methods given in the *USDCM* were improved by developing splash-over velocity coefficients specifically for the Type 13 and 16 combination inlets. While splash-over velocity was not specifically sought in the testing, it was determined analytically from the collected test data for the combination inlets. This was done by utilizing the accepted calculation procedures given in the *USDCM* to back-calculate the splash-over velocity for each test. A third-order polynomial regression was then fitted to the calculated splash-over velocity data to provide updated coefficients. The splash-over velocity coefficients are reflective of the combination-inlet performance, not the grate-only inlet performance, and provide a considerably improved fit to the observed efficiency data with efficiency errors averaging 10%. *USDCM* calculation procedures for the Type R curb inlet were improved by re-developing the regression coefficient and exponents for the original equation. The form of the original equation was preserved, and the overall fit to the observed efficiency data was improved considerably with efficiency errors averaging 3.8%.

Development of independent empirical equations by dimensional analysis provided an alternative approach to the currently used UDFCD methods. Physically-meaningful parameters were combined to produce a single, dimensionally consistent, equation for each inlet. These equations were found to predict efficiency values that differed by an average of 5% from the observed test data for each of the Type 13, 16, and R inlets. A comparison, by depth and inlet type, for all methods is presented in Table 5-3. In this table, each method is compared to the observed test data for maximum and average efficiency error. The original UDFCD methods were most accurate at the lowest test depth of 0.333 ft for the Type 13 and 16 inlets. For the Type R inlet they were most accurate at larger depths. Improved UDFCD methods show significant improvement at larger depths. Empirical equations were most accurate at 0.5- and 1-ft depths. Recommendations for calculation method use are given in the conclusion chapter of this report. A tabular, test-by-test efficiency calculation comparison is presented in Appendix H.

Table 5-3: Efficiency error by depth and inlet type

Average Efficiency Error (%)				Maximum Efficiency Error (%)			
Depth (ft)	UDFCD	UDFCD New	Empirical	Depth (ft)	UDFCD	UDFCD New	Empirical
Type 16				Type 16			
0.333	10.8	9.7	10.3	0.333	28.1	28.1	21.9
0.5	19.9	11.6	2.8	0.5	39.0	37.7	9.2
1	22.3	6.0	2.3	1	35.4	23.4	5.5
Type 13				Type 13			
0.333	8.9	7.2	8.6	0.333	22.2	22.2	15.5
0.5	22.4	12.2	2.9	0.5	32.3	31.0	8.1
1	25.3	6.7	1.5	1	34.0	16.4	4.2
Type R				Type R			
0.333	11.6	6.5	10.0	0.333	30.2	15.7	29.1
0.5	5.8	4.1	4.0	0.5	13.0	11.9	17.9
1	2.1	0.9	1.2	1	4.6	3.7	3.8

An efficiency comparison was made between a combination inlet, a grate-only inlet, and a curb-only inlet for single Type 13 and 16 configurations. An average difference of 3% efficiency was observed when the combination and the grate-only inlets were compared, and an average difference of 12% efficiency was observed when the combination and curb-only inlets were compared. Lastly, the relevance of uniform flow in the model was examined by repeating the analysis with the observed test data adjusted to conditions of uniform flow. An average efficiency difference of approximately 3%, as calculated by all methods, was noted between uniform and non-uniform flow conditions in the model. From this small difference, the existence or non-existence of uniform flow in the model was found to not affect the analysis significantly.

6 CONCLUSIONS AND RECOMMENDATIONS

6.1 Conclusions

The data collected in this study, and the analysis performed, provided considerable insight into the performance of the Type 13, 16, and R inlets under varying hydraulic conditions. Physically-meaningful test conditions, that are likely to be encountered in the field, were created in the model to supply a more complete body of test data than was previously available. The on-grade test data were analyzed and improved methods were developed for determining inlet efficiency. These improvements included: extending the currently used UDFCD methods (from *HEC-22*) to include the Type 13 and 16 combination inlets, modifying the currently used UDFCD methods for the Type R curb inlet, and developing independent empirical equations for each of the three inlet types. The original UDFCD methods and equations were preserved in the analysis. Empirical equations presented were developed independently from the UDFCD methods, are dimensionally consistent, and provide a simple approach for calculation of inlet efficiency. Physically-meaningful parameters, which can be easily determined by a user, were combined using dimensional analysis to produce an equation for each of the Type 13 combination, Type 16 combination, and Type R curb inlets to predict inlet efficiency.

6.2 Recommendations for Inlet Efficiency Calculation

The following guidance is provided for interpretation and use of the design criteria developed in this study. Current UDFCD methods do not allow for determination of the true efficiency for a combination inlet, which should take into account both the grate and the curb openings. Design of combination inlets is typically done by assuming the grate portion of the inlet acts alone (UDFCD, 2008). Both the empirical equations and the improved UDFCD calculations presented in this report take into account the full capacity of the grate and the curb opening. When the improved UDFCD methods were compared to the empirical equations for the Type 13 and 16 combination inlets, the empirical equations were better able to predict the

test data for typical design depths of 0.5 to 1 ft. A 5% reduction in average efficiency error was noted, and a 10% reduction in maximum efficiency error was noted for all test depths over the improved UDFCD methods. UDFCD methods for these inlets were shown to rely heavily on theoretical parameters that can not be physically determined by a user; parameters are instead determined from complex empirical relationships. A comparison between splash-over velocity curves developed for the Type 13 and 16 combination inlets and those for the most similar grate inlets from the *USDCM* revealed significant differences. The equations provided in the *USDCM* give an unrealistically high splash-over velocity (on the order of 30 ft/s) for a 10-ft Type 13 or 16 combination inlet, which is in sharp contrast to the 4 ft/s determined from the test data. Original and improved UDFCD methods were most accurate at the lowest flow depth of 0.333 ft. Beyond that depth, the accuracy was very poor. This is likely due to the limitations of the FHWA model used to collect data for development of the equations. For the Type R curb inlet, the improved UDFCD methods were slightly better able to predict the observed efficiency data than the empirical equation for all test depths. A 1.2% improvement in average efficiency error was noted over the empirical equation, and a 15% reduction in maximum efficiency error was noted for all test depths. Typical design depths are 0.5 ft and greater for selection and placement of street inlets (UDFCD, 2008). With this in mind, recommendations for which calculation method to use are given as follows: for the Type 13 and 16 combination inlets the empirical equations are recommended, for the Type R curb inlet the improved UDFCD methods are recommended. For illustration purposes, the observed test data on efficiency are plotted with the empirical efficiency and the efficiency determined from the improved UDFCD methods in Figure 6-1 through Figure 6-3.

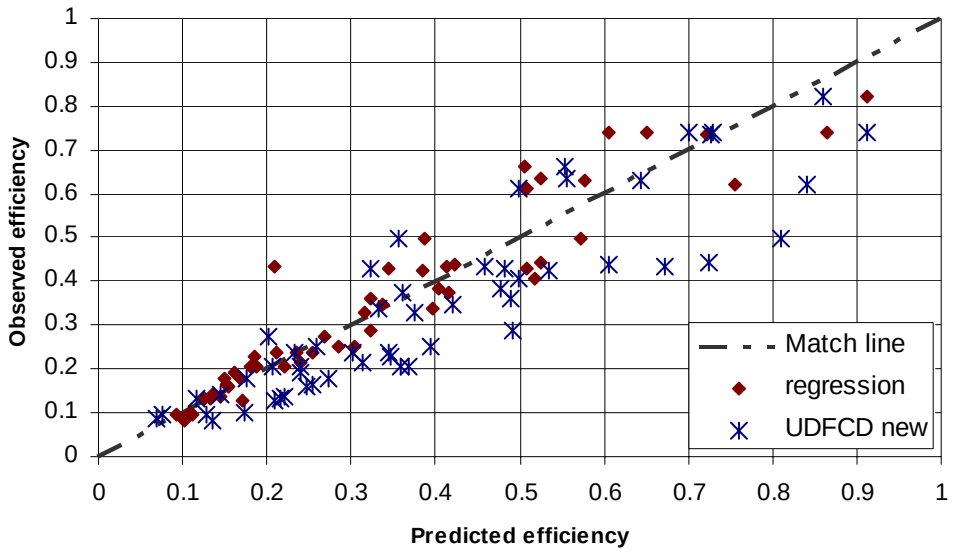

Figure 6-1: Type 13 combination-inlet efficiency from all improved methods

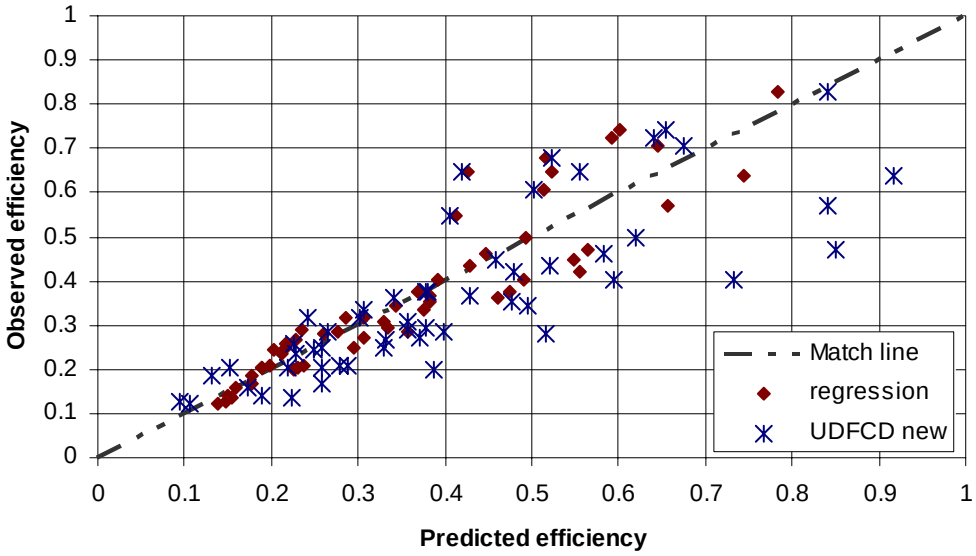

Figure 6-2: Type 16 combination-inlet efficiency from all improved methods

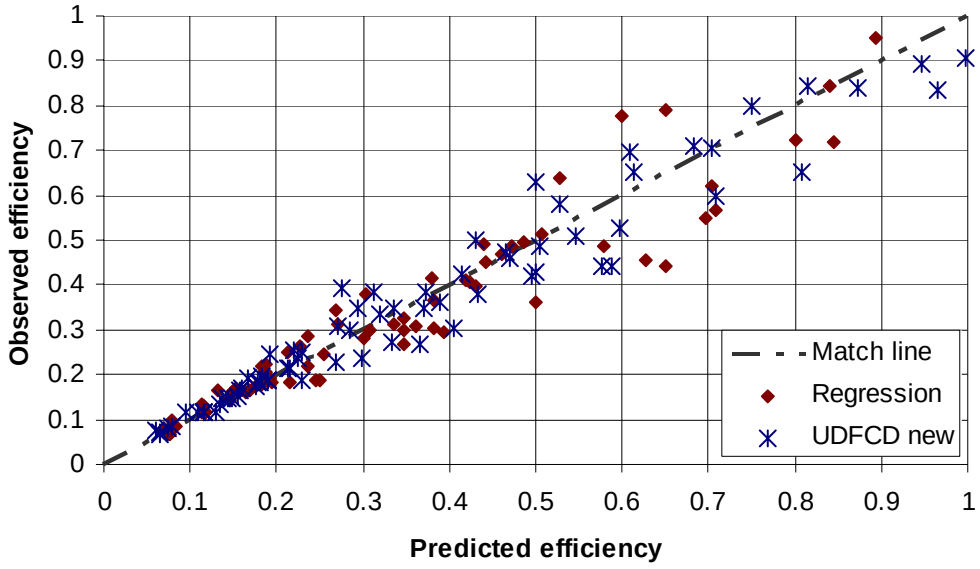

Figure 6-3: Type R curb inlet efficiency from all improved methods

6.3 Recommendations for Further Research

After examining the collected test data, and completing the analysis presented in this report, the need for several types of additional data became apparent. For the on-grade condition, use of the grate-only inlet configuration was done only for one inlet. In contrast, the combination inlet was used in numbers ranging from one to three inlets. Because of this, the body of test data for the grate-only inlet is incomplete when compared to the combination inlet. By gathering more data for the grate-only inlet, and performing a similar analysis to the one presented in this study, accurate methods could be developed for use of the Type 13 and 16 grates in varying numbers. As a minimum, the use of both Type 13 and 16 grates for two and three inlets at the 2% longitudinal and 1% lateral slope configuration would provide considerable insight. These slopes were the median of the ranges used in this study. At three depths per grate this would require a total of twelve tests.

Characteristics of two inlets used in this study resulted in high efficiency. The Type 16 grate has directional vanes that capture frontal flow very well. Although the grate is placed in a slight depression in the combination-inlet configuration, the depression is not as pronounced as for the Type R inlet. The Type R curb inlet has a local depression, well below the gutter flow line, that results in a high degree of capture of frontal and side flow. By combining these two

design characteristics, higher efficiency would result than either is capable of independently. The local depression would act to reduce splash-over and capture more side flow, while the directional vanes would capture frontal flow. A full testing program similar to this study would be required to develop design equations, or extend the UDFCD methods, for such an inlet. Engineering application of the Type 13 grate inlet typically involves placing a single grate in a sump condition with no curb component (such as in a parking lot or field). Placing a single Type 13 grate in such a configuration typically exposes it to direct flow from all sides. In the testing program performed for this study, the inlet was placed adjacent to a curb and exposed to lateral flow from three sides. Only at the 1-ft flow depth was it exposed to flow from over the curb. Testing the Type 13 grate in a true sump condition, where it is exposed to flow from all sides, would provide additional useful data. A slightly different model than the one used in this study would be necessary to collect data on this configuration.

For the analysis presented in this report, the observed test data were used in UDFCD methods developed from the original FHWA model data. The purpose was to adapt the UDFCD methods to include the inlets tested in this study. The converse of that analysis would be to use the FHWA model data in the empirical equations developed in this report. A comparison could then be made between the two methods and their ability to be adapted to suit other inlet types.

The additional testing suggested in this section would complete the body of knowledge available for common application of the Type 13, 16, and R inlets. The UDFCD methods could be easily extended to encompass the additional data, and independent design equations similar to those presented in this study could be developed for the additional configurations.

7 REFERENCES

Bos, M. G. (1989). Discharge Measurement Structures. Third Edition revised, The Netherlands: Institute for Land Reclamation and Improvement.

Chaudhry, M. H. (2008). Open Channel Flow. Second Edition, New York, NY: Springer.

Federal Highway Administration (2001). Hydraulic Engineering Circular No. 22, Second Edition, Urban Drainage Design Manual. Publication FHWA-NHI-01-021, Springfield, VA: U. S. National Technical Information Service.

Federal Highway Administration (1977). Hydraulic and Safety Characteristics of Selected Grate Inlets on Continuous Grades, Vol 1. Publication FHWA-RD-77-24, Springfield, VA: U. S. National Technical Information Service.

Fox, R. W. (2006). Introduction to Fluid Mechanics. Sixth Edition, New York, NY: John Wiley and Sons, Inc.

Julien, P. Y. (2002). River Mechanics. New York, NY: Cambridge University Press.

Li, W. H. (1956). Design of Storm-Water Inlets. The Johns Hopkins University, Baltimore, MD.

U. S. Bureau of Reclamation (2001). Water Measurement Manual. Third Edition, U. S. Department of the Interior, Denver, CO.

Urban Drainage and Flood Control District (2008). Urban Storm Drainage Criteria Manual. Denver, CO.

Uyumaz, A. (2002). Urban Drainage with Curb Opening Inlets. In: Global Solutions for Urban Drainage, Proceedings of the Ninth International Conference on Urban Drainage, American Society of Civil Engineers.

APPENDIX A

USDCM GRATE INLET SCHEMATICS

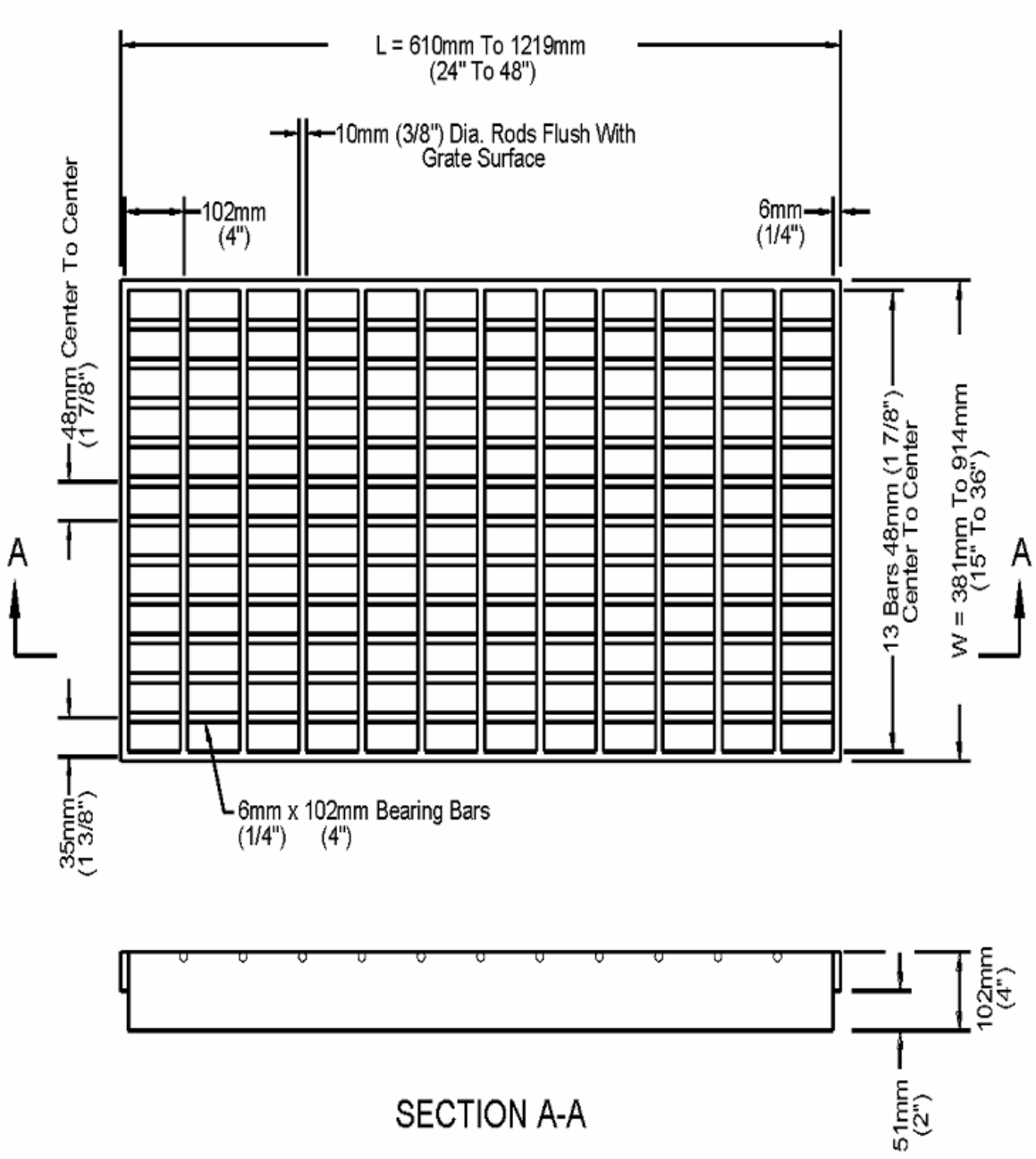

(P-1-7/8 grate does not have the 10-mm transverse rods)

Figure A-1: Bar P-1-7/8 and Bar P-1-7/8-4 grates (UDFCD, 2008)

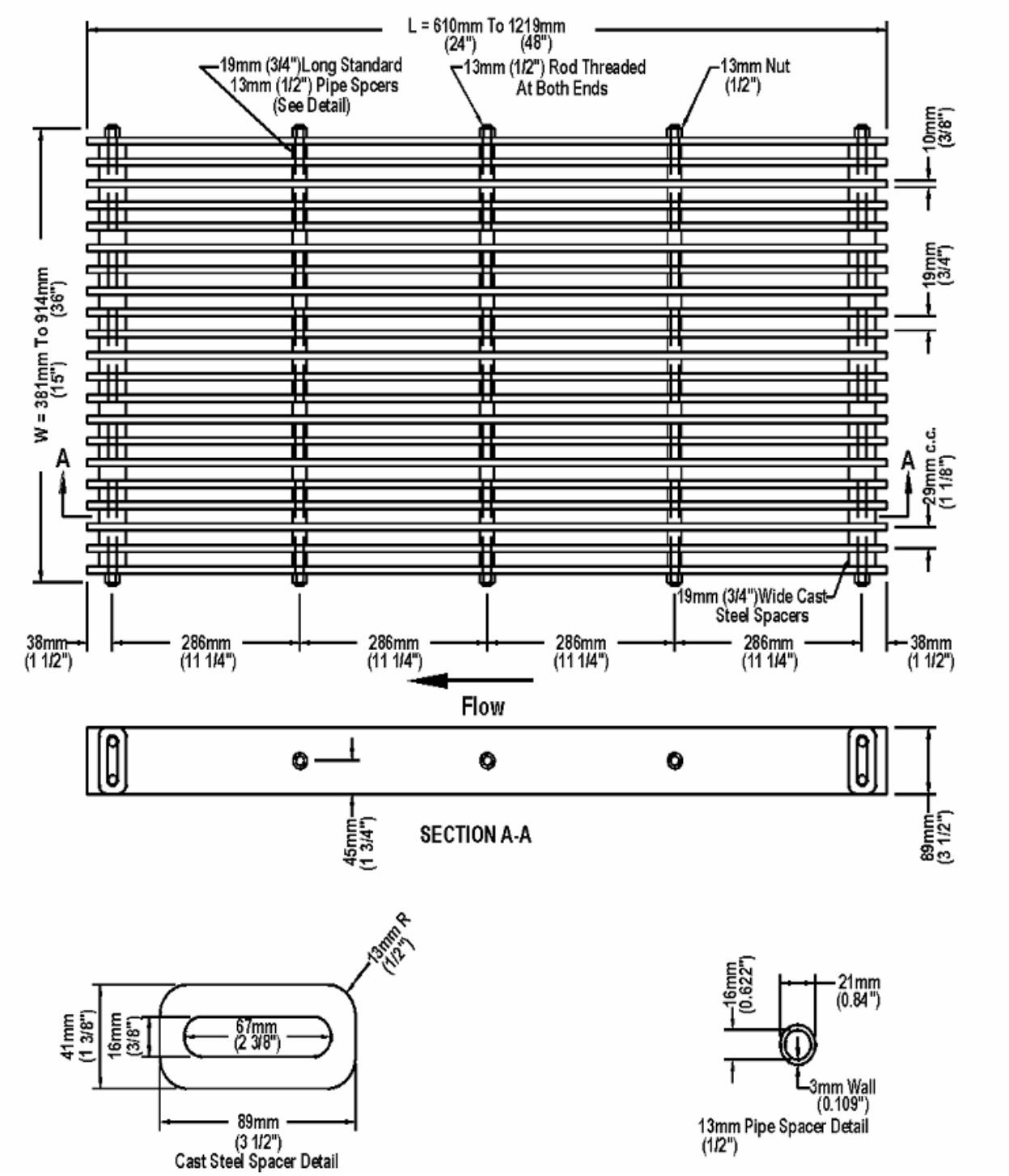

Figure A-2: Bar P-1-1/8 grate (UDFCD, 2008)

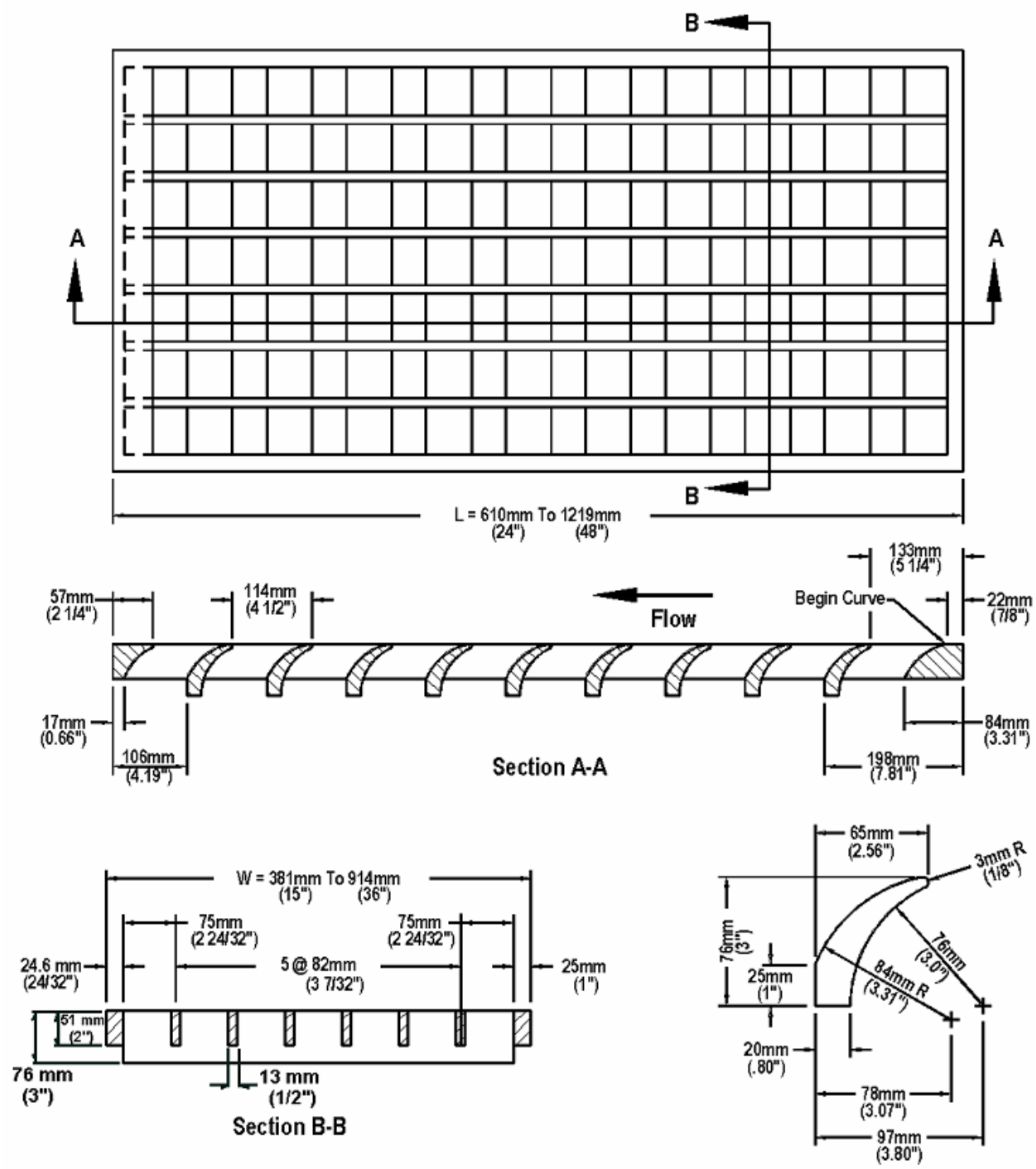

Figure A-3: Curved vane grate (UDFCD, 2008)

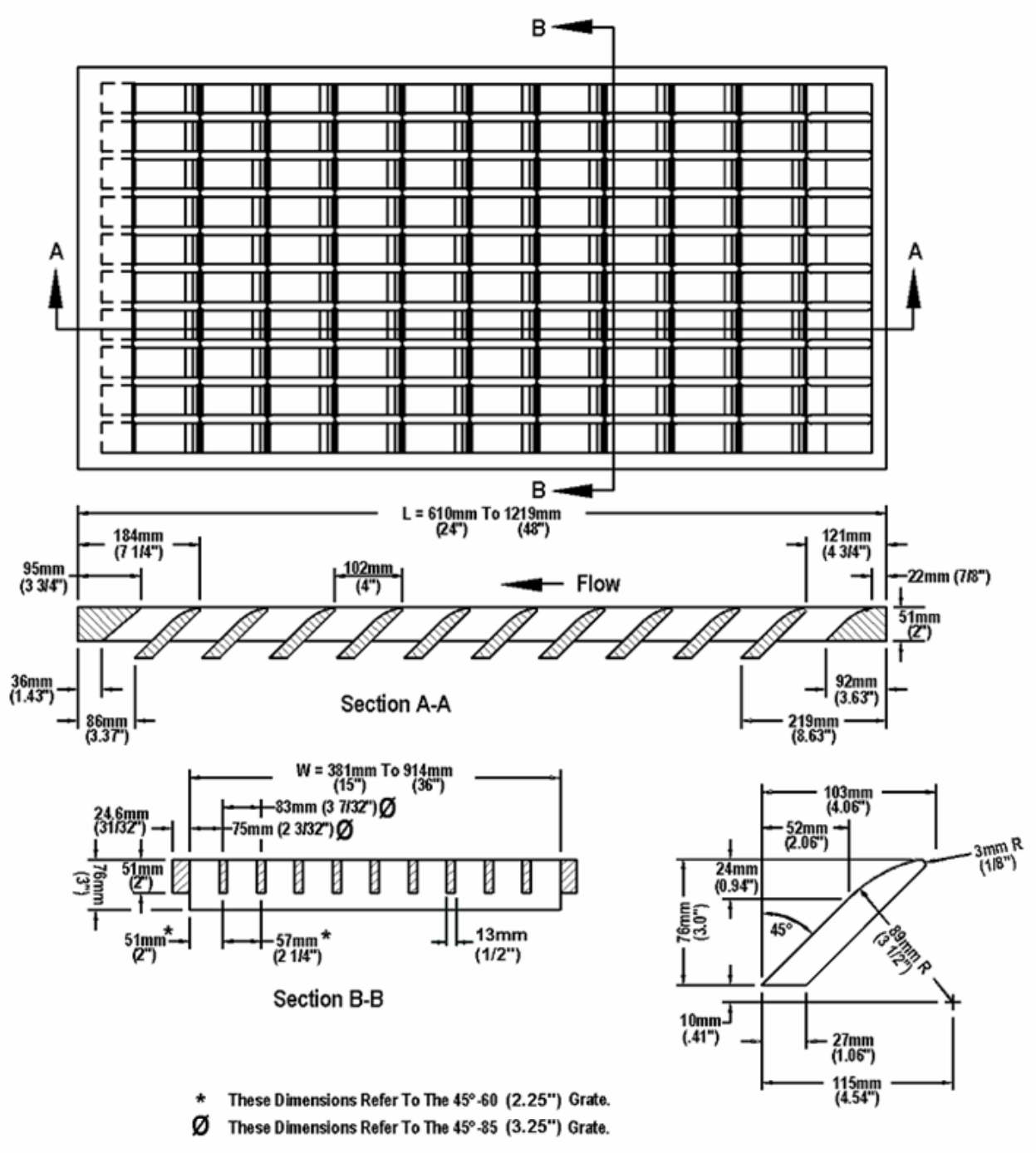

Figure A-4: 45º-tilt bar grate (UDFCD, 2008)

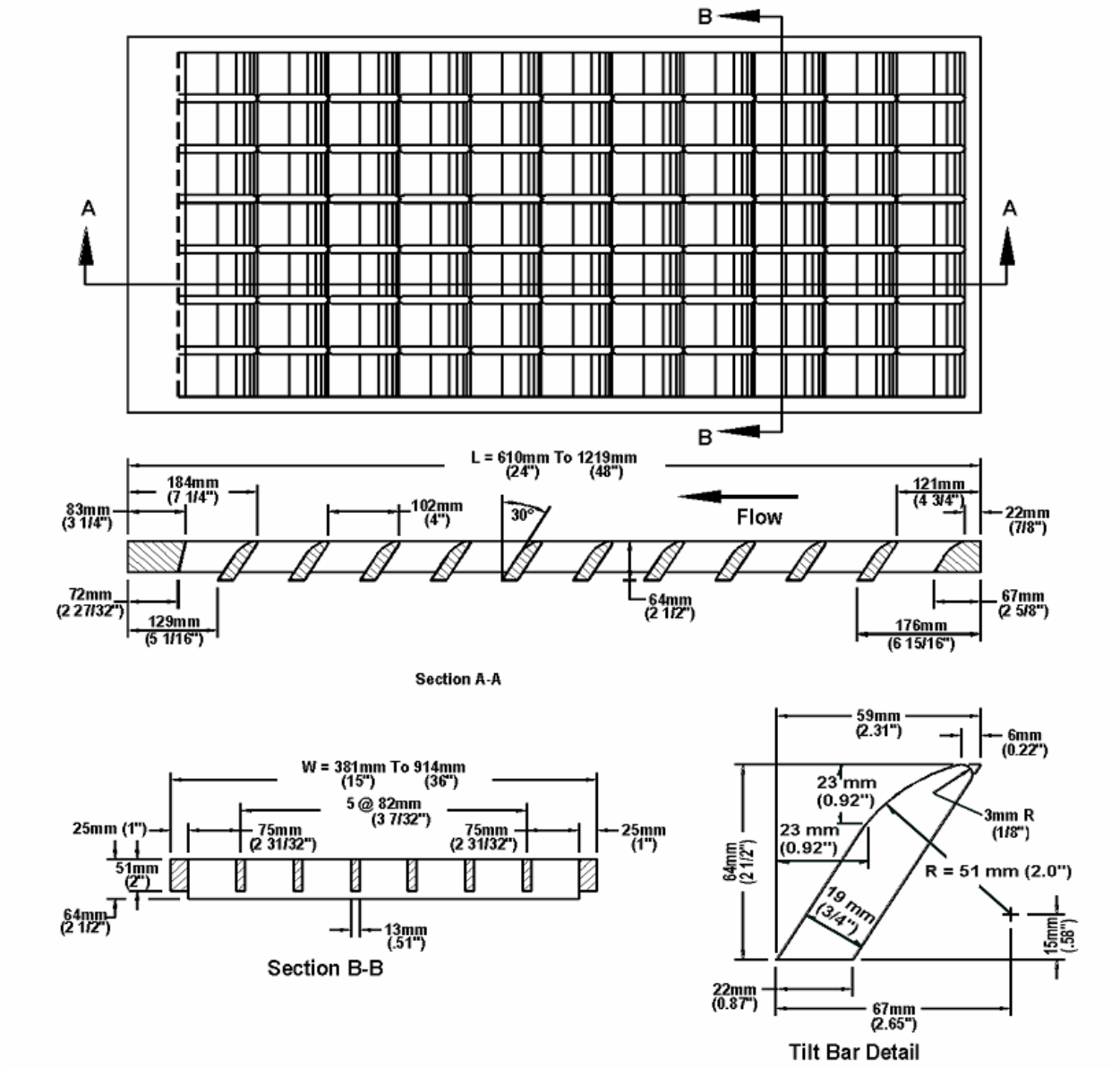

Figure A-5: 30°-tilt bar grate (UDFCD, 2008)

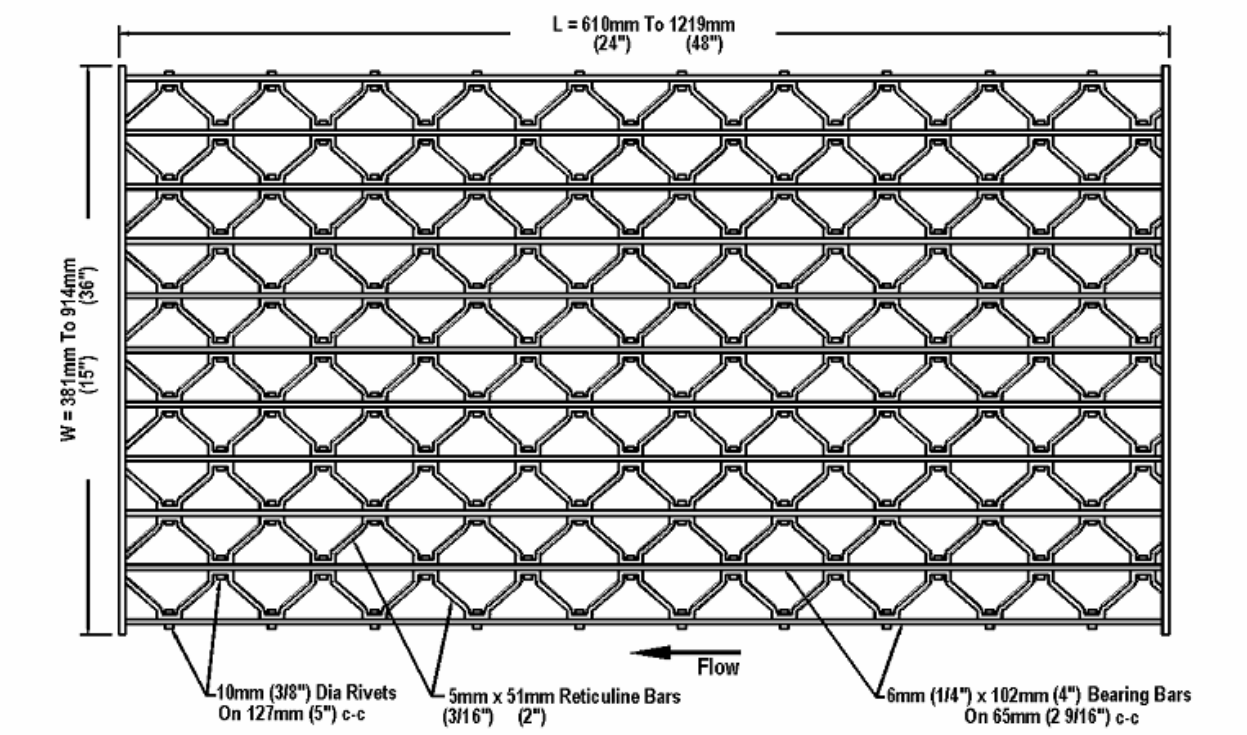

Figure A-6: Reticuline grate (UDFCD, 2008)

APPENDIX B

ON-GRADE TEST DATA

B.1 On-grade Test Results

All three inlets (Types 13, 16, and R) were tested in the on-grade condition at various slopes.

Table B-1: 0.5% and 1% on-grade test data

Test ID Number	Configuration	Longitudinal Slope (%)	Cross Slope (%)	Flow Depth (ft)	Prototype Total Flow (cfs)	Efficiency (%)	Top Width at Control (ft)	Top Width Down-stream of Inlets (ft)
44	15-ft Type R (R15)	0.5	1	0.333	4.4	89.3	16.0	10.2
45	15-ft Type R (R15)	0.5	1	0.501	20.3	50.8	17.5	16.0
46	15-ft Type R (R15)	0.5	1	0.999	128.8	23.6	18.2	18.2
47	12-ft Type R (R12)	0.5	1	0.333	3.9	84.0	16.0	10.0
48	12-ft Type R (R12)	0.5	1	0.501	21.8	37.9	18.2	18.2
49	12-ft Type R (R12)	0.5	1	0.999	126.3	19.5	18.2	18.2
50	9-ft Type R (R9)	0.5	1	0.333	4.2	70.4	16.0	12.0
51	9-ft Type R (R9)	0.5	1	0.501	21.5	34.8	18.2	18.2
52	9-ft Type R (R9)	0.5	1	0.999	127.8	14.5	18.2	18.2
53	5-ft Type R (R5)	0.5	1	0.333	4.4	50.0	16.0	15.6
54	5-ft Type R (R5)	0.5	1	0.501	22.3	24.5	18.2	18.2
55	5-ft Type R (R5)	0.5	1	0.999	125.5	8.3	18.2	18.2
56	Triple No. 13	0.5	1	0.333	4.4	82.1	15.8	9.0
57	Triple No. 13	0.5	1	0.501	20.6	43.2	18.2	18.2
58	Triple No. 13	0.5	1	0.999	126.6	22.7	18.2	18.2
59	Double No. 13	0.5	1	0.333	4.7	73.3	16.0	10.7
60	Double No. 13	0.5	1	0.501	22.6	35.9	18.2	18.2
61	Double No. 13	0.5	1	0.999	127.8	16.2	18.2	18.2
62	Single No. 13	0.5	1	0.333	4.8	61.3	16.0	15.8
63	Single No. 13	0.5	1	0.501	26.2	23.8	18.2	18.2
64	Single No. 13	0.5	1	0.999	126.4	9.9	18.2	18.2
65	Single No. 16	0.5	1	0.333	5.1	60.6	16.0	15.8
66	Single No. 16	0.5	1	0.501	21.4	28.5	18.2	18.2
67	Single No. 16	0.5	1	0.999	126.9	13.5	18.2	18.2
68	Double No. 16	0.5	1	0.333	5.3	70.6	17.0	12.8
69	Double No. 16	0.5	1	0.501	23.2	34.2	18.2	18.2
70	Double No. 16	0.5	1	0.999	124.7	20.9	18.2	18.2
71	Triple No. 16	0.5	1	0.333	4.5	82.8	15.7	9.0
72	Triple No. 16	0.5	1	0.501	23.7	40.1	18.2	18.2
73	Triple No. 16	0.5	1	0.999	125.8	26.9	18.2	18.2

Table B-2: 0.5% and 2% on-grade test data

Test ID Number	Configuration	Longi-tudinal Slope (%)	Cross Slope (%)	Flow Depth (ft)	Proto-type Total Flow (cfs)	Efficiency (%)	Top Width at Control (ft)	Top Width Down-stream of Inlets (ft)
74	Triple No. 16	0.5	2	0.333	3.4	63.6	14.0	13.6
75	Triple No. 16	0.5	2	0.501	11.2	47.2	18.2	13.8
76	Triple No. 16	0.5	2	0.999	93.8	28.2	18.2	18.2
77	Double No. 16	0.5	2	0.333	3.3	57.1	14.0	13.4
78	Double No. 16	0.5	2	0.501	11.2	40.3	18.2	14
79	Double No. 16	0.5	2	0.999	94.5	19.8	18.2	18.2
80	Single No. 16	0.5	2	0.333	3.7	50.0	14.0	13.6
81	Single No. 16	0.5	2	0.501	11.5	35.1	18.2	14
82	Single No. 16	0.5	2	0.999	95.6	17.0	18.2	18.2
83	Single No. 16, Grate only	0.5	2	0.501	11.4	35.6	18.2	13.9
84	Single No. 16, Grate only	0.5	2	0.999	94.3	14.9	18.2	18.2
85	Single No. 16, grate and 4-in. opening	0.5	2	0.501	11.2	34.7	18.2	14
86	Single No. 16, grate and 4-in. opening	0.5	2	0.999	95.4	16.2	18.2	18.2
87	Single No. 16, Debris Test 1	0.5	2	0.333	3.4	50.0	14.0	13.4
88	Single No. 16, Debris Test one	0.5	2	0.501	10.9	34.3	18.2	13.9
89	Single No. 16, Debris Test two	0.5	2	0.333	3.3	47.6	14.0	13.6
90	Single No. 16, Debris Test two	0.5	2	0.501	10.9	32.9	18.2	13.9
91	Single No. 13	0.5	2	0.333	3.0	63.2	12.0	13.4
92	Single No. 13	0.5	2	0.501	10.1	38.5	18.2	18.2
93	Single No. 13	0.5	2	0.999	95.1	13.1	18.2	18.2
94	Single No. 13, Debris Test one	0.5	2	0.333	3.7	45.8	14.0	13.6
95	Single No. 13, Debris Test one	0.5	2	0.501	11.8	32.9	18.2	14
96	Single No. 13, Debris Test two	0.5	2	0.333	3.4	54.5	14.0	13.5
97	Single No. 13, Debris Test two	0.5	2	0.501	12.0	33.8	14.0	13.7
98	Single No. 13, Grate only	0.5	2	0.501	10.4	34.3	18.2	13.9
99	Single No. 13, Grate only	0.5	2	0.999	93.2	11.0	18.2	18.2
100	Single No. 13, Grate and 4-in. Opening	0.5	2	0.501	11.2	34.7	18.2	13.9
101	Single No. 13, Grate and 4-in. Opening	0.5	2	0.999	94.3	12.7	18.2	18.2
102	Single No. 13, Curb opening only	0.5	2	0.501	11.2	23.6	18.2	14
103	Single No. 13, Curb opening only	0.5	2	0.999	94.3	7.1	18.2	18.2
104	Double No. 13	0.5	2	0.333	3.3	61.9	14.0	13.3
105	Double No. 13	0.5	2	0.501	11.2	44.4	18.2	18.2
106	Double No. 13	0.5	2	0.999	98.2	20.5	18.2	18.2
107	Triple No. 13	0.5	2	0.333	3.6	73.9	14.0	13.3
108	Triple No. 13	0.5	2	0.501	13.4	50.0	18.2	18.2
109	Triple No. 13	0.5	2	0.999	108.3	43.3	18.2	18.2
110	5-ft Type R (R5)	0.5	2	0.333	3.0	57.9	14.0	13.3
111	5-ft Type R (R5)	0.5	2	0.501	11.1	39.4	18.2	13.8
112	5-ft Type R (R5)	0.5	2	0.999	93.2	11.7	18.2	18.2
113	5-ft Type R (R5), w/ 4-in. Curb Opening	0.5	2	0.501	11.2	38.9	18.2	13.8
114	5-ft Type R (R5), w/ 4-in. Curb Opening	0.5	2	0.999	94.3	9.8	18.2	18.2

Test ID Number	Configuration	Longi-tudinal Slope (%)	Cross Slope (%)	Flow Depth (ft)	Proto-type Total Flow (cfs)	Efficiency (%)	Top Width at Control (ft)	Top Width Down-stream of Inlets (ft)
115	5-ft Type R (R5), w/Horizontal Safety Bar	0.5	2	0.501	11.1	39.4	18.2	13.8
116	9-ft Type R (R9)	0.5	2	0.333	3.1	65.0	14.0	13.1
117	9-ft Type R (R9)	0.5	2	0.501	11.2	47.2	18.2	13.7
118	9-ft Type R (R9)	0.5	2	0.999	93.8	19.3	18.2	18.2
119	12-ft Type R (R12)	0.5	2	0.333	2.8	83.3	14.0	13.1
120	12-ft Type R (R12)	0.5	2	0.501	10.9	52.9	18.2	13.7
121	12-ft Type R (R12)	0.5	2	0.999	93.8	25.4	18.2	18.2
122	15-ft Type R (R15)	0.5	2	0.333	3.3	90.5	14.0	13
123	15-ft Type R (R15)	0.5	2	0.501	10.9	60.0	18.2	13.6
124	15-ft Type R (R15)	0.5	2	0.999	94.3	30.7	18.2	18.2

Table B-3: 2% and 1% on-grade test data

Test ID Number	Configuration	Longi-tudinal Slope (%)	Cross Slope (%)	Flow Depth (ft)	Proto-type Total Flow (cfs)	Efficiency (%)	Top Width at Control (ft)	Top Width Down-stream of Inlets (ft)
125	15-ft Type R (R15)	2	1	0.333	14.8	44.2	18.2	16
126	15-ft Type R (R15)	2	1	0.501	33.5	30.2	18.2	18.2
127	15-ft Type R (R15)	2	1	0.999	178.5	17.6	18.2	18.2
128	12-ft Type R (R12)	2	1	0.333	13.4	43.0	18.2	16
129	12-ft Type R (R12)	2	1	0.501	32.9	27.0	18.2	18.2
130	12-ft Type R (R12)	2	1	0.999	176.1	14.7	18.2	18.2
131	9-ft Type R (R9)	2	1	0.333	13.4	36.0	18.2	16
132	9-ft Type R (R9)	2	1	0.501	29.6	22.6	18.2	18.2
133	9-ft Type R (R9)	2	1	0.999	173.0	11.4	18.2	18.2
134	5-ft Type R (R5)	2	1	0.333	13.1	25.0	18.2	16
135	5-ft Type R (R5)	2	1	0.501	28.4	16.5	18.2	18.2
136	5-ft Type R (R5)	2	1	0.999	179.0	7.6	18.2	18.2
137	Triple No. 16	2	1	0.333	13.2	44.7	18.2	16
138	Triple No. 16	2	1	0.501	39.9	30.9	18.2	18.2
139	Triple No. 16	2	1	0.999	155.1	23.6	18.2	18.2
140	Double No. 16	2	1	0.333	14.7	36.2	18.2	16
141	Double No. 16	2	1	0.501	32.7	27.1	18.2	18.2
142	Double No. 16	2	1	0.999	177.1	18.7	18.2	18.2
143	Single No. 16	2	1	0.333	15.3	28.6	18.2	16
144	Single No. 16	2	1	0.501	34.0	20.6	18.2	18.2
145	Single No. 16	2	1	0.999	176.6	12.3	18.2	18.2
146	Single No. 13	2	1	0.333	15.9	27.5	18.2	16
147	Single No. 13	2	1	0.501	33.7	20.4	18.2	18.2
148	Single No. 13	2	1	0.999	166.6	9.4	18.2	18.2
149	Double No. 13	2	1	0.333	14.3	33.7	18.2	16
150	Double No. 13	2	1	0.501	33.7	23.6	18.2	18.2
151	Double No. 13	2	1	0.999	176.6	13.3	18.2	18.2
152	Triple No. 13	2	1	0.333	13.1	42.9	18.2	16
153	Triple No. 13	2	1	0.501	31.0	28.6	18.2	18.2
154	Triple No. 13	2	1	0.999	177.7	17.7	18.2	18.2

Table B-4: 2% and 2% on-grade test data

Test ID Number	Configuration	Longi-tudinal Slope (%)	Cross Slope (%)	Flow Depth (ft)	Proto-type Total Flow (cfs)	Efficiency (%)	Top Width at Control (ft)	Top Width Down-stream of Inlets (ft)
155	Triple No. 13	2	2	0.333	7.8	74.0	16.0	8.3
156	Triple No. 13	2	2	0.501	22.1	43.7	18.2	18.2
157	Triple No. 13	2	2	0.999	163.2	19.1	18.2	18.2
158	Double No. 13	2	2	0.333	8.1	63.5	16.0	8.3
159	Double No. 13	2	2	0.501	23.4	34.7	18.2	18.2
160	Double No. 13	2	2	0.999	161.3	14.3	18.2	18.2
161	Single No. 13	2	2	0.333	7.8	50.0	14.8	9
162	Single No. 13	2	2	0.501	24.8	23.9	18.2	18.2
163	Single No. 13	2	2	0.999	155.9	8.9	18.2	18.2
164	Single No. 13, Debris Test one	2	2	0.333	7.3	40.4	14.0	8.3
165	Single No. 13, Debris Test one	2	2	0.501	24.0	17.5	18.2	18.2
166	Single No. 13, Debris Test two	2	2	0.333	7.2	47.8	14.0	8.3
167	Single No. 13, Debris Test two	2	2	0.501	24.0	19.5	18.2	18.2
168	Single No. 13, Grate Only	2	2	0.501	23.2	19.5	18.2	18.2
169	Single No. 13, Grate Only	2	2	0.999	154.3	6.6	18.2	18.2
170	Single No. 13, Grate and 4-in. Opening	2	2	0.501	22.3	25.2	18.2	15.8
171	Single No. 13, Grate and 4-in. Opening	2	2	0.999	164.1	8.2	18.2	18.2
172	Single No. 13, Curb opening only	2	2	0.501	24.2	9.7	18.2	18.2
173	Single No. 13, Curb opening only	2	2	0.999	155.9	3.7	18.2	18.2
174	Single No. 16	2	2	0.333	7.9	54.9	14.0	8.6
175	Single No. 16	2	2	0.501	22.3	31.5	18.2	15.6
176	Single No. 16	2	2	0.999	162.9	12.6	18.2	18.2
177	Single No. 16, Grate only	2	2	0.501	22.9	27.2	18.2	15.7
178	Single No. 16, Grate only	2	2	0.999	162.9	10.3	18.2	18.2
179	Single No. 16, Grate and 4-in. Opening	2	2	0.501	22.3	28.7	18.2	18.2
180	Single No. 16, Grate and 4-in. Opening	2	2	0.999	164.1	11.5	18.2	18.2
181	Single No. 16, Debris Test one	2	2	0.333	8.1	53.8	14.0	8.9
182	Single No. 16, Debris Test one	2	2	0.501	24.0	27.3	18.2	18.2
183	Single No. 16, Debris Test two	2	2	0.333	8.4	51.9	14.0	8.9
184	Single No. 16, Debris Test two	2	2	0.501	24.9	25.6	18.2	18.2
185	Double No. 16	2	2	0.333	7.9	64.7	14.0	8.3
186	Double No. 16	2	2	0.501	23.7	36.8	18.2	18.2
187	Double No. 16	2	2	0.999	163.7	20.3	18.2	18.2
188	Triple No. 16	2	2	0.333	8.4	72.2	14.0	8.3
189	Triple No. 16	2	2	0.501	22.6	46.2	18.2	18.2
190	Triple No. 16	2	2	0.999	162.9	25.7	18.2	18.2
191	5-ft Type R (R5)	2	2	0.333	7.3	38.3	17.8	11.3
192	5-ft Type R (R5)	2	2	0.501	22.9	18.4	18.2	18.2
193	5-ft Type R (R5)	2	2	0.999	166.0	7.1	18.2	18.2
194	5-ft Type R (R5), w/ 4-in. Curb Opening	2	2	0.999	166.8	5.4	18.2	18.2
195	5-ft Type R (R5), w/ 4-in. Curb Opening	2	2	0.501	22.8	18.5	18.2	18.2

Test ID Number	Configuration	Longi-tudinal Slope (%)	Cross Slope (%)	Flow Depth (ft)	Proto-type Total Flow (cfs)	Efficiency (%)	Top Width at Control (ft)	Top Width Down-stream of Inlets (ft)
196	5-ft Type R (R5), w/ Horizontal Safety Bar	2	2	0.501	23.1	18.2	18.2	18.2
197	9-ft Type R (R9)	2	2	0.333	6.2	65.0	11.0	6.8
198	9-ft Type R (R9)	2	2	0.501	21.8	33.6	18.2	14.3
199	9-ft Type R (R9)	2	2	0.999	166.0	11.6	18.2	18.2
200	12-ft Type R (R12)	2	2	0.333	7.5	70.8	14.0	9.8
201	12-ft Type R (R12)	2	2	0.501	21.7	42.4	18.2	15.8
202	12-ft Type R (R12)	2	2	0.999	166.8	15.2	18.2	18.2
203	15-ft Type R (R15)	2	2	0.333	7.0	84.4	14.0	8.3
204	15-ft Type R (R15)	2	2	0.501	21.5	48.6	18.2	15.8
205	15-ft Type R (R15)	2	2	0.999	166.8	18.8	18.2	18.2

Table B-5: 4% and 1% on-grade test data

Test ID Number	Configuration	Longi-tudinal Slope (%)	Cross Slope (%)	Flow Depth (ft)	Proto-type Total Flow (cfs)	Efficiency (%)	Top Width at Control (ft)	Top Width Down-stream of Inlets (ft)
206	15-ft Type R (R15)	4	1	0.333	13.1	44.0	18.2	16
207	15-ft Type R (R15)	4	1	0.501	38.3	26.8	18.2	18.2
208	15-ft Type R (R15)	4	1	0.999	143.4	18.6	18.2	18.2
209	12-ft Type R (R12)	4	1	0.333	12.6	42.0	18.2	16
210	12-ft Type R (R12)	4	1	0.501	38.3	23.6	18.2	18.2
211	12-ft Type R (R12)	4	1	0.999	152.9	14.9	18.2	18.2
212	9-ft Type R (R9)	4	1	0.333	13.9	34.8	18.2	16
213	9-ft Type R (R9)	4	1	0.501	38.2	18.8	18.2	18.2
214	9-ft Type R (R9)	4	1	0.999	141.5	11.7	18.2	18.2
215	5-ft Type R (R5)	4	1	0.333	13.7	21.6	18.2	16
216	5-ft Type R (R5)	4	1	0.501	38.2	11.4	18.2	18.2
217	5-ft Type R (R5)	4	1	0.999	140.3	6.9	18.2	18.2
218	Triple No. 16	4	1	0.333	12.6	42.0	18.2	16
219	Triple No. 16	4	1	0.501	38.2	29.4	18.2	18.2
220	Triple No. 16	4	1	0.999	145.7	24.8	18.2	18.2
221	Double No. 16	4	1	0.333	13.2	37.6	18.2	16
222	Double No. 16	4	1	0.501	36.6	25.1	18.2	18.2
223	Double No. 16	4	1	0.999	145.0	20.4	18.2	18.2
224	Single No. 16	4	1	0.333	13.1	33.3	18.2	16
225	Single No. 16	4	1	0.501	37.9	20.2	18.2	18.2
226	Single No. 16	4	1	0.999	141.2	14.0	18.2	18.2
227	Single No. 13	4	1	0.333	12.9	25.3	18.2	16
228	Single No. 13	4	1	0.501	37.7	12.8	18.2	18.2
229	Single No. 13	4	1	0.999	142.6	8.4	18.2	18.2
230	Double No. 13	4	1	0.333	13.2	37.6	18.2	16
231	Double No. 13	4	1	0.501	36.6	21.3	18.2	18.2
232	Double No. 13	4	1	0.999	138.7	13.5	18.2	18.2
233	Triple No. 13	4	1	0.333	12.6	40.7	18.2	16
234	Triple No. 13	4	1	0.501	38.2	24.9	18.2	18.2
235	Triple No. 13	4	1	0.999	146.8	17.9	18.2	18.2

Table B-6: 4% and 2% on-grade test data

Test ID Number	Configuration	Longi-tudinal Slope (%)	Cross Slope (%)	Flow Depth (ft)	Proto-type Total Flow (cfs)	Efficiency (%)	Top Width at Control (ft)	Top Width Down-stream of Inlets (ft)
236	Triple No. 13	4	2	0.333	8.4	74.1	15.5	7.7
237	Triple No. 13	4	2	0.501	25.7	42.4	18.2	14.3
238	Triple No. 13	4	2	0.999	128.6	20.5	18.2	18.2
239	Double No. 13	4	2	0.333	8.3	66.0	15.5	7.8
240	Double No. 13	4	2	0.501	26.0	32.9	18.2	14.3
241	Double No. 13	4	2	0.999	127.8	15.9	18.2	18.2
242	Single No. 13	4	2	0.333	9.0	43.1	15.5	7.7
243	Single No. 13	4	2	0.501	27.3	20.6	18.2	13.7
244	Single No. 13	4	2	0.999	129.7	9.5	18.2	18.2
245	Single No. 13, Debris Test one	4	2	0.333	8.6	34.5	16.0	8.6
246	Single No. 13, Debris Test one	4	2	0.501	26.5	15.9	17.5	14.3
247	Single No. 13, Debris Test two	4	2	0.333	8.4	40.7	16.0	8
248	Single No. 13, Debris Test two	4	2	0.501	27.1	16.7	18.2	14.3
249	Single No. 13, Curb opening only	4	2	0.501	26.5	9.4	18.2	14.3
250	Single No. 13, Curb opening only	4	2	0.999	119.2	4.7	18.2	18.2
251	Single No. 13, Grate Only	4	2	0.501	21.8	19.3	18.2	9.8
252	Single No. 13, Grate Only	4	2	0.999	117.7	6.5	18.2	18.2
253	Single No. 13, Grate and 4-in. Opening	4	2	0.501	24.5	21.7	18.2	14.3
254	Single No. 13, Grate and 4-in. Opening	4	2	0.999	113.3	9.9	18.2	18.2
255	Single No. 16, Grate and 4-in. Opening	4	2	0.501	28.2	31.5	18.2	14.3
256	Single No. 16, Grate and 4-in. Opening	4	2	0.999	123.1	15.3	18.2	18.2
257	Single No. 16, Grate only	4	2	0.501	30.4	28.7	18.2	12.8
258	Single No. 16, Grate only	4	2	0.999	133.4	12.7	18.2	18.2
259	Single No. 16, Debris Test one	4	2	0.333	8.1	55.8	18.2	7.4
260	Single No. 16, Debris Test one	4	2	0.501	26.5	25.9	18.2	14.3
261	Single No. 16, Debris Test two	4	2	0.333	8.1	48.1	18.2	8
262	Single No. 16, Debris Test two	4	2	0.501	26.8	17.4	18.2	14.3
263	Single No. 16	4	2	0.333	7.5	64.6	14.6	7.8
264	Single No. 16	4	2	0.501	28.1	31.7	18.2	14.3
265	Single No. 16	4	2	0.999	129.4	15.7	18.2	18.2
266	Double No. 16	4	2	0.333	8.7	67.9	14.6	7.8
267	Double No. 16	4	2	0.501	26.5	37.6	18.2	14.3
268	Double No. 16	4	2	0.999	130.9	24.6	18.2	18.2
269	Triple No. 16	4	2	0.333	8.4	74.1	14.6	7.7
270	Triple No. 16	4	2	0.501	25.7	43.6	18.2	14.3
271	Triple No. 16	4	2	0.999	127.8	29.0	18.2	18.2
272	5-ft Type R (R5)	4	2	0.333	8.1	34.6	16.0	8.6
273	5-ft Type R (R5)	4	2	0.501	26.7	17.0	18.2	14.3
274	5-ft Type R (R5)	4	2	0.999	118.9	7.9	18.2	18.2
275	5-ft Type R (R5), w/ 4-in. Curb Opening	4	2	0.501	27.4	16.5	18.2	14.3
276	5-ft Type R (R5), w/ 4-in. Curb Opening	4	2	0.999	128.6	6.2	18.2	18.2

Test ID Number	Configuration	Longi-tudinal Slope (%)	Cross Slope (%)	Flow Depth (ft)	Proto-type Total Flow (cfs)	Efficiency (%)	Top Width at Control (ft)	Top Width Down-stream of Inlets (ft)
277	5-ft Type R (R5), w/ Horizontal Safety Bar	4	2	0.501	26.7	16.4	18.2	14.3
278	9-ft Type R (R9)	4	2	0.333	7.9	62.7	16.0	8.6
279	9-ft Type R (R9)	4	2	0.501	25.9	30.1	18.2	14.3
280	9-ft Type R (R9)	4	2	0.999	117.7	13.2	18.2	18.2
281	12-ft Type R (R12)	4	2	0.333	8.7	69.6	16.0	8
282	12-ft Type R (R12)	4	2	0.501	25.3	38.3	18.2	14.3
283	12-ft Type R (R12)	4	2	0.999	113.8	18.2	18.2	18.2
284	15-ft Type R (R15)	4	2	0.333	7.8	80.0	16.0	7.7
285	15-ft Type R (R15)	4	2	0.501	23.4	46.0	18.2	14.3
286	15-ft Type R (R15)	4	2	0.999	123.1	21.3	18.2	18.2

Table B-7: Additional debris tests (4% and 1% on-grade)

Test ID Number*	Configuration**	Longi-tudinal Slope (%)	Cross Slope (%)	Flow Depth (ft)	Proto-type Total Flow (cfs)	Efficiency (%)	Top Width at Control (ft)	Top Width Down-stream of Inlets (ft)
AT287	Single No. 13 - 25% flat	4	1	0.333	14.50	21.51	18.2	16.0
AT288	Single No. 13 - 25% flat	4	1	0.501	38.03	11.48	18.2	18.2
AT291	Double No. 13 - 25% flat	4	1	0.333	14.65	27.66	18.2	16.0
AT293	Double No. 13 - 25% flat	4	1	0.501	38.81	18.88	18.2	18.2
AT303	Triple No. 13 - 25% flat	4	1	0.333	14.34	40.22	18.2	16.0
AT306	Triple No. 13 - 25% flat	4	1	0.501	37.57	24.90	18.2	18.2
245	Single No. 13 - 50% flat	4	1	0.333	8.57	34.55	18.2	16.0
246	Single No. 13 - 50% flat	4	1	0.501	26.50	15.88	18.2	18.2
AT295	Double No. 13 - 50% flat	4	1	0.333	14.50	33.33	18.2	16.0
AT297	Double No. 13 - 50% flat	4	1	0.501	38.35	17.48	18.2	18.2
AT300	Triple No. 13 - 50% flat	4	1	0.333	14.65	39.36	18.2	16.0
AT301	Triple No. 13 - 50% flat	4	1	0.501	38.03	24.59	18.2	18.2
261	Single No. 16 - 25% 3d	4	1	0.333	8.11	48.08	18.2	16.0
262	Single No. 16 - 25% 3d	4	1	0.501	26.81	17.44	18.2	18.2
AT296	Double No. 16 - 25% 3d	4	1	0.333	14.34	34.78	18.2	16.0
AT298	Double No. 16 - 25% 3d	4	1	0.501	38.03	16.39	18.2	18.2
AT299	Triple No. 16 - 25% 3d	4	1	0.333	14.65	36.17	18.2	16.0
AT302	Triple No. 16 - 25% 3d	4	1	0.501	37.88	21.40	18.2	18.2
AT289	Single No. 16 - 50% 3d	4	1	0.333	14.19	27.47	18.2	16.0
AT290	Single No. 16 - 50% 3d	4	1	0.501	38.03	11.89	18.2	18.2
AT292	Double No. 16 - 50% 3d	4	1	0.333	14.65	34.04	18.2	16.0
AT294	Double No. 16 - 50% 3d	4	1	0.501	38.50	16.60	18.2	18.2
AT304	Triple No. 16 - 50% 3d	4	1	0.333	14.34	35.87	18.2	16.0
AT305	Triple No. 16 - 50% 3d	4	1	0.501	37.72	20.66	18.2	18.2

*AT – additional test
**flat – type 1 debris; 3d – type 2 debris

APPENDIX C

SUMP TEST DATA

C.1 Sump Test Data

All three inlets (Types 13, 16, and R) were tested in the sump condition.

Table C-1: Sump test data

Test ID Number	Configuration	Longitudinal Slope (%)	Cross Slope (%)	Flow Depth (ft)	Prototype Flow (cfs)
1	Triple No. 13	0	1	0.333	2.5
2	Triple No. 13	0	1	0.501	8.6
3	Triple No. 13	0	1	0.999	42.2
4	Double No. 13	0	1	0.333	2.3
5	Double No. 13	0	1	0.501	7.8
6	Double No. 13	0	1	0.999	27.1
7	Single No. 13	0	1	0.333	2.0
8	Single No. 13	0	1	0.501	5.9
9	Single No. 13	0	1	0.999	15.3
10	Single No. 13, Curb opening only	0	1	0.501	5.1
11	Single No. 13, Curb opening only	0	1	0.999	6.1
12	Single No. 13, Grate only	0	1	0.501	10.3
13	Single No. 13, Grate only	0	1	0.999	11.4
14	Single No. 13, w/ 4-in. opening	0	1	0.501	5.8
15	Single No. 13, w/ 4-in. opening	0	1	0.999	15.1
16	Single No. 16, Grate only	0	1	0.501	3.6
17	Single No. 16, Grate only	0	1	0.999	13.7
18	Single No. 16, w/ 4-in. opening	0	1	0.501	5.5
19	Single No. 16, w/ 4-in. opening	0	1	0.999	7.5
20	Single No. 16	0	1	0.333	2.3
21	Single No. 16	0	1	0.501	6.2
22	Single No. 16	0	1	0.999	13.9
23	Double No. 16	0	1	0.333	2.5
24	Double No. 16	0	1	0.501	7.6
25	Double No. 16	0	1	0.999	26.5
26	Triple No. 16	0	1	0.333	2.8
27	Triple No. 16	0	1	0.501	8.4
28	Triple No. 16	0	1	0.999	37.4
29	5-ft Type R (R5)	0	1	0.333	2.2
30	5-ft Type R (R5)	0	1	0.501	7.3
31	5-ft Type R (R5)	0	1	0.999	12.6
32	5-ft Type R (R5), w/ 4-in. Curb Opening	0	1	0.501	6.4
33	5-ft Type R (R5), w/ 4-in. Curb Opening	0	1	0.999	8.9
34	5-ft Type R (R5), Horizontal Safety Bar	0	1	0.501	7.3
35	9-ft Type R (R9)	0	1	0.333	2.5
36	9-ft Type R (R9)	0	1	0.501	8.7
37	9-ft Type R (R9)	0	1	0.999	24.2
38	12-ft Type R (R12)	0	1	0.333	2.8
39	12-ft Type R (R12)	0	1	0.501	10.0
40	12-ft Type R (R12)	0	1	0.999	32.9
41	15-ft Type R (R15)	0	1	0.333	2.8
42	15-ft Type R (R15)	0	1	0.501	10.1
43	15-ft Type R (R15)	0	1	0.999	42.1

For the additional sump tests, only the Type 13 and 16 were tested at two additional flow depths (0.75 and 1.5 ft).

Table C-2: Additional sump test data

Test ID Number	Configuration	Longitudinal Slope (%)	Cross Slope (%)	Flow Depth (ft)	Prototype Flow (cfs)
AT1	Triple No. 16	0	1	0.75	21.8
AT2	Triple No. 16	0	1	1.5	52.7
AT3	Double No. 16	0	1	0.75	17.9
AT4	Double No. 16	0	1	1.5	33.8
AT5	Single No. 16	0	1	0.75	10.9
AT6	Single No. 16	0	1	1.5	17.6
AT7	Single No. 13	0	1	0.75	11.5
AT8	Single No. 13	0	1	1.5	19.2
AT9	Double No. 13	0	1	0.75	16.7
AT10	Double No. 13	0	1	1.5	40.1
AT11	Triple No. 13	0	1	0.75	20.3
AT12	Triple No. 13	0	1	1.5	59.4

APPENDIX D

INLET CONSTRUCTION DRAWINGS

D.1 Inlet Drawings

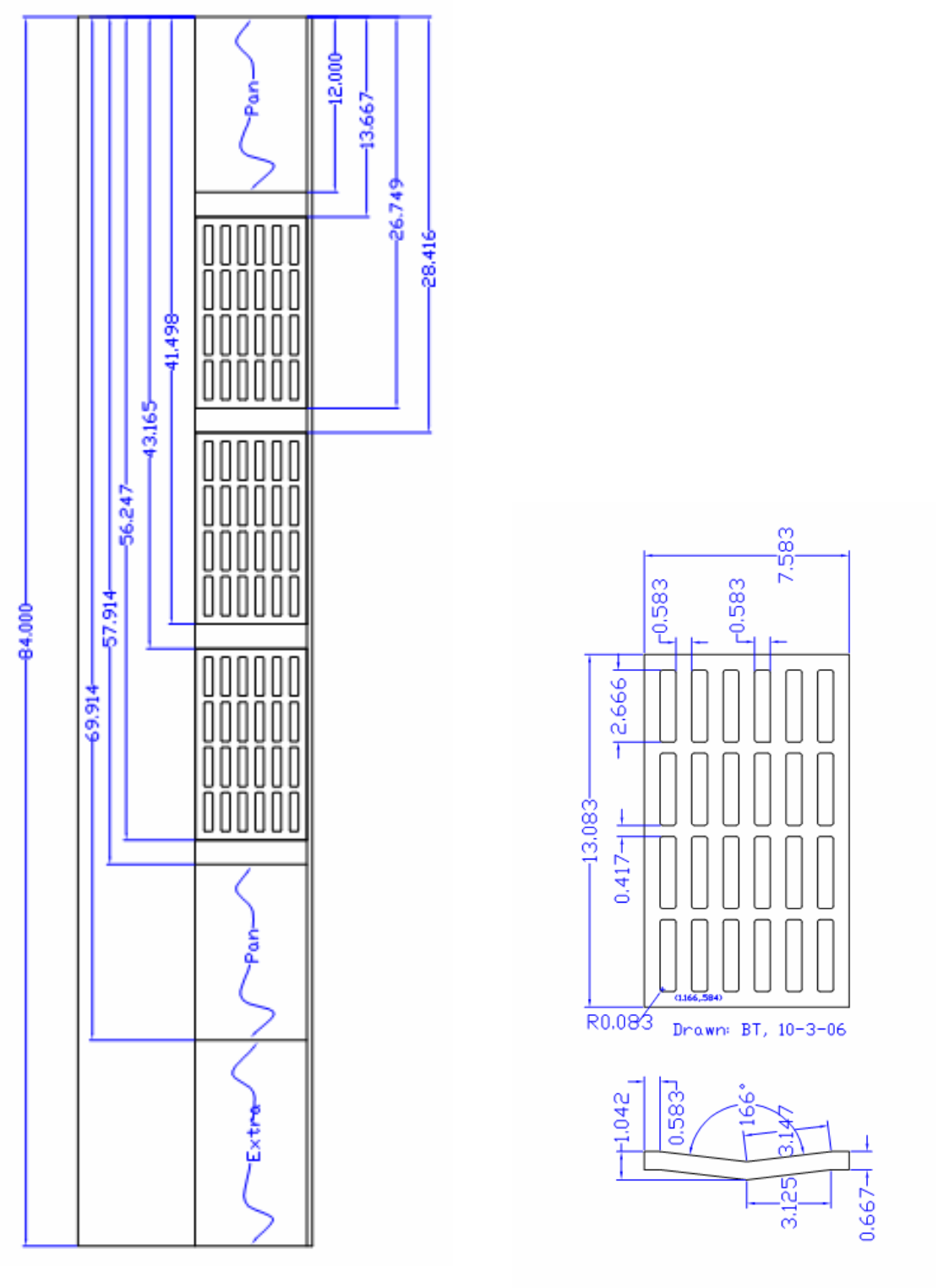

(a) (b)

Figure D-1: Type 13 inlet specifications

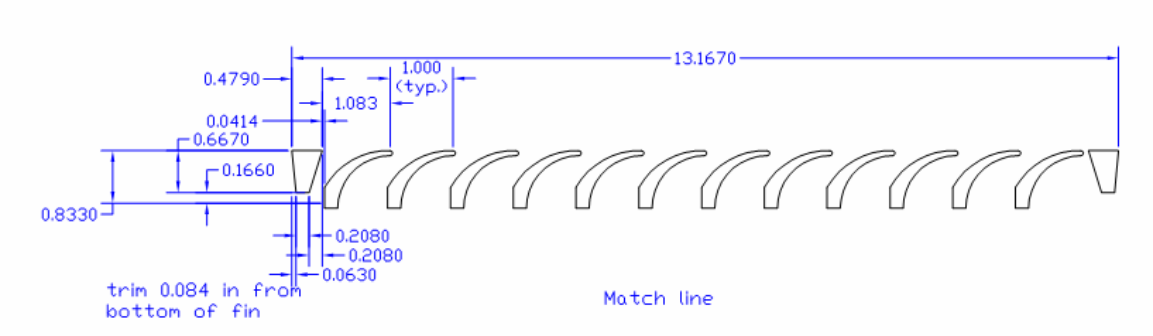

(a)

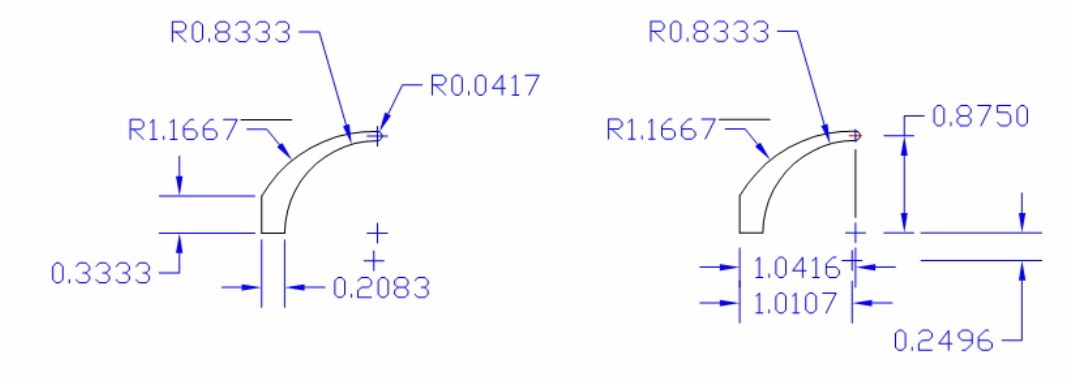

(b)

Figure D-2: Type 16 inlet specifications

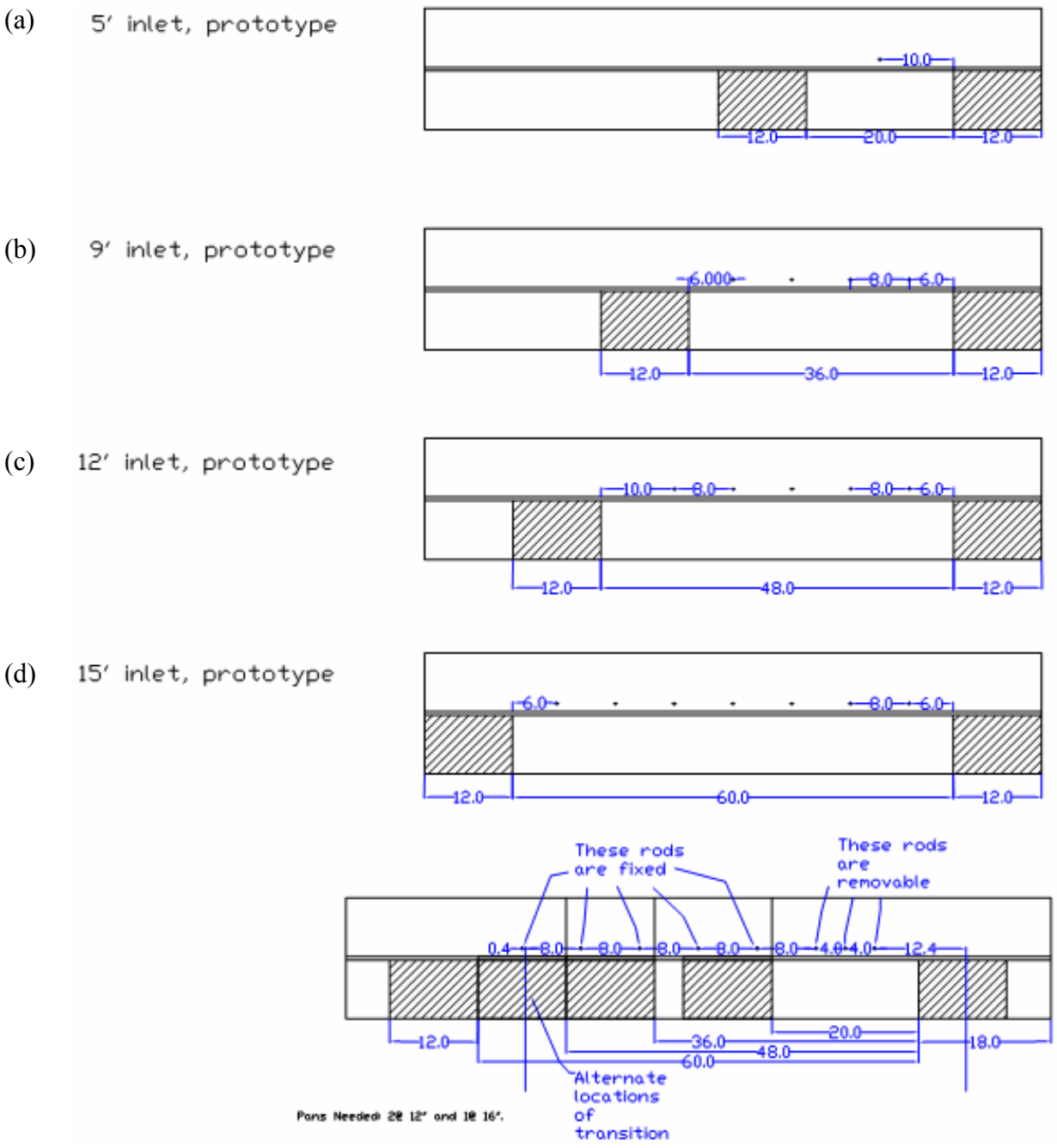

Figure D-3: Type R curb inlet specifications (plan view)

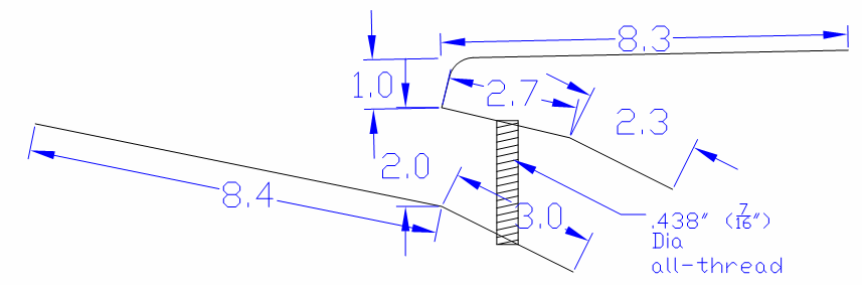

(a)

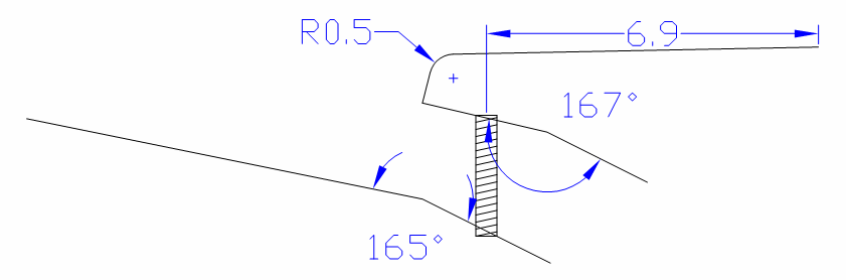

(b)

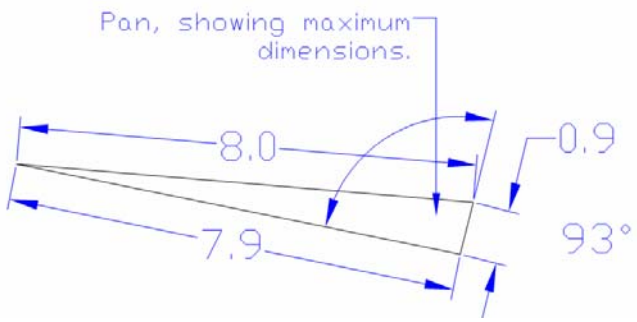

(c)

Figure D-4: Type R curb inlet specifications (profile view)

APPENDIX E

DATA COLLECTION

UDFCD Curb and Grate Study Data Sheet

Date: _____ Test ID Number: _____
Operators (*first initial and last name*): _____
Start Time: _____ End Time: _____
Water Temperature (ºF): _____

Model Information

Cross Slope: 1% 2% Longitudinal Slope: 0% 0.5% 2% 4%
Model Configuration (*circle one*): Denver Type 13 Denver Type 16 Type R
Inlet Configuration (*circle one*): Single Double Triple 5-ft 9-ft 12-ft 15-ft
Debris: Y N 4-ft curb opening: Y N
Other: _____

Discharge Information

Venturi Reading (cfs): _____
Mag Meter Reading (cfs): _____
Annubar (cfs): _____
Through Grates (ft of head): _____
Bypassing Grates (ft of head): _____

Flow Characteristics

Extent of Flow (station and distance from river right wall): ***See Back of Sheet***
Depth of Flow, at 5 ft Upstream, Model: _____
Gutter Flow Line Depth: _____

Verbal Description of Flow into Inlets

Note: Upstream grate is #1, second is #2, and the furthest downstream is # 3.
Approximate distribution of flow through inlets: _____

_____
_____
_____
_____
_____
_____

(*Over*)

Extent of Flow

Station (x)	Position (y)	Notes

Notes and Observations: _____

UDFCD Sheet (Page 2 of 2)

APPENDIX F

ADDITIONAL PARAMETERS

F.1 Additional Parameters Used in Regressions and UDFCD Methods

From the collected test data, several parameters such as top width (*Tw*), cross-sectional flow area (*A*), wetted perimeter (*Wp*), critical depth (*depth*), Froude number (*Fr*), Manning's roughness coefficient (*n*), and flow velocity (*velocity*) were determined at the prototype scale and are given here for use by the UDFCD in data analysis. These are organized by the inlet type used and are given for all the on-grade tests.

Table F-1: Additional parameters for the Type 13 inlet tests

Test ID Number	*depth* (ft)	*Tw* (ft)	*A* (ft^2)	*Wp* (ft)	*Fr*	*n*	*velocity* (ft/s)
62	0.111	16	1.92	16.23	1.28	0.0124	2.517
63	0.167	18.15	5.18	18.65	1.67	0.0109	5.056
64	0.333	20.165	15.48	21.675	1.64	0.0126	8.167
91	0.111	12	1.42	12.22	1.07	0.0172	2.086
92	0.167	18.15	3.92	18.5	0.98	0.0207	2.585
93	0.333	20.165	14.2	21.525	1.41	0.0170	6.696
94	0.111	12	1.42	12.22	1.35	0.0136	2.635
95	0.167	18.15	3.92	18.5	1.15	0.0177	3.022
96	0.111	12	1.42	12.22	1.24	0.0148	2.415
97	0.167	18.15	3.92	18.5	1.16	0.0175	3.062
98	0.167	18.15	3.92	18.5	1.01	0.0201	2.664
99	0.333	20.165	14.2	21.525	1.38	0.0174	6.565
100	0.167	18.15	3.92	18.5	1.09	0.0187	2.863
101	0.333	20.165	14.2	21.525	1.39	0.0172	6.641
102	0.167	18.15	3.92	18.5	1.09	0.0187	2.863
103	0.333	20.165	14.2	21.525	1.39	0.0172	6.641
146	0.111	18.15	2.14	18.39	3.81	0.0071	7.430
147	0.167	18.15	5.18	18.65	2.14	0.0145	6.500
148	0.333	20.165	15.48	21.675	2.17	0.0164	10.765
161	0.111	16	1.79	16.22	2.29	0.0124	4.354
162	0.167	18.15	3.92	18.5	2.40	0.0132	6.323
163	0.333	20.165	14.2	21.525	2.31	0.0162	10.977
164	0.111	16	1.79	16.22	2.16	0.0132	4.093
165	0.167	18.15	3.92	18.5	2.32	0.0136	6.124
166	0.111	16	1.79	16.22	2.11	0.0134	4.006
167	0.167	18.15	3.92	18.5	2.32	0.0136	6.124
168	0.167	18.15	3.92	18.5	2.25	0.0140	5.925
169	0.333	20.165	14.2	21.525	2.28	0.0163	10.868
170	0.167	18.15	3.92	18.5	2.16	0.0146	5.686
171	0.333	20.165	14.2	21.525	2.43	0.0153	11.559
172	0.167	18.15	3.92	18.5	2.34	0.0135	6.164
173	0.333	20.165	14.2	21.525	2.31	0.0162	10.977
227	0.111	18.15	2.14	18.39	3.10	0.0119	6.046

Test ID Number	*depth* (ft)	*Tw* (ft)	*A* (ft^2)	*Wp* (ft)	*Fr*	*n*	*velocity* (ft/s)
228	0.167	18.15	5.18	18.65	2.40	0.0177	7.282
229	0.333	20.165	15.48	21.675	1.85	0.0262	9.214
242	0.111	15.5	1.79	16.72	2.62	0.0139	5.051
243	0.167	18.15	3.92	18.5	2.64	0.0159	6.959
244	0.333	20.165	14.2	21.525	1.92	0.0259	9.133
245	0.111	15.5	1.79	16.72	2.48	0.0147	4.790
246	0.167	18.15	3.92	18.5	2.56	0.0164	6.760
247	0.111	15.5	1.79	16.72	2.44	0.0150	4.703
248	0.167	18.15	3.92	18.5	2.62	0.0160	6.919
249	0.167	18.15	3.92	18.5	2.56	0.0164	6.760
250	0.333	20.165	14.2	21.525	1.76	0.0282	8.398
251	0.167	18.15	3.92	18.5	2.11	0.0199	5.567
252	0.333	20.165	14.2	21.525	1.74	0.0286	8.288
253	0.167	18.15	3.92	18.5	2.37	0.0178	6.243
254	0.333	20.165	14.2	21.525	1.68	0.0296	7.981
59	0.111	16	1.92	16.23	1.24	0.0128	2.436
60	0.167	18.15	5.18	18.65	1.44	0.0126	4.363
61	0.333	20.165	15.48	21.675	1.66	0.0125	8.257
104	0.111	12	1.42	12.22	1.18	0.0156	2.305
105	0.167	18.15	3.92	18.5	1.09	0.0187	2.863
106	0.333	20.165	14.2	21.525	1.45	0.0165	6.916
149	0.111	18.15	2.14	18.39	3.44	0.0079	6.701
150	0.167	18.15	5.18	18.65	2.14	0.0145	6.500
151	0.333	20.165	15.48	21.675	2.29	0.0155	11.409
158	0.111	16	1.79	16.22	2.39	0.0119	4.528
159	0.167	18.15	3.92	18.5	2.26	0.0139	5.965
160	0.333	20.165	14.2	21.525	2.39	0.0156	11.362
230	0.111	18.15	2.14	18.39	3.18	0.0116	6.191
231	0.167	18.15	5.18	18.65	2.33	0.0182	7.072
232	0.333	20.165	15.48	21.675	1.80	0.0270	8.962
239	0.111	15.5	1.79	16.72	2.39	0.0153	4.615
240	0.167	18.15	3.92	18.5	2.52	0.0167	6.641
241	0.333	20.165	14.2	21.525	1.89	0.0263	9.002
56	0.111	16	1.92	16.23	1.16	0.0137	2.273
57	0.167	18.15	5.18	18.65	1.31	0.0138	3.972
58	0.333	20.165	15.48	21.675	1.64	0.0126	8.177
107	0.111	12	1.42	12.22	1.29	0.0142	2.525
108	0.167	18.15	3.92	18.5	1.30	0.0157	3.420
109	0.333	20.165	14.2	21.525	1.60	0.0150	7.629
152	0.111	18.15	2.14	18.39	3.14	0.0086	6.119
153	0.167	18.15	5.18	18.65	1.98	0.0157	5.988
154	0.333	20.165	15.48	21.675	2.31	0.0154	11.480
155	0.111	16	1.79	16.22	2.29	0.0124	4.354
156	0.167	18.15	3.92	18.5	2.14	0.0147	5.647
157	0.333	20.165	14.2	21.525	2.41	0.0154	11.493
233	0.111	18.15	2.14	18.39	3.03	0.0122	5.900

Test ID Number	*depth* (ft)	*Tw* (ft)	*A* (ft^2)	*Wp* (ft)	*Fr*	*n*	*velocity* (ft/s)
234	0.167	18.15	5.18	18.65	2.43	0.0175	7.373
235	0.333	20.165	15.48	21.675	1.91	0.0255	9.486
236	0.111	15.5	1.79	16.72	2.44	0.0150	4.703
237	0.167	18.15	3.92	18.5	2.49	0.0169	6.561
238	0.333	20.165	14.2	21.525	1.90	0.0261	9.056
AT287	0.111	18.15	2.14	18.39	3.48	0.0106	6.774
AT288	0.167	18.15	5.18	18.65	2.42	0.0175	7.343
AT291	0.111	18.15	2.14	18.39	3.51	0.0105	6.847
AT293	0.167	18.15	5.18	18.65	2.47	0.0172	7.493
AT303	0.111	18.15	2.14	18.39	3.44	0.0108	6.701
AT306	0.167	18.15	5.18	18.65	2.39	0.0178	7.252
AT295	0.111	18.15	2.14	18.39	3.48	0.0106	6.774
AT297	0.167	18.15	5.18	18.65	2.44	0.0174	7.403
AT300	0.111	18.15	2.14	18.39	3.51	0.0105	6.847
AT301	0.167	18.15	5.18	18.65	2.42	0.0175	7.343

Table F-2: Additional parameters for the Type 16 inlet tests

Test ID Number	*depth* (ft)	*Tw* (ft)	*A* (ft^2)	*Wp* (ft)	*Fr*	*n*	*velocity* (ft/s)
65	0.111	17	1.88	17.22	1.45	0.0108	2.736
66	0.167	18.15	5.18	18.65	1.36	0.0133	4.123
67	0.333	20.165	15.48	21.675	1.65	0.0126	8.197
80	0.111	12	1.42	12.22	1.35	0.0136	2.635
81	0.167	18.15	3.92	18.5	1.12	0.0182	2.943
82	0.333	20.165	14.2	21.525	1.41	0.0170	6.729
83	0.167	18.15	3.92	18.5	1.10	0.0184	2.903
84	0.333	20.165	14.2	21.525	1.39	0.0172	6.641
85	0.167	18.15	3.92	18.5	1.09	0.0187	2.863
86	0.333	20.165	14.2	21.525	1.41	0.0170	6.718
87	0.111	12	1.42	12.22	1.24	0.0148	2.415
88	0.167	18.15	3.92	18.5	1.06	0.0192	2.784
89	0.111	12	1.42	12.22	1.18	0.0156	2.305
90	0.167	18.15	3.92	18.5	1.06	0.0192	2.784
143	0.111	18.15	2.14	18.39	3.66	0.0074	7.138
144	0.167	18.15	5.18	18.65	2.16	0.0143	6.560
145	0.333	20.165	15.48	21.675	2.29	0.0155	11.409
174	0.111	14	1.6	14.22	2.59	0.0110	4.969
175	0.167	18.15	3.92	18.5	2.16	0.0146	5.686
176	0.333	20.165	14.2	21.525	2.41	0.0155	11.471
177	0.167	18.15	3.92	18.5	2.22	0.0142	5.846
178	0.333	20.165	14.2	21.525	2.41	0.0155	11.471
179	0.167	18.15	3.92	18.5	2.16	0.0146	5.686
180	0.333	20.165	14.2	21.525	2.43	0.0153	11.559
181	0.111	14	1.6	14.22	2.64	0.0108	5.066
182	0.167	18.15	3.92	18.5	2.32	0.0136	6.124
183	0.111	14	1.6	14.22	2.74	0.0104	5.261
184	0.167	18.15	3.92	18.5	2.41	0.0131	6.362
224	0.111	18.15	2.14	18.39	3.14	0.0118	6.119
225	0.167	18.15	5.18	18.65	2.41	0.0176	7.313
226	0.333	20.165	15.48	21.675	1.83	0.0265	9.123
255	0.167	18.15	3.92	18.5	2.73	0.0149	7.198
256	0.333	20.165	14.2	21.525	1.82	0.0264	8.672
257	0.167	18.15	3.92	18.5	2.94	0.0139	7.754
258	0.333	20.165	14.2	21.525	1.97	0.0244	9.397
259	0.111	14.6	1.66	14.82	2.55	0.0144	4.883
260	0.167	18.15	3.92	18.5	2.56	0.0159	6.760
261	0.111	14.6	1.66	14.82	2.55	0.0144	4.883
262	0.167	18.15	3.92	18.5	2.59	0.0157	6.840
263	0.111	14.6	1.66	14.82	2.36	0.0161	4.507
264	0.167	18.15	3.92	18.5	2.71	0.0155	7.158
265	0.333	20.165	14.2	21.525	1.91	0.0260	9.111
68	0.111	17	1.88	17.22	1.49	0.0105	2.819
69	0.167	18.15	5.18	18.65	1.48	0.0123	4.484

Test ID Number	*depth* (ft)	*Tw* (ft)	*A* (ft^2)	*Wp* (ft)	*Fr*	*n*	*velocity* (ft/s)
70	0.333	20.165	15.48	21.675	1.62	0.0128	8.056
77	0.111	12	1.42	12.22	1.18	0.0156	2.305
78	0.167	18.15	3.92	18.5	1.09	0.0187	2.863
79	0.333	20.165	14.2	21.525	1.40	0.0172	6.652
140	0.111	18.15	2.14	18.39	3.51	0.0077	6.847
141	0.167	18.15	5.18	18.65	2.08	0.0149	6.319
142	0.333	20.165	15.48	21.675	2.30	0.0154	11.439
185	0.111	14	1.6	14.22	2.59	0.0110	4.969
186	0.167	18.15	3.92	18.5	2.29	0.0138	6.044
187	0.333	20.165	14.2	21.525	2.42	0.0154	11.526
221	0.111	18.15	2.14	18.39	3.18	0.0116	6.191
222	0.167	18.15	5.18	18.65	2.33	0.0182	7.072
223	0.333	20.165	15.48	21.675	1.88	0.0258	9.365
266	0.111	14.6	1.66	14.82	2.75	0.0138	5.259
267	0.167	18.15	3.92	18.5	2.56	0.0164	6.760
268	0.333	20.165	14.2	21.525	1.94	0.0257	9.221
71	0.111	17	1.88	17.22	1.27	0.0123	2.405
72	0.167	18.15	5.18	18.65	1.51	0.0120	4.574
73	0.333	20.165	15.48	21.675	1.63	0.0127	8.126
74	0.111	12	1.42	12.22	1.24	0.0148	2.415
75	0.167	18.15	3.92	18.5	1.09	0.0187	2.863
76	0.333	20.165	14.2	21.525	1.39	0.0173	6.608
137	0.111	18.15	2.14	18.39	3.18	0.0085	6.191
138	0.167	18.15	5.18	18.65	2.54	0.0122	7.704
139	0.333	20.165	15.48	21.675	2.02	0.0176	10.019
188	0.111	14	1.6	14.22	2.74	0.0104	5.261
189	0.167	18.15	3.92	18.5	2.19	0.0144	5.766
190	0.333	20.165	14.2	21.525	2.41	0.0155	11.471
218	0.111	18.15	2.14	18.39	3.03	0.0122	5.900
219	0.167	18.15	5.18	18.65	2.43	0.0175	7.373
220	0.333	20.165	15.48	21.675	1.89	0.0257	9.415
269	0.111	14.6	1.66	14.82	2.65	0.0143	5.071
270	0.167	18.15	3.92	18.5	2.49	0.0169	6.561
271	0.333	20.165	14.2	21.525	1.89	0.0263	9.002
AT296	0.111	18.15	2.14	18.39	3.44	0.0108	6.701
AT298	0.167	18.15	5.18	18.65	2.42	0.0175	7.343
AT299	0.111	18.15	2.14	18.39	3.51	0.0105	6.847
AT302	0.167	18.15	5.18	18.65	2.41	0.0176	7.313
AT289	0.111	18.15	2.14	18.39	3.40	0.0109	6.629
AT290	0.167	18.15	5.18	18.65	2.42	0.0175	7.343
AT292	0.111	18.15	2.14	18.39	3.51	0.0105	6.847
AT294	0.167	18.15	5.18	18.65	2.45	0.0173	7.433
AT304	0.111	18.15	2.14	18.39	3.44	0.0108	6.701
AT305	0.167	18.15	5.18	18.65	2.40	0.0177	7.282
AT303	0.111	18.15	2.14	18.39	3.44	0.0108	6.701
AT306	0.167	18.15	5.18	18.65	2.39	0.0178	7.252

Test ID Number	*depth* (ft)	*Tw* (ft)	*A* (ft^2)	*Wp* (ft)	*Fr*	*n*	*velocity* (ft/s)
AT295	0.111	18.15	2.14	18.39	3.48	0.0106	6.774
AT297	0.167	18.15	5.18	18.65	2.44	0.0174	7.403
AT300	0.111	18.15	2.14	18.39	3.51	0.0105	6.847
AT301	0.167	18.15	5.18	18.65	2.42	0.0175	7.343

Table F-3: Additional parameters for the Type R curb inlet tests

Test ID Number	*depth* (ft)	*Tw* (ft)	*A* (ft^2)	*Wp* (ft)	*Fr*	*n*	*velocity* (ft/s)
44	0.111	16.000	1.92	1.809	1.16	0.0137	2.273
45	0.167	17.500	4.96	4.793	1.35	0.0139	4.086
46	0.333	20.165	15.48	15.147	1.67	0.0124	8.318
47	0.111	16.000	1.92	1.809	1.03	0.0153	2.030
48	0.167	18.150	5.18	5.013	1.39	0.0131	4.213
49	0.333	20.165	15.48	15.147	1.64	0.0127	8.157
50	0.111	16.000	1.92	1.809	1.12	0.0142	2.192
51	0.167	18.150	5.18	5.013	1.37	0.0132	4.153
52	0.333	20.165	15.48	15.147	1.66	0.0125	8.257
53	0.111	16.000	1.92	1.809	1.16	0.0137	2.273
54	0.167	18.150	5.18	5.013	1.42	0.0128	4.303
55	0.333	20.165	15.48	15.147	1.63	0.0127	8.106
122	0.111	14.000	1.6	1.489	1.07	0.0172	2.046
123	0.167	18.150	3.92	3.753	1.06	0.0192	2.784
124	0.333	20.165	14.2	13.867	1.39	0.0172	6.641
119	0.111	14.000	1.6	1.489	0.91	0.0200	1.754
120	0.167	18.150	3.92	3.753	1.06	0.0192	2.784
121	0.333	20.165	14.2	13.867	1.39	0.0173	6.608
116	0.111	14.000	1.6	1.489	1.02	0.0180	1.949
117	0.167	18.150	3.92	3.753	1.09	0.0187	2.863
118	0.333	20.165	14.2	13.867	1.39	0.0173	6.608
110	0.111	14.000	1.6	1.489	0.96	0.0190	1.851
111	0.167	18.150	3.92	3.753	1.07	0.0190	2.823
112	0.333	20.165	14.2	13.867	1.38	0.0174	6.565
113	0.167	18.150	3.92	3.753	1.09	0.0187	2.863
114	0.333	20.165	14.2	13.867	1.39	0.0172	6.641
115	0.167	18.150	3.92	3.753	1.07	0.0190	2.823
125	0.111	18.150	2.14	2.029	3.55	0.0076	6.920
126	0.167	18.150	5.18	5.013	2.13	0.0145	6.470
127	0.333	20.165	15.48	15.147	2.32	0.0153	11.530
128	0.111	18.150	2.14	2.029	3.21	0.0084	6.264
129	0.167	18.150	5.18	5.013	2.09	0.0148	6.350
130	0.333	20.165	15.48	15.147	2.29	0.0155	11.379
131	0.111	18.150	2.14	2.029	3.21	0.0084	6.264
132	0.167	18.150	5.18	5.013	1.89	0.0164	5.718
133	0.333	20.165	15.48	15.147	2.25	0.0158	11.177
134	0.111	18.150	2.14	2.029	3.14	0.0086	6.119
135	0.167	18.150	5.18	5.013	1.81	0.0172	5.477
136	0.333	20.165	15.48	15.147	2.33	0.0153	11.560
203	0.111	14.000	1.6	1.489	2.29	0.0124	4.384
204	0.167	18.150	3.92	3.753	2.08	0.0152	5.488
205	0.333	20.165	14.2	13.867	2.47	0.0151	11.746
200	0.111	14.000	1.6	1.489	2.44	0.0117	4.676
201	0.167	18.150	3.92	3.753	2.10	0.0150	5.527

Test ID Number	*depth* (ft)	*Tw* (ft)	*A* (ft^2)	*Wp* (ft)	*Fr*	*n*	*velocity* (ft/s)
202	0.333	20.165	14.2	13.867	2.47	0.0151	11.746
197	0.111	11.000	1.34	1.229	2.35	0.0122	4.653
198	0.167	18.150	3.92	3.753	2.11	0.0149	5.567
199	0.333	20.165	14.2	13.867	2.46	0.0152	11.691
191	0.111	17.800	1.95	1.839	2.00	0.0141	3.757
192	0.167	18.150	3.92	3.753	2.22	0.0142	5.846
193	0.333	20.165	14.2	13.867	2.46	0.0152	11.691
194	0.333	20.165	14.2	13.867	2.47	0.0151	11.746
195	0.167	18.150	3.92	3.753	2.20	0.0143	5.806
196	0.167	18.150	3.92	3.753	2.23	0.0141	5.885
206	0.111	18.150	2.14	2.029	3.14	0.0118	6.119
207	0.167	18.150	5.18	5.013	2.44	0.0174	7.403
208	0.333	20.165	15.48	15.147	1.86	0.0261	9.264
209	0.111	18.150	2.14	2.029	3.03	0.0122	5.900
210	0.167	18.150	5.18	5.013	2.44	0.0174	7.403
211	0.333	20.165	15.48	15.147	1.99	0.0245	9.878
212	0.111	18.150	2.14	2.029	3.33	0.0111	6.483
213	0.167	18.150	5.18	5.013	2.43	0.0175	7.373
214	0.333	20.165	15.48	15.147	1.84	0.0264	9.143
215	0.111	18.150	2.14	2.029	3.29	0.0112	6.410
216	0.167	18.150	5.18	5.013	2.43	0.0175	7.373
217	0.333	20.165	15.48	15.147	1.82	0.0267	9.063
284	0.111	16.000	1.79	1.679	2.29	0.0165	4.354
285	0.167	18.150	3.92	3.753	2.26	0.0186	5.965
286	0.333	20.165	14.2	13.867	1.82	0.0273	8.672
281	0.111	16.000	1.79	1.679	2.57	0.0147	4.877
282	0.167	18.150	3.92	3.753	2.44	0.0172	6.442
283	0.333	20.165	14.2	13.867	1.68	0.0295	8.014
278	0.111	16.000	1.79	1.679	2.34	0.0162	4.441
279	0.167	18.150	3.92	3.753	2.50	0.0168	6.601
280	0.333	20.165	14.2	13.867	1.74	0.0286	8.288
272	0.111	16.000	1.79	1.679	2.39	0.0159	4.528
273	0.167	18.150	3.92	3.753	2.58	0.0163	6.800
274	0.333	20.165	14.2	13.867	1.76	0.0283	8.376
275	0.167	18.15	3.92	3.753	2.65	0.0159	6.999
276	0.333	20.165	14.2	13.867	1.90	0.0261	9.056
277	0.167	18.15	3.92	3.753	2.58	0.0163	6.800
AT302	0.167	18.15	5.18	18.65	2.41	0.0176	7.313
AT289	0.111	18.15	2.14	18.39	3.40	0.0109	6.629
AT290	0.167	18.15	5.18	18.65	2.42	0.0175	7.343
AT292	0.111	18.15	2.14	18.39	3.51	0.0105	6.847
AT294	0.167	18.15	5.18	18.65	2.45	0.0173	7.433
AT304	0.111	18.15	2.14	18.39	3.44	0.0108	6.701
AT305	0.167	18.15	5.18	18.65	2.40	0.0177	7.282
AT303	0.111	18.15	2.14	18.39	3.44	0.0108	6.701
AT306	0.167	18.15	5.18	18.65	2.39	0.0178	7.252

Test ID Number	*depth* (ft)	*Tw* (ft)	*A* (ft^2)	*Wp* (ft)	*Fr*	*n*	*velocity* (ft/s)
AT295	0.111	18.15	2.14	18.39	3.48	0.0106	6.774
AT297	0.167	18.15	5.18	18.65	2.44	0.0174	7.403
AT300	0.111	18.15	2.14	18.39	3.51	0.0105	6.847
AT301	0.167	18.15	5.18	18.65	2.42	0.0175	7.343

APPENDIX G

REGRESSION ANALYSIS STATISTICS

G.1 Statistical Qualities

The following data are taken directly from the SAS application and organized by inlet type:

The REG Procedure
Model: MODEL1
Dependent Variable: logE

Number of Observations Read 54
Number of Observations Used 54

Analysis of Variance

Source	DF	Sum of Squares	Mean Square	F Value	Pr > F
Model	3	2.20663	0.73554	149.59	<.0001
Error	50	0.24585	0.00492		
Corrected Total	53	2.45248			

Root MSE	0.07012	R-Square	0.8998
Dependent Mean	-0.48707	Adj R-Sq	0.8937
Coeff Var	-14.39675		

Parameter Estimates

Variable	Label	DF	Parameter Estimate	Standard Error	t Value	Pr > |t|
Intercept	Intercept	1	-1.02291	0.04068	-25.15	<.0001
logLh	logLh	1	0.57349	0.13006	4.41	<.0001
logFr	logFr	1	0.75556	0.09620	7.85	<.0001
log3	log3	1	-0.92041	0.09428	-9.76	<.0001

Correlation of Estimates

Variable	Intercept	logLh	logFr	log3
Intercept	1.0000	0.3767	0.0139	-0.1676
logLh	0.3767	1.0000	0.9120	-0.9639
logFr	0.0139	0.9120	1.0000	-0.9318
log3	-0.1676	-0.9639	-0.9318	1.0000

Note: logLh = log(h/L), logFr = log(V^2T/gA), log3 = log(V^2/gL)

(a)

Figure G-1: Type 16 combination inlet

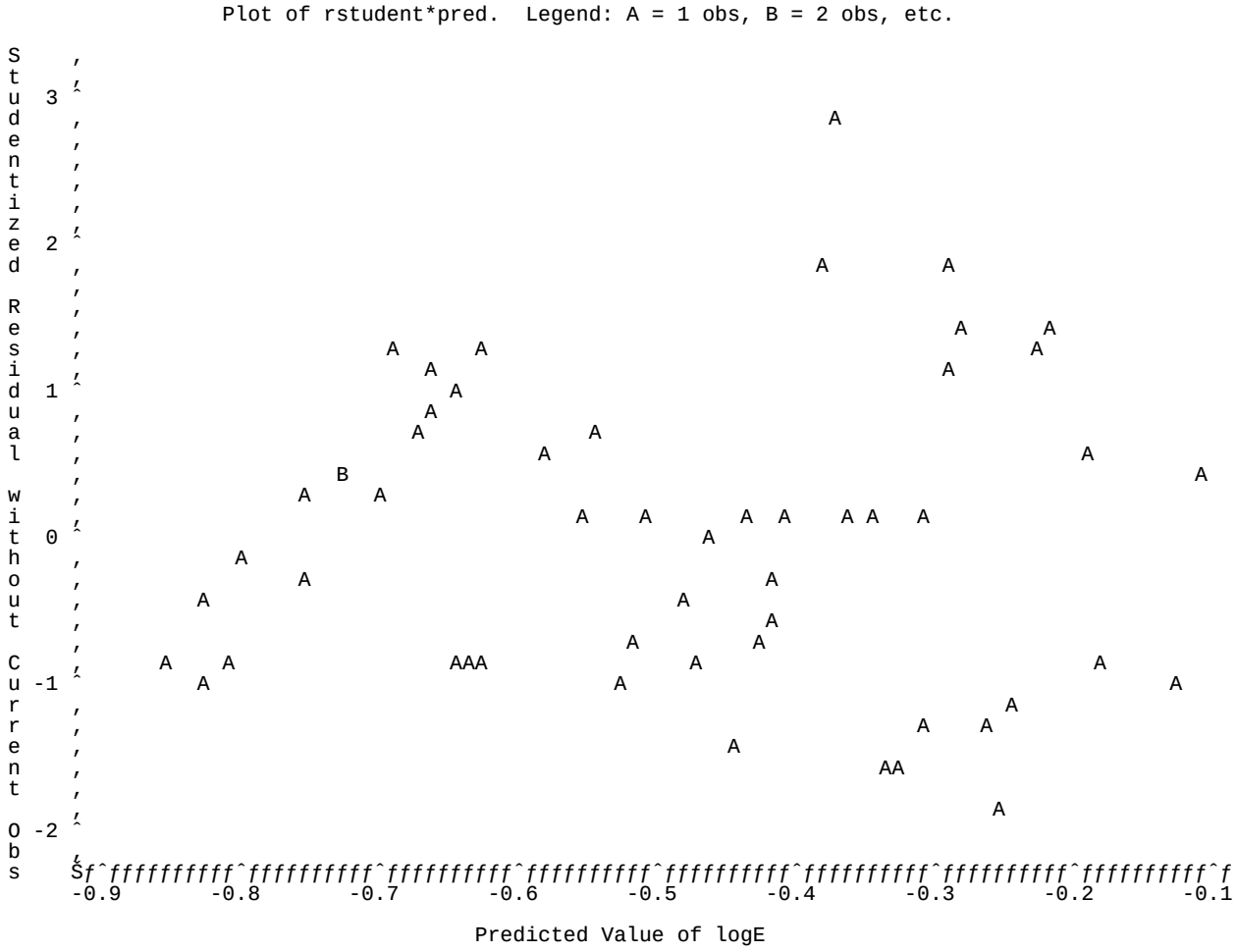

(b)

Figure G-1 (cont.): Type 16 combination inlet

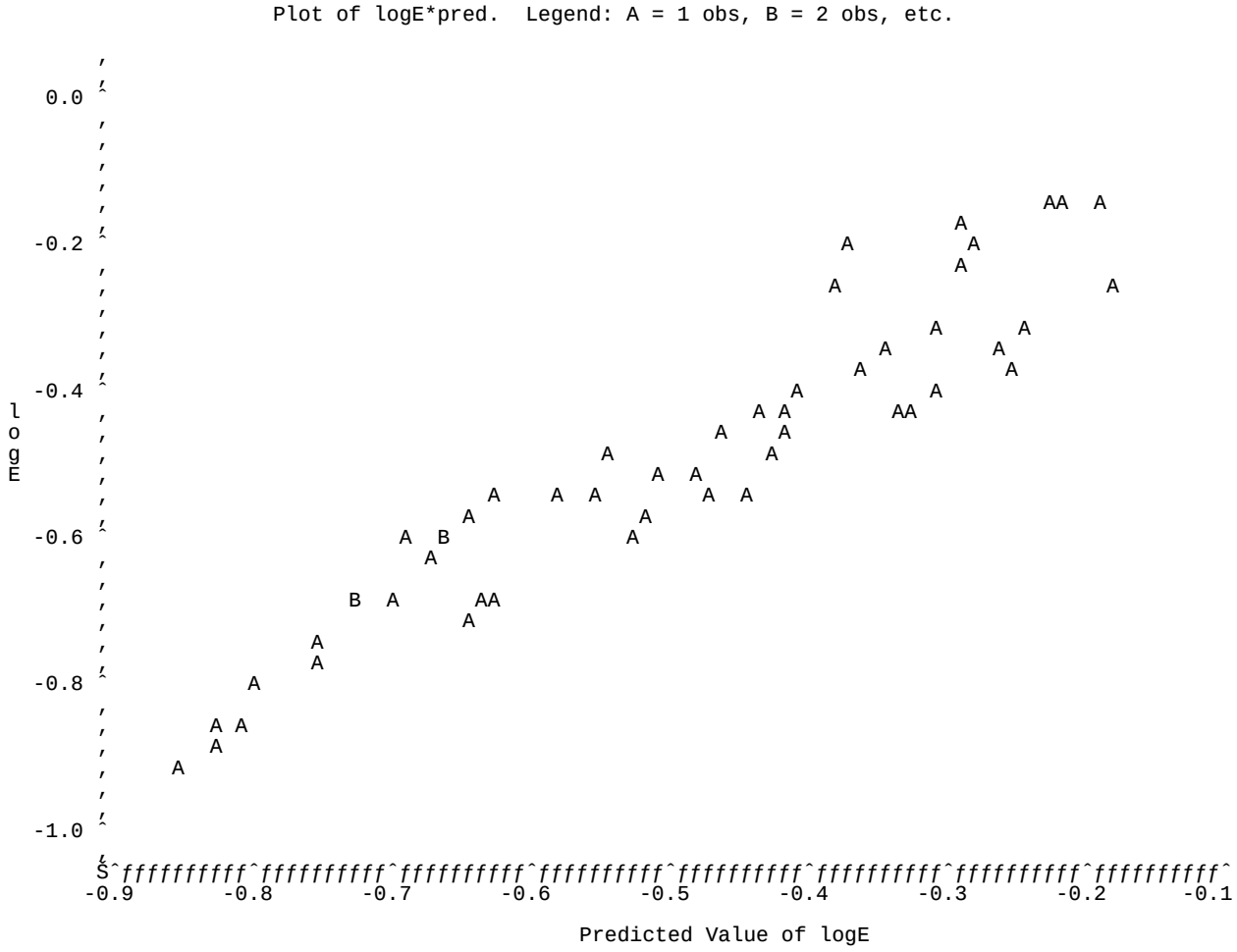

(c)

Figure G-1 (cont.): Type 16 combination inlet

The REG Procedure
Model: MODEL1
Dependent Variable: logE

Number of Observations Read 53
Number of Observations Used 53

Analysis of Variance

Source	DF	Sum of Squares	Mean Square	F Value	Pr > F
Model	3	3.81553	1.27184	325.37	<.0001
Error	49	0.19154	0.00391		
Corrected Total	52	4.00707			

Root MSE	0.06252	R-Square	0.9522
Dependent Mean	-0.54874	Adj R-Sq	0.9493
Coeff Var	-11.39360		

Parameter Estimates

Variable	Label	DF	Parameter Estimate	Standard Error	t Value	Pr > |t|
Intercept	Intercept	1	-1.20291	0.03673	-32.75	<.0001
logLh	logLh	1	0.66466	0.11875	5.60	<.0001
logFr	logFr	1	0.83532	0.08911	9.37	<.0001
log3	log3	1	-1.13773	0.08641	-13.17	<.0001

Correlation of Estimates

Variable	Intercept	logLh	logFr	log3
Intercept	1.0000	0.3470	-0.0169	-0.1383
logLh	0.3470	1.0000	0.9139	-0.9661
logFr	-0.0169	0.9139	1.0000	-0.9385
log3	-0.1383	-0.9661	-0.9385	1.0000

Note: $\log Lh = \log(h/L)$, $\log Fr = \log(V^2T/gA)$, $\log 3 = \log(V^2/gL)$

(a)

Figure G-2: Type 13 combination inlet

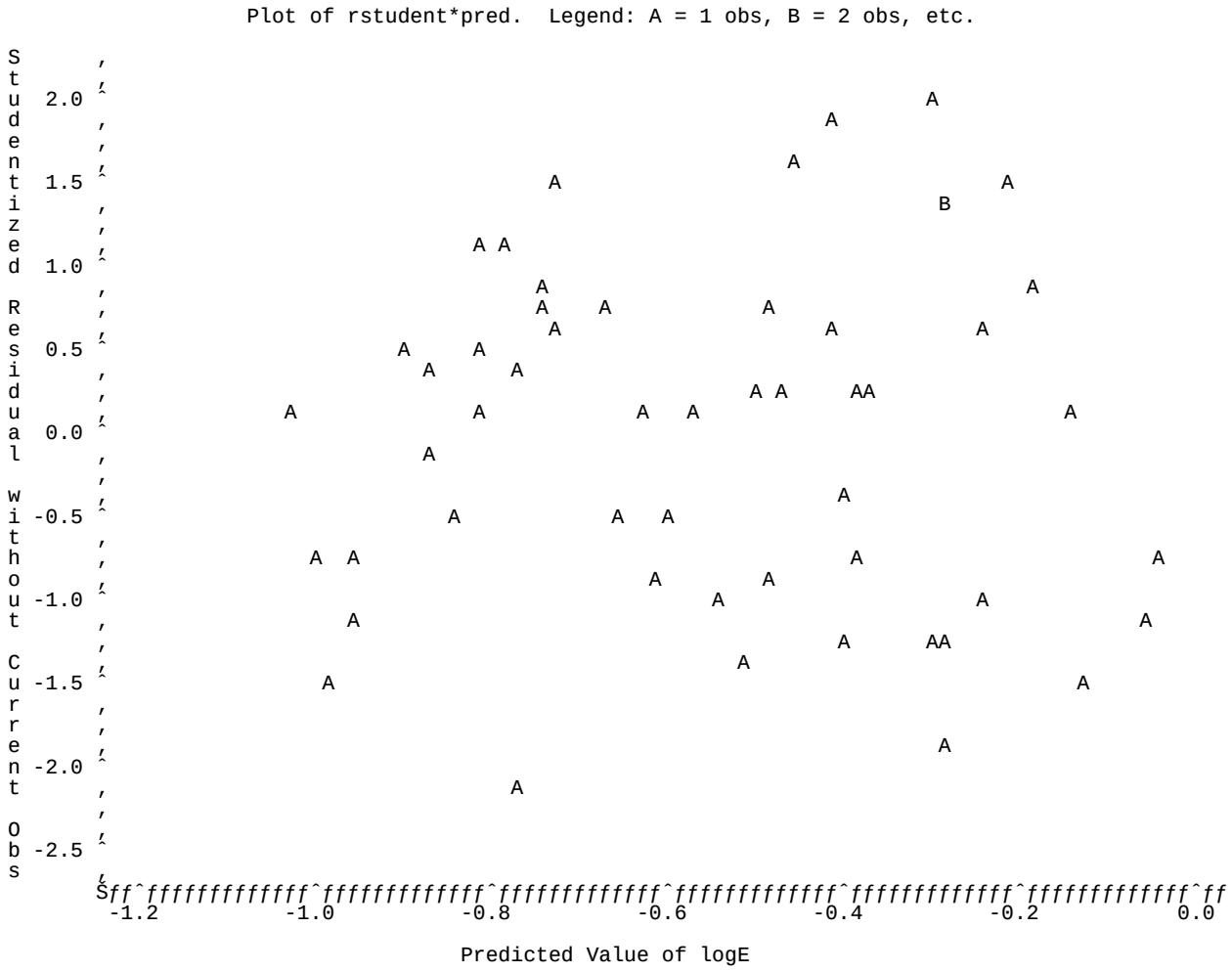

(b)

Figure G-2 (cont.): Type 13 combination inlet

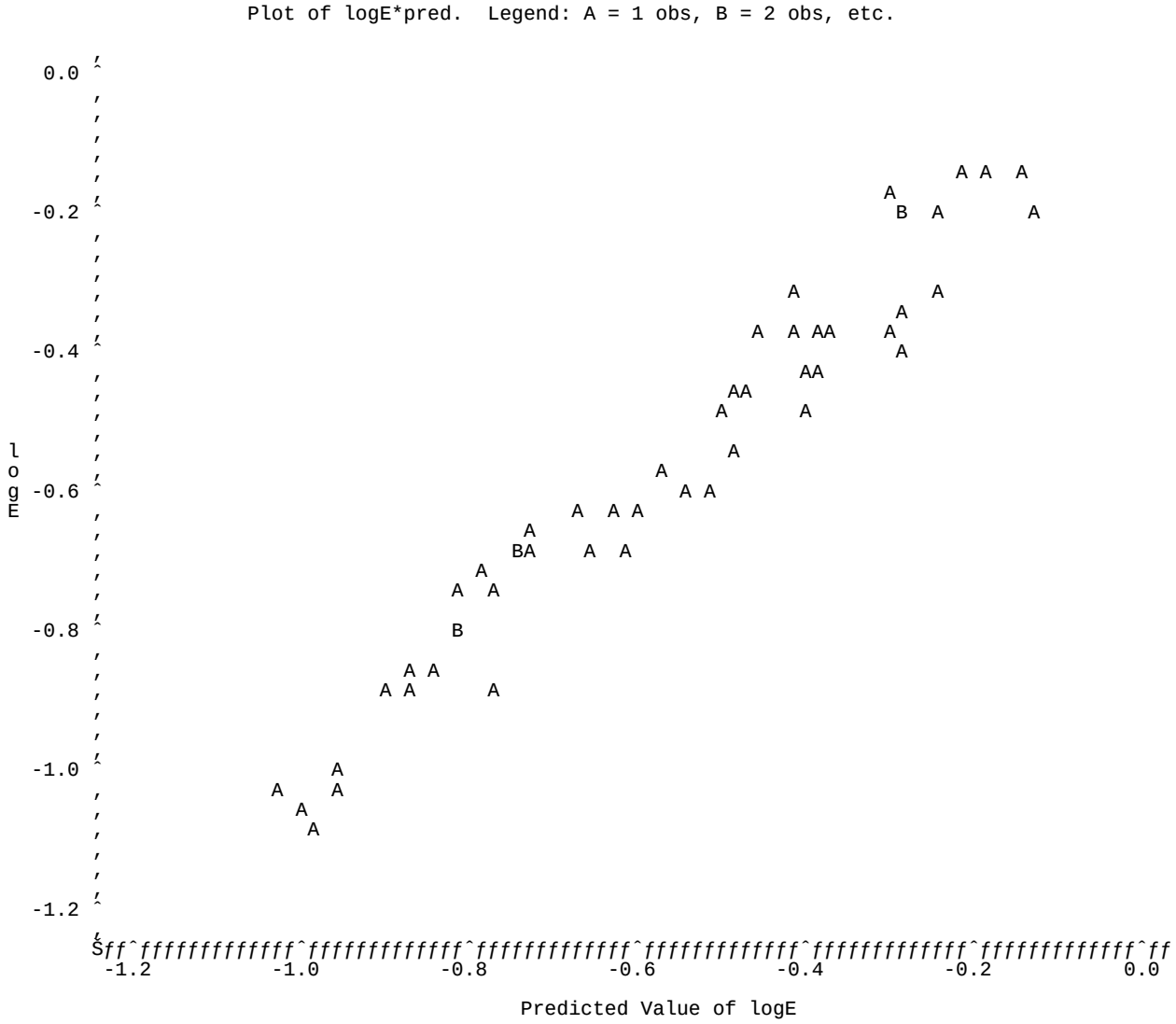

(c)

Figure G-2 (cont.): Type 13 combination inlet

The REG Procedure
Model: MODEL1
Dependent Variable: logE

Number of Observations Read	71
Number of Observations Used	71

Analysis of Variance

Source	DF	Sum of Squares	Mean Square	F Value	Pr > F
Model	3	5.87247	1.95749	412.60	<.0001
Error	67	0.31786	0.00474		
Corrected Total	70	6.19033			

Root MSE	0.06888	R-Square	0.9487
Dependent Mean	-0.54896	Adj R-Sq	0.9464
Coeff Var	-12.54716		

Parameter Estimates

Variable	Label	DF	Parameter Estimate	Standard Error	t Value	Pr > |t|
Intercept	Intercept	1	-1.11977	0.10801	-10.37	<.0001
log2	log2	1	0.54531	0.04650	11.73	<.0001
logSc	logSc	1	0.23115	0.05647	4.09	0.0001
log3	log3	1	-0.87850	0.03173	-27.69	<.0001

Correlation of Estimates

Variable	Intercept	log2	logSc	log3
Intercept	1.0000	-0.1435	0.9215	0.3006
log2	-0.1435	1.0000	0.2123	-0.8321
logSc	0.9215	0.2123	1.0000	-0.0809
log3	0.3006	-0.8321	-0.0809	1.0000

Note: log2 = log(V^2/gh), log3 = log(V^2/gL), log*Sc* = log(*cross slope*)

(a)

Figure G-3: Type R curb inlet

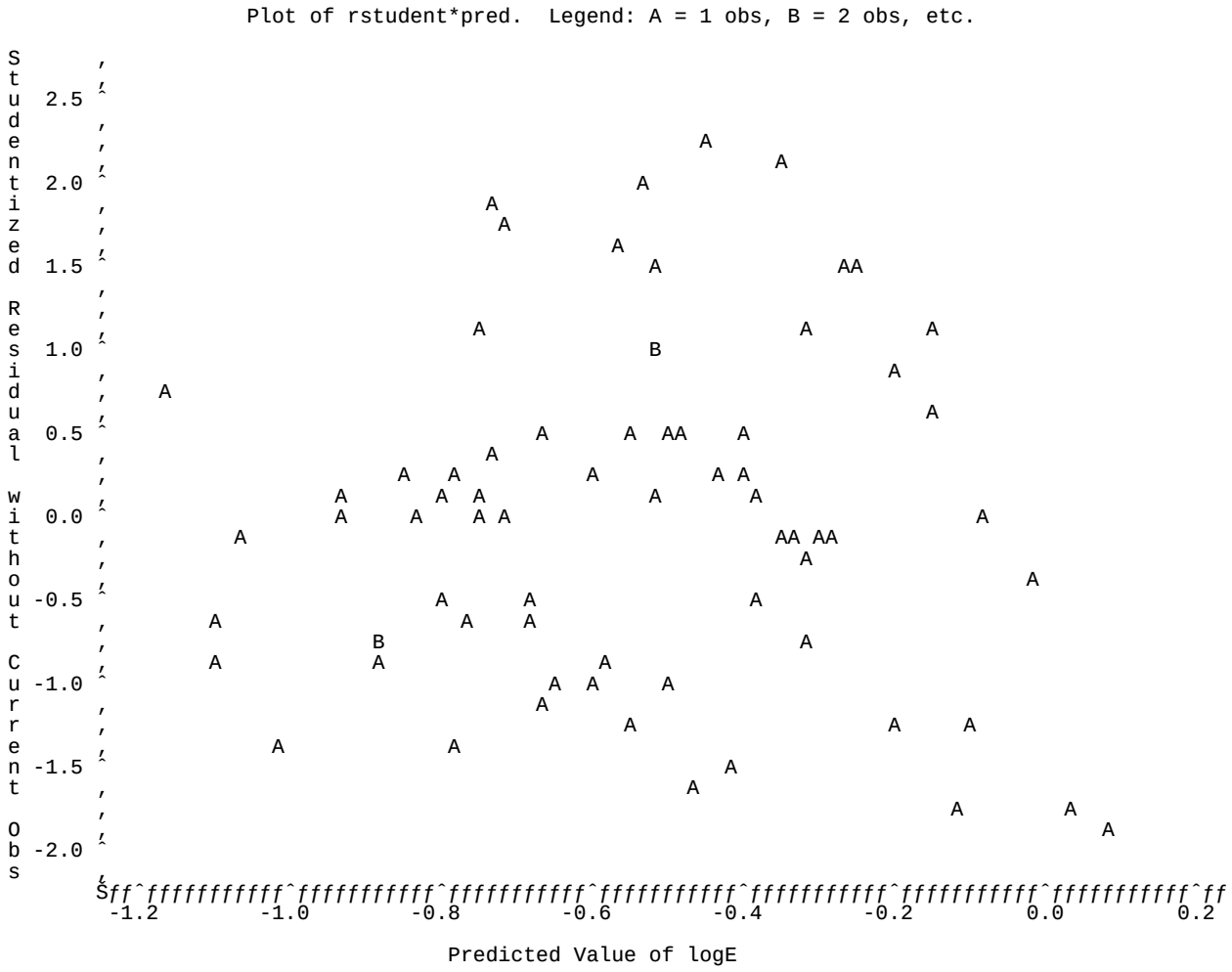

(b)

Figure G-3 (cont.): Type R curb inlet

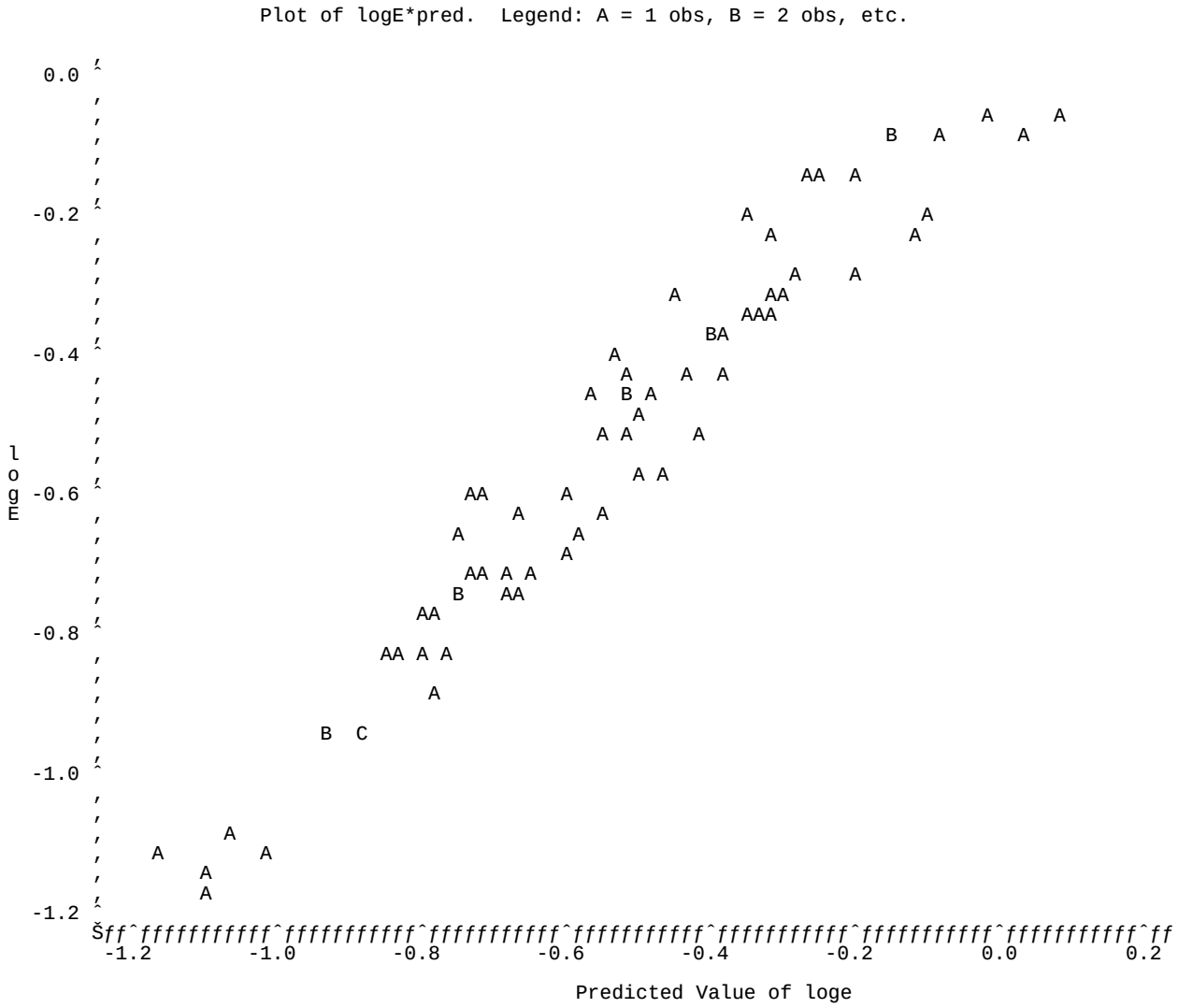

(c)

Figure G-3 (cont.): Type R curb inlet

APPENDIX H

CALCULATED EFFICIENCY

H.1 Efficiency Determined from Empirical Equations and Improved UDFCD Methods

Table H-1: Type 13 combination-inlet calculated efficiency

Test ID Number	Depth (ft)	Grates	Flow (cfs)	Efficiency		
				Observed	Regression	UDFCD New
62	0.333	1	4.83	0.61	0.51	0.50
63	0.501	1	26.19	0.24	0.21	0.30
64	0.999	1	126.42	0.10	0.11	0.17
91	0.333	1	2.96	0.63	0.58	0.64
92	0.501	1	10.13	0.38	0.40	0.48
93	0.999	1	95.09	0.13	0.13	0.22
146	0.333	1	15.90	0.27	0.27	0.20
147	0.501	1	33.67	0.20	0.18	0.24
148	0.999	1	166.64	0.09	0.09	0.08
161	0.333	1	7.79	0.50	0.39	0.36
162	0.501	1	24.78	0.24	0.23	0.23
163	0.999	1	155.88	0.09	0.10	0.07
227	0.333	1	12.94	0.25	0.30	0.26
228	0.501	1	37.72	0.13	0.17	0.21
229	0.999	1	142.63	0.08	0.10	0.13
242	0.333	1	9.04	0.43	0.34	0.32
243	0.501	1	27.28	0.21	0.22	0.21
244	0.999	1	129.69	0.09	0.11	0.13
59	0.333	2	4.68	0.73	0.72	0.73
60	0.501	2	22.60	0.36	0.32	0.49
61	0.999	2	127.82	0.16	0.15	0.25
104	0.333	2	3.27	0.62	0.75	0.84
105	0.501	2	11.22	0.44	0.53	0.72
106	0.999	2	98.20	0.20	0.18	0.36
149	0.333	2	14.34	0.34	0.40	0.33
150	0.501	2	33.67	0.24	0.25	0.34
151	0.999	2	176.61	0.13	0.12	0.12
158	0.333	2	8.11	0.63	0.53	0.56
159	0.501	2	23.38	0.35	0.34	0.42
160	0.999	2	161.34	0.14	0.13	0.14
230	0.333	2	13.25	0.38	0.42	0.36
231	0.501	2	36.63	0.21	0.24	0.31
232	0.999	2	138.73	0.13	0.14	0.22
239	0.333	2	8.26	0.66	0.51	0.55
240	0.501	2	26.03	0.33	0.32	0.38
241	0.999	2	127.82	0.16	0.15	0.25
56	0.333	3	4.36	0.82	0.91	0.86
57	0.501	3	20.58	0.43	0.41	0.67
58	0.999	3	126.57	0.23	0.18	0.35

Test ID Number	Depth (ft)	Grates	Flow (cfs)	Efficiency		
				Observed	Regression	UDFCD New
107	0.333	3	3.59	0.74	0.87	0.91
108	0.501	3	13.41	0.50	0.57	0.81
109	0.999	3	108.34	0.43	0.21	0.46
152	0.333	3	13.09	0.43	0.51	0.48
153	0.501	3	31.02	0.29	0.32	0.49
154	0.999	3	177.70	0.18	0.15	0.17
155	0.333	3	7.79	0.74	0.65	0.73
156	0.501	3	22.13	0.44	0.42	0.61
157	0.999	3	163.21	0.19	0.16	0.24
233	0.333	3	12.63	0.41	0.52	0.50
234	0.501	3	38.19	0.25	0.28	0.39
235	0.999	3	146.84	0.18	0.17	0.27
236	0.333	3	8.42	0.74	0.61	0.70
237	0.501	3	25.72	0.42	0.38	0.53
238	0.999	3	128.60	0.20	0.19	0.37

Table H-2: Type 16 combination-inlet calculated efficiency

Test ID Number	Depth (ft)	Grates	Flow (cfs)	Efficiency		
				Observed	Regression	UDFCD New
65	0.333	1	5.14	0.61	0.51	0.56
66	0.501	1	21.36	0.28	0.28	0.39
67	0.999	1	126.89	0.14	0.16	0.25
80	0.333	1	3.74	0.50	0.49	0.63
81	0.501	1	11.54	0.35	0.38	0.40
82	0.999	1	95.55	0.17	0.18	0.20
143	0.333	1	15.28	0.29	0.36	0.40
144	0.501	1	33.98	0.21	0.24	0.27
145	0.999	1	176.61	0.12	0.14	0.07
174	0.333	1	7.95	0.55	0.41	0.46
175	0.501	1	22.29	0.31	0.31	0.29
176	0.999	1	162.89	0.13	0.15	0.06
224	0.333	1	13.09	0.33	0.38	0.33
225	0.501	1	37.88	0.20	0.23	0.18
226	0.999	1	141.23	0.14	0.15	-0.08
263	0.333	1	7.48	0.65	0.43	0.37
264	0.501	1	28.06	0.32	0.29	0.21
265	0.999	1	129.38	0.16	0.16	-0.05
68	0.333	2	5.30	0.71	0.65	0.78
69	0.501	2	23.23	0.34	0.34	0.58
70	0.999	2	124.70	0.21	0.20	0.34
77	0.333	2	3.27	0.57	0.66	0.84
78	0.501	2	11.22	0.40	0.49	0.73
79	0.999	2	94.46	0.20	0.23	0.37
140	0.333	2	14.65	0.36	0.46	0.59
141	0.501	2	32.73	0.27	0.31	0.38
142	0.999	2	177.08	0.19	0.18	0.13
185	0.333	2	7.95	0.65	0.52	0.69
186	0.501	2	23.69	0.37	0.38	0.47
187	0.999	2	163.67	0.20	0.19	0.15
221	0.333	2	13.25	0.38	0.48	0.48
222	0.501	2	36.63	0.25	0.29	0.26
223	0.999	2	144.97	0.20	0.19	-0.04
266	0.333	2	8.73	0.68	0.52	0.57
267	0.501	2	26.50	0.38	0.37	0.35
268	0.999	2	130.94	0.25	0.20	0.01
71	0.333	3	4.52	0.83	0.78	0.89
72	0.501	3	23.69	0.40	0.39	0.73
73	0.999	3	125.80	0.27	0.23	0.45
74	0.333	3	3.43	0.64	0.74	0.92
75	0.501	3	11.22	0.47	0.56	0.86
76	0.999	3	93.84	0.28	0.26	0.53
137	0.333	3	13.25	0.45	0.55	0.74
138	0.501	3	39.91	0.31	0.33	0.49

Test ID Number	Depth (ft)	Grates	Flow (cfs)	Efficiency		
				Observed	Regression	UDFCD New
139	0.999	3	155.10	0.24	0.21	0.19
188	0.333	3	8.42	0.72	0.59	0.83
189	0.501	3	22.60	0.46	0.45	0.64
190	0.999	3	162.89	0.26	0.22	0.25
218	0.333	3	12.63	0.42	0.56	0.61
219	0.501	3	38.19	0.29	0.33	0.35
220	0.999	3	145.75	0.25	0.22	0.01
269	0.333	3	8.42	0.74	0.60	0.72
270	0.501	3	25.72	0.44	0.43	0.50
271	0.999	3	127.82	0.29	0.24	0.08

Table H-3: Type R curb inlet calculated efficiency

Test ID Number	Depth (ft)	Length (ft)	Flow (cfs)	Efficiency		
				Observed	Regression	UDFCD New
44	0.333	15	4.36	0.89	0.95	0.95
45	0.501	15	20.26	0.51	0.51	0.55
46	0.999	15	128.76	0.24	0.22	0.22
47	0.333	12	3.90	0.84	0.84	0.87
48	0.501	12	21.82	0.38	0.41	0.43
49	0.999	12	126.26	0.20	0.18	0.18
50	0.333	9	4.21	0.70	0.62	0.70
51	0.501	9	21.51	0.35	0.32	0.34
52	0.999	9	127.82	0.15	0.14	0.14
53	0.333	5	4.36	0.50	0.36	0.43
54	0.501	5	22.29	0.24	0.19	0.19
55	0.999	5	125.48	0.08	0.08	0.08
122	0.333	15	3.27	0.90	1.00	1.00
123	0.501	15	10.91	0.60	0.78	0.71
124	0.999	15	94.31	0.31	0.30	0.27
119	0.333	12	2.81	0.83	1.00	0.96
120	0.501	12	10.91	0.53	0.64	0.60
121	0.999	12	93.84	0.25	0.25	0.22
116	0.333	9	3.12	0.65	0.79	0.81
117	0.501	9	11.22	0.47	0.49	0.46
118	0.999	9	93.84	0.19	0.19	0.17
110	0.333	5	2.96	0.58	0.49	0.53
111	0.501	5	11.07	0.39	0.29	0.28
112	0.999	5	93.22	0.12	0.11	0.09
125	0.333	15	14.81	0.44	0.45	0.58
126	0.501	15	33.51	0.30	0.38	0.40
127	0.999	15	178.48	0.18	0.18	0.18
128	0.333	12	13.41	0.43	0.40	0.50
129	0.501	12	32.89	0.27	0.31	0.33
130	0.999	12	176.14	0.15	0.15	0.14
131	0.333	9	13.41	0.36	0.31	0.39
132	0.501	9	29.62	0.23	0.26	0.27
133	0.999	9	173.03	0.11	0.11	0.11
134	0.333	5	13.09	0.25	0.19	0.23
135	0.501	5	28.37	0.16	0.16	0.16
136	0.999	5	178.95	0.08	0.07	0.06
203	0.333	15	7.01	0.84	0.72	0.82
204	0.501	15	21.51	0.49	0.50	0.50
205	0.999	15	166.79	0.19	0.20	0.19
200	0.333	12	7.48	0.71	0.57	0.68
201	0.501	12	21.67	0.42	0.40	0.42
202	0.999	12	166.79	0.15	0.17	0.15
197	0.333	9	6.24	0.65	0.44	0.61
198	0.501	9	21.82	0.34	0.31	0.32

Test ID Number	Depth (ft)	Length (ft)	Flow (cfs)	Efficiency		
				Observed	Regression	UDFCD New
199	0.999	9	166.01	0.12	0.13	0.12
191	0.333	5	7.33	0.38	0.30	0.31
192	0.501	5	22.91	0.18	0.18	0.18
193	0.999	5	166.01	0.07	0.08	0.07
206	0.333	15	13.09	0.44	0.49	0.59
207	0.501	15	38.35	0.27	0.35	0.37
208	0.999	15	143.41	0.19	0.20	0.19
209	0.333	12	12.63	0.42	0.41	0.50
210	0.501	12	38.35	0.24	0.28	0.30
211	0.999	12	152.92	0.15	0.16	0.15
212	0.333	9	13.87	0.35	0.30	0.37
213	0.501	9	38.19	0.19	0.22	0.23
214	0.999	9	141.54	0.12	0.13	0.12
215	0.333	5	13.72	0.22	0.18	0.22
216	0.501	5	38.19	0.11	0.13	0.13
217	0.999	5	140.29	0.07	0.08	0.07
284	0.333	15	7.79	0.80	0.72	0.75
285	0.501	15	23.38	0.46	0.47	0.47
286	0.999	15	123.15	0.21	0.25	0.21
281	0.333	12	8.73	0.70	0.55	0.61
282	0.501	12	25.25	0.38	0.37	0.37
283	0.999	12	113.79	0.18	0.22	0.18
278	0.333	9	7.95	0.63	0.45	0.50
279	0.501	9	25.88	0.30	0.28	0.28
280	0.999	9	117.69	0.13	0.16	0.13
272	0.333	5	8.11	0.35	0.27	0.29
273	0.501	5	26.66	0.17	0.16	0.16
274	0.999	5	118.94	0.08	0.10	0.07

ELECTRONIC DATA SUPPLEMENT

CONTENTS AND ORGANIZATION

(stored on a 16-GB SDHC™ card)

Folder	Files and/or Sub-folders
Client Final Report	Microsoft Word® (.doc) and Adobe® Acrobat® (.pdf) files for both single- and double-sided printing; and SureThing (.std) CD label file
Analysis	Microsoft Excel® (.xls) files
*Data and Photographs**	0.5% long 1% cross 0.5% long 2% cross 2% long 1% cross 2% long 2% cross 4% long 1% cross 4% long 2% cross Additional model photographs Additional tests Grate-inlet combination pictures Inlet construction Sump tests

*The reader is referred to the UDFCD for obtaining photographs and video documentation.